Global Journal of Science Frontier Research: A
Physics and Space Science
Volume 15 Issue 3 Version 1.0 Year 2015
Type : Double Blind Peer Reviewed International Research Journal
Publisher: Global Journals Inc. (USA)
Online ISSN: 2249-4626 & Print ISSN: 0975-5896

First Observations of Thermal Surface Energy and of the Thermal Evolution Process

By A. Titov

Yeditepe University, Turkey

Abstract- Using a developed technique of synchronous differential temperature measurements, the existence of the thermal surface energy (TSE) has been demonstrated with a huge signal-to-noise ratio in material artifacts, made of a homogeneous material, when these artefacts are irradiated by an external electromagnetic (EM) field. The TSE, presenting the energy of the oriented motion of the coupled field-particles system inside a solid-state artifact, is shown experimentally to be linearly related to the Poynting vector of the external EM field, and it results in the appearance of the thermal hysteresis effect, which is irreversible in time and has no symmetry in spaceThe experiments, presented in this paper, have shown that the principle of superposition is not valid for EM fields in case of TSE, so that the *thermal evolution process*, which inevitably includes the changing in time and in space the variations of the thermal surface energy, *is characterized by the infinite number of correlated influence factors*.

Keywords: *surface energy, temperature definition, hysteresis, fourier theory, evolution process.*

GJSFR-A Classification : *FOR Code: M00*

Strictly as per the compliance and regulations of :

First Observations of Thermal Surface Energy and of the Thermal Evolution Process

A. Titov

Abstract- Using a developed technique of synchronous differential temperature measurements, the existence of the thermal surface energy (TSE) has been demonstrated with a huge signal-to-noise ratio in material artifacts, made of a homogeneous material, when these artefacts are irradiated by an external electromagnetic (EM) field. The TSE, presenting the energy of the oriented motion of the coupled field-particles system inside a solid-state artifact, is shown experimentally to be linearly related to the Poynting vector of the external EM field, and it results in the appearance of the thermal hysteresis effect, which is irreversible in time and has no symmetry in space. The experiments, presented in this paper, have shown that the principle of superposition is not valid for EM fields in case of TSE, so that the *thermal evolution process*, which inevitably includes the changing in time and in space the variations of the thermal surface energy, *is characterized by the infinite number of correlated influence factors*. It is shown experimentally that the dependences on time of the thermal evolution process are specific for any particular point on the artifact surface, and that the corresponding hysteresis effect at each point is characterized by its local time. It is found also that the properties of the material artifact, at any time moment in the Universal Coordinated Time, depend crucially on the choice of the observation point on the artifact surface, and *the properties of the artifact at any point are continuously changing in time as a result of its interaction with the external EM field.* The presented studies give an experimental confirmation of Niels Bohr's fundamental observation that, in the general case, the adequate description of material objects in terms of the isotropic and homogeneous concepts of time and space is not possible. The new concept of temperature, presented in the paper, as the energy of the field-particle system of a macroscopic material object, which can be detected by its EM radiation and which includes the oriented motion of this system, is sufficient for the description of the thermal surface energy and extends the notion of temperature to open systems, beyond the approximation of the thermodynamic equilibrium conditions.

Keywords: surface energy, temperature definition, hysteresis, fourier theory, evolution process.

I. Introduction

In the opening speech at the XVII World Congress of the International Measurement Confederation, held in Rio de Janeiro in 2006, the Director of the National Metrology Institute Prof. A. Brandy was discussing the observation of American scientist "new discoveries are in the next decimal unit", and in this way he was emphasizing the role of precise measurements and Metrology in scientific and industrial progress. The term "discovery" is used in the observation quite intentionally, meaning that with the experimental progress even the well-established physical concepts can be found in contradiction with the results of measurements, which are based on new methods or which realize significantly smaller level of uncertainties. This observation is in agreement with Niels Bohr's views on epistemology, who in accordance with L. Rosenfeld [1] has re-discovered dialectics and who "vividly realized that our proud theories are but temporary resting places of the mind on the unending road to knowledge. Such resting places, however, there must be, where we may taste the joys of knowledge, feel that we have reached a certain harmony between our mental picture of the world and our experience of it". In this respect, we can remind the original N. Bohr observation "*Isolated material particles are abstractions*, their properties being definable and observable only through their interaction with other systems". In 1958 Werner Heisenberg, when discussing the Copenhagen interpretation of Quantum theory, wrote "Our scientific work in physics consists in asking questions about nature in the language that we possess and trying to get an answer from experiment by the means at our disposal… It is understandable that in our scientific relation to nature our own activity becomes very important when *we have to deal with parts of nature into which we can penetrate only by using the most elaborate tools*". From these observations, it is easier to understand N. Bohr's remarks: "We must be clear that when it comes to atoms, language can be used only as in poetry. The poet, too, is not nearly so concerned with describing facts as with creating images and establishing mental connections."

"*Physics is to be regarded* not so much as the study of something *a priory* given, but rather *as the development of methods of ordering and surveying human experience*. In this respect our task must be to account for such experience in a manner independent of individual subjective judgment and therefore objective in the sense that it can be unambiguously communicated in ordinary human language."

"What is that we human beings ultimately depend on? We depend on our words. We are suspended in language. Our task is to communicate experience and ideas to others."

"In physics we again and again learn that *our task is not to investigate the essence of things*-we do not

Author: Physics Department, Yeditepe University, Istanbul, Turkey. e-mail: atitov@yeditepe.edu.tr

at all know what this would mean; *but to develop those concepts that allow us to speak with each other about the events of nature in a fruitful manner*."

"'There is no quantum world. There is only an abstract quantum physical description. It is wrong to think that the task of physics is to find out how nature *is*. Physics concerns what we can *say* about Nature."

And quite interesting, but somewhat simplified summary of the ideas of N. Bohr we can find in the University text-book on Physics by D. Giancoly [2]. When discussing the wave-particle duality of light, D. Giancoly writes: "Part of the difficulty stems from how we think. Visual pictures (or models) in our minds are based on what we see in the everyday world. We apply the concepts of waves and particles to light because in the macroscopic world we see that energy is transferred from place to place by these two methods. We cannot see directly whether light is a wave, or particle– so *we do indirect experiments*. *To explain the experiments, we apply the models* of waves or of particles to the nature of light. *But these are the abstractions of the human mind*. There is no reason why light should conform to these models (or visual images) taken from macroscopic world. *The best we can do is recognize that our knowledge is limited to the indirect experiments*, and that in terms of everyday language and images, light reveals both wave and particle properties." [2a].

The new, revolutionary insights to N. Bohr's epistemology are giving the philosophical observations of Albert Einstein, associated with the last period of his scientific activity: "*No amount of experimentation can ever prove me right; a single experiment can prove me wrong*". This quote is of paramount importance and shows the crucial difference in the roles of the experimental and theoretical studies. Only one experiment can show that the theory is wrong. From the same observation it follows that in accordance with Karl Popper philosophical views no finite number of experiments can prove that the theory is correct, as only one experiment, performed under basically new conditions, can demonstrate the evident inconsistence of the approximations of the theoretical model of this theory with the properties of Nature. In this respect, it is also important to remind two other fundamental philosophical observations of A. Einstein: "I don't believe in mathematics.", and "As far as the laws of mathematics refer to reality, they are not certain; and as far as they are certain, they do not refer to reality".

These observations appear very close to one of the most important Niels Bohr's philosophical statements, which can be even found nowadays in the University text-books. For example, D. Giancoly in [2b] writes: "Perhaps the most important and influential philosopher of quantum mechanics was Bohr. *He argued that a space-time description of actual atoms and electrons is not possible*". The confirmation of this N. Bohr's point of view can be found in the letter of 1926 by Erwin Schrödinger to W. Wien: "*Bohr's standpoint, that a space-time description is impossible*, I reject a *limine*. Physics does not consist only of atomic research, science does not consist only of physics, and life does not consist only of science. The aim of atomic research is to fit our empirical knowledge concerning it into our other thinking. *All of this other thinking, so far as it concerns the outer world, is active in space and time. If it cannot be fitted into space and time, then it fails in its whole aim and one does not know what purpose it really serves*".

As it is clear from this quote, E. Schrödinger could not accept Niels Bohr's dialectic point of view, which, in Schrödinger's opinion, was in contradiction with the fundamental principles of the theoretical physics, existing at that time. In this respect, it is interesting to pay attention to the opinion of Paul A. M. Dirac, who in his article "*Reminiscences about a Great Physicist"* (published in 1990) wrote about N. Bohr:" *his arguments were mainly of a qualitative nature, and I was not able to really pinpoint the facts behind them. What I wanted was statements which could be expressed in terms of equations, and Bohr's work very seldom provided such statements*. I am really not sure how much later my work was influenced by these lectures of Bohr's... He certainly did not have a direct influence because *he did not stimulate one to think of new equations*". Probably, due to these reasons many theorists prefer to send this Bohr's observation to oblivion, in spite of fact that Albert Einstein (who is known for his "epoch-making contributions to the progress of natural philosophy") has written about Niels Bohr: "Not often in life has a human being caused me such joy by his mere presence as you did." and "*Nobody knows how the stand of our knowledge about the atom would be without him*. Personally, Bohr is one of the amiable colleagues I have met. *He utters his opinions like one perpetually groping and never like one who believes himself to be in possession of the truth*". These A. Einstein's observations are very close to the opinion of Robert Oppenheimer, who describing the process of great synthesis of atomic physics in 1920s, wrote: "It was a heroic time. It was not the doing of any one man; it involved the collaboration of scores of scientists from many different lands. *But from the first to last the deeply creative, subtle and critical spirit of Niels Bohr guided, restrained, deepened and finally transmuted the enterprise*". The estimate of Niels Bohr contribution by Arnold Sommerfeld is quite similar:"The theory of spectral lines will bear the name of Bohr for all time".

An important feature of N. Bohr's method of investigation was pointed out by W. Heisenberg in "*Physics and Philosophy"* (1958), where he wrote: "The first thing Bohr said to me was that it would only then be profitable to work with him if I understood that he was a dilettante. The only way I knew to react to this

unexpected statement was with a polite smile of disbelief. But evidently Bohr was serious. *He explained how he had to approach every new question from a starting point of total ignorance.* It is perhaps better to say that Bohr's strength lay in his formidable intuition and insight rather than erudition". Isidor I. Rabi in the book "*The Physicists*" (1978) adds to this:" When Bohr is about everything is somehow different. Even the dullest gets a fit of brilliancy". An interesting real episode is described in [1], when "one of Bohr's most faithful and eminent disciples, Weisskopf, who, after having discovered, not without effort, the explanation of a tricky case of complementarity put to him by a doubting experimenter, exclaimed, "*Bohr always wins!*".

Naturally, the conclusion under which conditions the space-time description of material systems is valid and in which cases (in accordance with N. Bohr statement) it is not possible, can be given only by the experiment, and it does not depend on how many prominent physicists supported, or rejected this observation. The presented quotes only emphasize specific features and differences of the points of view of several outstanding scientists on the basic philosophical problems of Physics and can help to elucidate the idea of the comparison of the mentioned philosophical standpoints with the results of the presented experimental studies, which are also supporting A. Einstein's observation about a quite special role of the experiment in the comprehension of the properties of Nature.

Speaking about the progress in high-precision experimental studies of the properties of macroscopic material objects, it is worth noting here that with the development of a new methods of optical length measurements by optical interferometry [3a] and with development of optical interferometers with the resolution below 0.05nm [3b, 3c], we have managed to demonstrate in [3d] the *process of gradual changes of the properties of the parts of the measurement system only as a result of electromagnetic interaction between them*. For example, the plots of Figs. 3 and 4 in [3d] characterize the surface deformations of the mono-crystal reference plate, arising in the wringing contact between the gauge block (GB) and the reference plate [4] as a result of electromagnetic interaction between the atoms of the reference plate and the atoms of the gauge block. In Fig.3 of [3d] we show the topography map of the surface deformations of crystalline plate, arising on the area of the plate surface that is not covered by the wringing contact. This map shows the value of the deformations (induced by the wringing contact) as a function of the location of the specified point of the free area of the plate relative to the position of the center of the wrung gauge block. The inset of Fig.3 presents the plots of the magnitudes of the surface deformations as a function of the time interval, elapsed after the realization of the wringing contact. These data are presented for a couple of points, located symmetrically relative to the GB center. And as it follows from the plots of Figs. 4 and 5 in [3d], the central length of a gauge block [4, 5] is not constant, but presents some function of the time interval elapsed after the realization of the wringing procedure. Besides that, the central length of a GB, the main parameter of a material length standard that is used for the most accurate realization of the Metre [6], is different from the length of a free GB (see Fig.15 in [3e]) as a result of the presence of the surface texture deformations in the wringing contact (see Figs. 12 and 14 in [3e]). Thus, the presented experimental data have clearly demonstrated the existence of the *self-ordering evolution process, when the properties of a material artifact (GB) are gradually changing in time as a result of EM interaction between the two parts of the investigated system (GB and plate)*, and the detection method is based on precise length measurements. But interferometric length measurements are closely related to temperature measurements, and in accordance with [5] temperature contribution gives one half of the total uncertainty of the long GB length measurement. For example, figure 4 in [5] shows that the 500mm GB (8 PTB 63) can be regarded as a very stable thermometer, as its length stability of ~10.6nm for the time period of ~20 years corresponds to the temperature stability of ~90μK/year and with the demonstrated uncertainty in a single measurement series of ~1mK. So, the presented above experimental results give a clear indication that the precise temperature measurements can be used for the detailed studies of the thermal self-ordering evolution process when interaction with the electromagnetic (EM) field is used both as a source of evolution process and also as a detection method of the induced variations of the properties of material objects. In this respect it is worthy of note that in recent years there were important advances in precise, traceable temperature measurements of material artifacts [3e-3h] in the temperature range close to 293.15K (20°C). (And all length measurement results should be reduced exactly to this temperature, in accordance with the established international practice). In [3e], for example, the temperature measurements in a water triple-point (WTP) cell [7a] with the random uncertainty of 1μK were demonstrated that gave the possibility to detect the evolution process in WTP cells, which are nowadays used for the definition of the temperature unit – Kelvin [7a]. In this case, the thermal evolution process manifests itself as a gradual change of the temperature of the standard (see Fig.8 in [3e]). The observed temperature of the WTP cell appears as a function of the time interval, elapsed after the application of the "thermal shock" that makes the ice mantle free [7a] in that temperature standard. When taking this time dependence into consideration and when comparing

the WTP cell temperatures, measured 1 hour after the application to the cell of the "thermal shock", the agreement between the two WTP cells, produced in Brazil and using the isotope composition of equatorial water [7a], was found to be less than 3μK (see Fig.2 in [3f]). Then, the similar approach was applied to the studies of gallium (Ga) standard [7a]: the mean temperature of the last hour of temperature plateau with the total duration of 16 hours in our standard was found to be the most reproducible one, and its time stability on a week interval (characterized by the standard deviation) was found to be about 2μK (see Fig.7 in [3e]), when measured by Rosemount standard platinum resistance thermometer [7a] (SPRT, model 162 CE) and a Guildline bridge (Model 9975), and about 12μK – for the measurements with a thermistor and high-precision Hp multi-meter (see Fig.9) [3g]. But the WTP and gallium standards are the only two standards that are needed to define traceable temperatures on ITS-90 [7a, 7b] close to 20 degrees C... So, when we combine this information with the possibility to perform the calibration of a couple of SPRT in a double-Dewar system within the uncertainty below 10μK (see Figs. 5 and 6 in [3h]) and with the demonstrated time stability of the whole measurement system of ~9.1μK/year (see Fig.1 in [3h]), it is becoming clear that the progress in the reproducibility of the temperature measurements relative to the thermodynamic temperature is about two orders of magnitude, as even the temperature differences between the most complete studies of the primary level constant volume gas thermometers, performed by the groups of R. C. Kemp and D. N. Astrov, are reaching the value of 2.5mK at 250K, and more than 4mK at 200K (see Fig.2 in [8]). So, *there is a unique opportunity to apply in practice N. Bohr's approach of "renovation of the philosophy of science"*[1] *and to check experimentally if the model assumptions and predictions of some well-established physical theories, such as Thermodynamics* [9a, 9b] *or Fourier thermal conduction theory (TCT)* [9c]*, are still in agreement with the new advances of experimental physics in the temperature field*.

Such study is acquiring special importance when we recall A. Einstein's warning, made in his classical paper [10] that "*classical thermodynamics can no longer be looked upon as applicable with precision…For the calculation of the free energy, the energy and the entropy of the boundary surface should also be considered*". And in his earlier paper, entitled "A Theory of the Foundations of Thermodynamics" [3], A. Einstein unambiguously defined the fundamental assumptions of thermodynamics, when writing:" *Let the system be isolated, i.e., the system considered should not interact with other systems*". And also there we find: "*Experience shows that after a certain time an isolated system assumes a state in which no perceptible quantity of the system undergoes any further changes in time; we call this state the stationary state*". So, in accordance with A. Einstein, Thermodynamics deals only with isolated systems, and when all the transient processes have already finished in it. The other very important theoretical observations, fundamental for the understanding of applicability of thermodynamics, can be found in a popular University text-book [9a, 9b], where it is specially emphasized that the basic thermodynamic concept of internal energy is closely related to the theoretical assumptions of adiabatic enclosure [9a] and quasi-static process [9a]. In [9a] it is specially noted that the thermodynamic temperature can be regarded as a function of state, *only if it is assumed* that for quasi-static processes the number of the influence parameters is equal to the number of the parameters, which are used for the description of the system under the thermal equilibrium conditions. In the description of an imaginary experiment (standard for thermodynamic courses), when an ideal gas is located inside the cylinder-piston system with adiabatic isolation [4a], we find the following paragraph on page 48 in [9a]: "In the limiting case of a *quasi-static process*, the internal pressure in gas is equal to the external pressure on the piston. Only under these conditions, the internal state of the gas can be characterized by only two parameters (pressure and volume), and only then the process can occur infinitely slow, passing through consecutive equilibrium conditions. In the opposite case, the motion of the piston occurs with acceleration, so that the different parts of the gas move with *finite velocities* and *for description of the internal state of the gas the infinite number of the parameters will be needed*". Thus, it follows from the university text-book that if the process is not quasi-static, the concept of thermodynamic temperature (as a function of state) loses its validity [9a, 9b]. It is also specially noted in [9a] that the thermal conductivity process presents a typical example when a relatively slow process can not be considered as a quasi-static process. This gives a clear indication that the notion of "temperature" in TCT cannot be associated with the thermodynamic temperature. This assertion also follows, naturally, from the assumptions of thermodynamics, indicated by A. Einstein in [11], as the system in TCT is not closed, and the main subject of TCT is the description of the transient process in that system. Unfortunately, in theoretical Physics there is no other definition of temperature except the thermodynamic one.

For the future comparison of the results of our experiments with theory, it is relevant to remind one important observation in [12], dealing with TCT. In the first chapters of this thick text-book, the authors find it necessary to attract the readers attention that the thermal conduction theory, describing the transient processes, is actually based on the result of a *single, one dimensional, steady-state experiment*, with the help

of which the heat flux density in a material artifact is related to the temperature gradient inside the artifact. This remark gives an indication that, most probably, already at that time some discrepancies between TCT and experiments were known. Evidently, only new precise experiments can help to establish the relations between the concept of thermodynamic temperature and the notion of "experimental" temperature, which presents a measure of the thermal energy in a specified part of a material artifact and which has been used by mankind for centuries.

In this paper, using the variation principle (the most general in experimental Physics) we demonstrate the existence of thermal surface energy (TSE). TSE is shown to present the energy of the oriented motion of charged particles inside a solid-state artifact and the energy of the guided electromagnetic (EM) field, which is propagating along the material artifact and which is always accompanying a non-uniform motion of charged particles [13a, 14a]. It is shown that TSE arises when there is an input of the thermal energy (positive or negative) to the system, and the main parameters of TSE (its magnitude and the direction of its increase) *are defined by the vector quantity* – the Poynting vector of the external EM field, which is produced by an external heat source and the material objects, surrounding the system. So, on one hand, we can say that TSE appears as a result of the EM field pressure [9g] and the specific features of the propagation of the wave momentum [15] (describing the coupled field-particle system [15]) in the vicinity of the boundary of the material artifact. On the other hand, we can also say that the TSE presents a new form of the fundamental collective R. Dicke effect [16], which is known to be related to the interaction of EM field with an ensemble of charged particles [17-19]. In the particular case of the system under consideration, the collective effect corresponds to very low levels of excitation of atomic system [18, 19], when as a result of the effect of trapping of EM radiation in the atomic system, the number of particles in the ensemble becomes a crucial parameter in the description of interaction in the field-particle system [17-19].

The most important results of this study are the following. First, it is experimentally shown that TSE, produced by the Poynting vector of the external heat source, results in the thermal hysteresis effect, which (as the other well-known hysteresis effects [9d, 9e]) is irreversible in time and has no spatial symmetry [9d, 9e]. Second, with very high signal-to-noise ratio it is demonstrated that *the principle of superposition is not valid for TSE*, so that all material artifacts in the presence of a single heat source are found to be in continuous, ever-lasting, non-linear interaction with each other and with the heat source through continuous radiation of EM field, just as a consequence of the existence of the TSE. The main properties of the interaction of EM field with material artifacts –the presence of the hysteresis effect, or the memory about the pre-history of the system, and the non-linearity of the coupled field –particle system, manifesting itself as the violation of the superposition principle for EM fields, lead to the "self-ordering" evolution process, in which the parameters and properties of each interacting artifact are gradually changing in response to the variations of the resulting EM field, which is produced by all interacting material artifacts. Among the gradually changing parameters and properties of the artifact it is possible to mention some quite general such as the length of an artifact and its aging, as well as some specific ones (such as variations in time and in space of stresses and deformations inside an artifact, particle mass transfer inside it, variations in time and in space of the total-energy density [15] and of the energy flux density [15] of the coupled field-particle system inside the material). The key features of the thermal evolution process are that *the properties of the artifact are specific for any particular point inside the artifact, as well as for the specific time moment*, and *the number of influence parameters, necessary for the description of the evolution process, is absolutely enormous* under the achieved accuracy level of the experimental studies. When speaking about the general case, we are to note first that the number of material objects, interacting through EM in the Universe, (or the number of influence factors) can be considered as infinite. Second, all of these objects are interacting with the common EM field, which is produced by these objects during the whole precedent time up to the moment of the performance of the particular measurement, and consequently, *all these influence factors are, at least, partially correlated and cannot be regarded as independent ones*. Third, the interaction between the material objects in the evolution process of system depends on the pre-history of each partner, or each object exhibits its specific hysteresis effect. Fourth, in the process of the EM interaction of the objects of the system with external partners, some of these partners can appear as new ones (with basically new physical properties) and some can disappear. Under these conditions, it should be clear that in the general case, the description of any material system, which always depends on the infinite number of correlated variables and which is always under the continuous evolution process, in terms of the existing mathematical tools is not possible. Thus, the *presented experimental studies give a definite indication of the validity of the fundamental philosophical observation of Niels Bohr that the space-time description of material systems in the general case is impossible*. The presented experiments also give the answer to the cited above Erwin Schrödinger's "other thinking" and to his claim: "The aim of atomic research is to fit our empirical knowledge concerning it *into our other thinking*. *All of this other thinking, so far as it concerns the outer world, is active in space and time. If it cannot be fitted into space and time, then it fails in its*

whole aim and one does not know what purpose it really serves".

Among the other fundamental results of this study is the demonstration that the basic assumption of the Fourier TCT that the thermal energy flux in material is determined only by the temperature gradient in it (which was borrowed from the existing at that time experimental physics) is not valid in the general case. It is only *approximately valid* in case of the fixed stationary conditions, when all the transients are finished in the system. Besides that, it follows from the study that *the precise knowledge of the temperature distribution on the surface of a material artifact at some fixed time instant,* which is used in formulation of TCT, *is impossible to realize experimentally in principle*. So, that the TCT can be regarded as some illustration of the A. Einstein observation that "when the laws of mathematics … are certain, they do not refer to reality".

Dealing with the thermodynamics, it is shown experimentally that the concepts of isolated system and of adiabatic enclosure can be treated only as unrealistic theoretical assumptions, which are in contradiction with numerous experimental observations in astronomy, biology (including molecular biology) and zoology. The ideas of the adiabatic enclosure and of the isolated system are in disagreement with the well-known experimental facts that the thermal EM radiation covers the whole spectrum of energies [2d] and all the materials are becoming relatively transparent at high enough frequencies [9g, 9h], so that from the university physics course we can find that the concept of thermodynamic temperature is not appropriate for plasma physics [9a], for example, where adiabatic enclosures do not exist in any approximation [9a]. For precise temperature measurements, achieved nowadays, the concept of thermodynamic temperature as a function of state is obsolete, and must be substituted by the more general concept of *temperature, which includes the energy of the oriented motion of the coupled field-particle system that can be detected through the radiated EM field by different types of thermometers*. Here, thermometers represent the devices, which effectively absorb the propagating EM field and which convert the oriented field propagation into the random motion of the particles of "thermometric fluid", by changing the resistance in SPRT [7b], for example, and simultaneously transferring the corresponding field impulse to the material surrounding.

It is also shown experimentally (see Fig.11) that that with the existing experimental tools the thermal evolution process can be detected during the time interval of a couple of minutes. It means that the wave momentum density and total-energy density inside the block [15] cannot be regarded as conserved quantities after that time interval.

II. Experiment

a) Experimental demonstration of thermal surface energy and of the asymmetry in space of the thermal evolution process

The main features of our experimental set-up, in which a 100-mm gauge block (GB) is located horizontally on three polished spheres inside a closed Dewar system, can be understood from the inset of Fig.1. The measurement system is located inside a laboratory with precise air temperature control with typical diurnal variations of about 50mK. Two thermistors R6 and R3, equipped with copper adapters covering the whole width of the GB, are located on one of the side surfaces of the GB. Thermistors are, practically, identical and are installed parallel to the gauging surfaces of the GB (Fig.1). A 100-Ohm platinum resistance thermometer (PRT), also equipped with a copper adapter, is located parallel to the adapters of the thermistors at exactly equal distances from them. We use a newly developed multi-channel synchronous detection technique (MSDT) [3f] to measure simultaneously, with high precision the variations of temperatures in the thermistor channels that are induced by the periodic modulation of the current in the PRT. Synchronous measurements of temperatures and of thermal velocities, available from all three thermometers, are realized by the program whose print-screen for the duration of 1.4 period of the modulation cycle is presented in Fig.1. The duration of the cycle is ~140 minutes. One fourth of the cycle duration, the PRT current is kept at the level of 5mA (heating period), and for the left part of the modulation cycle the current is equal to 1mA (cooling period). The PRT is connected to a programmed, high-precision DC bridge Mi-T615 (Canada), so that the accurate temperature measurements of the PRT during the whole modulation cycle are available. Meanwhile, the thermistors R6 and R3 (belonging to channels 1 and 2, respectively) are connected to precision multi-meters HP-3450A, so that synchronous differential temperature measurements between the channels 1 and 2 with the resolution of 1-2μK for the time duration of a few minutes can be achieved thanks to high sensitivity of the thermistors relative to PRT. The record in Fig.1 with a faster response time corresponds to the measured variations of the PRT resistance during the modulation cycle. The two other traces show the variations of the resistances of the thermistors, which have negative thermal coefficients. As a consequence of the used geometry, the system is extremely sensitive to any asymmetry in heat fluxes along the surface of the GB in the direction of the longest side of the GB. The key feature of the experiment is that both thermistors are calibrated to measure the temperature of the artifact surface in the close vicinity of its adapter [3i].

With the two cursors of the program (shown in Fig.1 as triangles), we specify the desired part of the record, and the program calculates the mean values of the temperature and of the temperature rate in each channel, using the calibration equations (temperature versus resistance) for each channel that are in advance stored in the program. In two separate windows, the program displays the initial and final moments of the measurement time interval that are defined by the position of the cursors on X-axis of the record. The larger window of the program shows the mean values of the temperature and of the temperature rate, obtained in one of the channels during the specified measurement time interval. The information about the results of the measurements in all of the channels for the sequence of the desired time intervals is written by the same program in a special file. These files contain the data of synchronous differential temperature measurements between the channels 1 and 2 as a function of time. As this information can be presented separately for high and low levels of the modulation current in the PRT, it can be processed using the MSD technique [3f. 3i]. The plots in Figs. 2, 4, 6 of this paper present the examples of the application of the MSD technique to the data of such files. The procedure of the calibration of the PRT and thermistors is described in detail in [3i, 3f] and the application of the MSD technique is outlined in [3h]. Here, we note that the records of Fig.1 correspond to measurements on a steel block with 10-mm separations between the adapters of the thermistors and the adapter of the PRT. The axis of thermistor R6 is located at the distance 4.5mm from the nearest gauging surface. In this case, one of the side surfaces of the thermistor adapter lies in the plane of the gauging surface of the block.

An observation of a paramount importance can be inferred already from the plots of Fig.1: though the separations of thermistors from the heat source are the same, the *induced temperature variations in the thermistor channels are different.* This means that the thermal transfer process is not symmetric in space, similar to the build-up processes of domains in ferromagnetic [4d] or ferroelectric materials [4e] under the application of the external fields. This also means that the basic assumption of the Fourier TCT, defining the energy flux in the material, is in contradiction with the experimental results obtained by the variation principle, the most general and powerful in experimental Physics. This will be demonstrated in detail, with extremely high signal-to-noise ratio when using the MSD technique. But this can be clearly observed even from the unprocessed results of the measurements of Fig.1. Indeed, from the corresponding temperature measurement results of Fig.1 we find that for the last 30 minutes of the cooling part of the cycle at I=1mA, which is presented first in this figure, the mean temperature, recorded by the thermistor R6, was 466μK higher than the mean temperature, obtained from the thermistor R3. For the second modulation cycle, which is shown completely in Fig.1 and which is marked by two cursors, this temperature difference **T[1,2]** was about 469μK.Thus, the stability in time of the reference points in Fig.1 was within 4μK. And it is important to realize that the temperature of the gauge block in the vicinity of the thermistor R6 *was higher* than the temperature of the block in the vicinity of the thermistor R3 for all reference points. And in contrast to the basic approximation of the TCT theory, it follows from Fig.1 that when the current in the PRT was increased to 5mA, the *flux of thermal energy to the unit volumes of the artifact in the vicinity of the R6 thermistor* (having already higher temperature) *was larger than the energy flux to the unit volumes in the vicinity of the R3 thermistor*, as the temperature rate, recorded by thermistor R6, was definitely larger than the temperature rate, recorded by thermistor R3!

In future, the mean temperature difference between the channels 1 and 2, recorded for the last 30 minutes of the cooling period (at I=1mA), we shall denote by the quantity **T[1,2]**. And all the data points, corresponding to the last 30 minutes of the cooling part of the modulation cycle, we shall call *the reference points*.

Now, the plot of Fig.2 will be used for illustrations of the application of the MSD technique. Here, the experimental conditions are the same as the ones in Fig.1. In Fig.2, the reference points are marked with rectangles. The averaging time for the reference points is chosen to be 5, or 10 minutes. All of these reference points are used to generate the linear fit, which is shown as a solid line and which is very close to abscissa axis. The equation of this fit is presented in Fig.2 in a separate text box. From this equation we find that for the initial time of the record (X=350min.) the fit value is -0.02μK, while for the end of the record (X=480 min.) it gives the value of 0.11μK. So, all the values of the reference function, given by the fit equation and representing the systematic offsets, are below ±0.15μK for the whole time interval of this observation. The random spread of the data points relative to this fit is also very small: a standard deviation of a single reference point relative to the linear fit is less than 3μK.

Using this fit as a reference, we can determine very precisely the difference between the simultaneous measurements of temperatures, realized by the channels 1 and 2 during the modulation cycle. This temperature difference, which is measured relative to the fit to the reference points, is denoted here by the quantity **ΔT[1,2]**. The experimental points of Fig.2, represented by dots, demonstrate the time dependence of the difference in the temperatures of the channels 1 and 2, when *these temperature variations are induced by the increased value of the PRT current* (I=5mA) *during the heating period of the modulation cycle*. The

measurement time intervals are 2 and 4 minutes at the beginning and at the end of the heating period of the cycle, respectively. It follows from Fig.2 that for all data points of the heating period the quantity **ΔT[1,2]** is positive, and the maximum value of **ΔT[1,2]** is surpassing by orders the uncertainty of the reference values. For example, the maximum value of the quantity **ΔT[1,2]** in Fig.2 is equal to 2620±3μK, while the systematic offset of the reference function is within ±0.15μK and the standard deviation of a single reference point is below 3μK.

It should be specially emphasized that the induced temperature difference **ΔT[1,2]** *is a vector quantity*. Its positive value indicates that the amount of thermal energy, delivered from the PRT during the heating period of the cycle to the elementary (unit) volume of the material artifact in the vicinity of the thermistor R6, is larger than the corresponding amount of the thermal energy, delivered to the elementary (unit) volume of the artifact in the vicinity of the thermistor R3. Thus, this experiment has given a first clear demonstration that, in spite of the fact that the thermistors are located on the surface of homogeneous artifact at the same distance from the heat source, the time averaged value of the heat flux of the thermal energy to the elementary volumes of the GB material, located in the vicinity of the nearest gauging surface of the artifact, is substantially higher than the time averaged value of the energy flux to the elementary volumes, located symmetrically relative to the heat source in the bulk material away from the gauging surface. We are to remind here that thermistor R6 is located closer to the gauging surface of the block, and we are analyzing the reaction of the system during the heating period of the modulation cycle when there is a positive net input of energy to the artifact. Thus, from Fig.2 it follows that *the larger average flux of thermal energy to the elementary volumes in the vicinity of the R6 thermistor occurs when for all time intervals of the heating period, the temperature difference between the PRT and R6 is smaller than the difference between the PRT and R3*. Naturally in this case, the projections of temperature gradients along the longer axis of the GB in the direction of the thermistor R6 were definitely smaller than the corresponding projections of the temperature gradients in the direction of the thermistor R3. So, we can infer from Figs. 1 and 2 that *at the initial stages of the heat transfer process there is an additional flux of thermal energy to the elementary volumes of the artifact in the vicinity of its boundary surface, which cannot be related to the thermal gradients in the artifact, as it supposed in TCT*.

Naturally, we can plot the induced temperature variations **ΔT[1,2]**, which are induced by the current switch from 5mA to 1mA. Such points for the cooling period of the cycle are shown by rhombi. It can be also inferred from Fig.2 that the excessive thermal energy, which is stored in the vicinity of the gauging surface close to the thermistor R6 during the relatively short part of the heating period of the cycle, is distributed over the whole length of the block, practically homogeneously, at the end of the cooling period of the modulation cycle.

To demonstrate in more detail the main properties of the heat propagation process at its early stages and to find the physical reason for the excessive energy flux, we studied experimentally the variations of the thermal velocities **ΔV[R6]** and **ΔV[R3]**, which were induced by 5mA current and were recorded simultaneously by both thermistors. Thus, this part of our study deals with *synchronous differential thermal velocity measurements*. Here, the mean values of the temperature velocities for both channels **(V[R6]** and **V[R3])** for any desired time interval can be found in the way similar to the measurement of the mean values of temperatures. For this it is necessary to specify the desired time interval with the two cursers of the program and to select the appropriate channel. Then the mean value of the thermal velocity will be found in the window of the program (Fig.1) together with the mean temperature value. Both calculations are performed by the program, using the experimentally obtained calibration equations for the responses of the thermistors that have been measured on the GB surface under the analogous external conditions [3i, 3f].

The velocity dependence for the thermistor R6 as a function of the measurement time for two modulations cycles (under the experimental conditions of Fig.1) are presented in Fig.3a. Dots correspond to the heating period of the modulation cycle, while rhombi show the measured values of the thermal velocity for the cooling period of the cycle. The data points for the last 30 minutes of the cooling period, where the slope of the experimental curve is already relatively small, are used as reference points. These points in Fig.3a are shown as rectangles. For all of the reference points of our experiment, with the duration of 16 hours, we find 6-th order polynomial fit using the least squares criteria. The corresponding curve of the fit is shown as a solid line in Fig.3a.

The velocity variations **ΔV[R6]**, which are induced by the switch of the PRT current from 1mA to 5mA and then back from 5ma to 1mA, are calculated as a difference between the measured values of the thermal velocity in the channel at a specified time and the value of the reference function at the same time. As it follows from Fig.3a, the values of the induced velocity **ΔV[R6]** are quite reproducible. For example, the mean maximum value of the quantity **ΔV[R6]**, averaged over the two cycles presented in Fig.3a, is 1686μK/min. Meanwhile, the scatter of the maximum values, recorded in both cycles relative to the mean value is within ±9μK/min. This scatter can be hardly seen in Fig.3a, as

it is much smaller than the dimensions of the data-points, used in the figure. The time averaging, which is used in the detection of the maximum of the curve in Fig.3a, is only 1 minute. But as a result of the use of the sensitive thermistors, the random uncertainty of the measurements, corresponding to 1 minute averaging time, is quite negligible in comparison with the dimensions of the data-points and does not affect, practically, the position of the points. It should be specially emphasized here that the slow drifts, which are typical for thermistors, are removed, practically completely, in MSD technique by the use of the reference fit, which establishes the recalibration of the thermistors sensitivities every cycle during the time interval, devoted to the measurement of the reference data-points.

The corresponding dependence of the quantity **ΔV[R6]**, which is averaged over the two cycles of Fig.3a, is presented in Fig.3b. Here again, the dots correspond to the heating period of the modulation cycle, and the rhombi show the obtained values of the thermal velocity **ΔV[R6]** for the cooling period of the cycle. The standard deviation of the reference points in Fig.3b relative to the fit is ~10.4μK/minute, and it shows that some systematic cooling of the system at the end of the cooling period of the modulation cycle is still observed. But as the maximum value of the quantity **ΔV[R6]** is ~1686μK/minute, it is clear that the measurements of the induced variations of the thermal velocities in this experiment are still performed with huge signal-to-noise ratios.

To demonstrate clearly the fundamental effect of the spatial asymmetry in the delivery of the thermal power to the elementary volumes, located at the same distance from the heat source on a rectangular block, made of homogeneous material, in Fig.3b we present also the induced velocity variations **ΔV[R3]**, corresponding to the simultaneously measured values in the other channel. For this dependence, the heating period of the cycle is shown by triangles, and the cooling period is presented by circles. Similar to the dependence **ΔV[R6]**, the maximum value of the induced velocity **ΔV[R3]** is observed, approximately, 2.5minutes after the increase of the modulation current in the PRT. But the value of **ΔV[R3]**, averaged over the same modulation cycles, is only about 1172μK/minute, instead of ~1686μK/minute in the other channel. It also follows from Fig.3b that the excessive energy flux to the elementary volumes in the vicinity of thermistor R6 is obtained during the first 15-20 minutes of the heating period of the modulation cycle, and for the rest time interval of the heating period, the induced variations of the thermal velocities in both channels are, practically, equal. In the explicit way, this statement follows from the plot of Fig.3c, where the difference between the quantities **ΔV[R6]** and **ΔV[R3]**, denoted by the quantity **ΔV[1,2]** is presented. From the plots of Figs.1 and 3b it follows that for the last 30-40 minutes of the cooling period of the modulation cycle, the differences **V[1,2]** between the measured values of thermal velocities **V[R6]** and **V[R3]** are usually within 1μK/minute, and the quantity **V[1,2]** for these points can be used as a reference points (rectangles in Fig.3c), relative to which the induced variations **ΔV[1,2]** could be very precisely determined. In this case we can use even a simple linear fit. The equation of this fit, corresponding to the reference points, averaged over two modulation cycles, is presented in the text box of Fig.3c. From the presented fit equation, we can infer that for the time interval between 360 and 440 minutes, the value of the reference function stays in the range of 0.26-0.31 μK/minute. So, for the differential thermal velocity measurements, the contribution to the error budget due to the possible choice of the reference function is, practically, equal to zero. It also means that practically the same results for the quantity **ΔV[1,2]** can be obtained by using the linear fit in Fig.3c, or by finding the differences between the quantities **ΔV[R6]** and **ΔV[R3]** (Fig.3b), calculated with the help of the 6-th order polynomial fits to the reference points in all modulation cycles of a whole measurement series. This is the consequence of a proper choices of the length of the modulation cycle and of the length of its cooling period, so that the mean thermal velocities, recorded by both channels, for the last 30 minutes of the cooling cycle coincide with each other to within a small fraction of 1μK/minute. This observation is supported by the experimental result that the standard deviation of the reference points relative to the linear fit in Fig.3c (that describes the uncertainty of the determination of a single reference point) is equal to 0.83μK/minute. So, the total uncertainty of a single measurement in Fig.3c is by orders of magnitude smaller than the maximum value of the difference in thermal velocities in the channels 1 and 2, which is induced by the variations of the PRT current.

It is also worth reminding here that the difference in thermal velocities **ΔV[1,2]**, presented in Fig.3c, is also a vector quantity, as it carries the information about the direction along the axis of the block between the positions of thermistors R3 and R6. For example, the positive value of **ΔV[1,2]** means that during the heating period of the modulation cycle (presented by dots in Fig.3c) *the thermal power*, delivered to the elementary volume of the artifact material in the vicinity of R6 thermistor, is larger than the thermal power, delivered to the corresponding volume of the artifact in the R3 vicinity. For the cooling period of the cycle, which is shown in Fig.3c by rhombi, the losses of thermal power from the elementary volumes in the vicinity of the R6 thermistor occur faster than from the elementary volumes, located at the same distance

from the heat source but in the direction of the bulk material away, from the gauging surface.

The physical meaning of the thermal power, recorded by thermometers, can be clarified from the basic Poynting theorem of classical electrodynamics [13a, 14b, 15]. In accordance with the integral form of Poynting theorem of classical electrodynamics [13a, 14b, 15], representing the continuity equation for the energy density and for the energy current density of EM field (or Poynting vector, see Eq. (2.13) in [15]), we find: the rate of the change in time of the electromagnetic energy within an artifact volume, plus the time rate of the total work, done by EM fields on charged particles within the artifact volume, are equal to the quantity of EM energy, which is delivered inside the artifact per unit time through its boundary surface by the Poynting vector of EM field [13a]. The differential form of this theorem states that the rate of the change of the total-energy density, written for the particle-field system within the artifact [15], is defined by the divergence of the total-energy current density (see Eq. (2.14), (2.18) in [15]). In other words, *the total power delivered to the elementary volume (dx dy dz), is defined by the total-energy flux of the coupled field-particle system [15] that is delivered inside to this elementary volume through its boundary surface*. So, the results of experiments in Fig.3c give a clear indication that the difference in thermal powers (i.e. the difference in the time derivatives of the total field-particle energies that is recorded by the two channels) is the consequence of the additional, systematic flux of energy to the volumes in the vicinity of the gauging surface (nearest to the heat source) relative to the volumes, which are located at the same distance from the heat source but in the opposite direction, away from the boundary of the artifact. From our experiments it can be also inferred (see below) that this additional total-energy current density, arises as a result of the reflection of the propagating wave momentum of the field-particle system from the gauging surface of the artifact, so that the reflected part of the field-particle system results in the appearance of the wave momentum [8] and the total-energy current densities [8], propagating some (relatively small) distance in the direction of the heat source.

It is also clearly seen from the plot of Fig.3c that this additional energy flux does exist only during a short, initial time of the heating period of the modulation cycle, but the additional thermal energy (see Fig.2) is stored in the vicinity of the boundary during the whole heating period. Besides that, the comparison of the dependences on time of the quantity **ΔV[1,2]** for the heating and for the cooling periods of the modulation cycle shows that the excessive heating of the elementary volumes in the vicinity of the R6 thermistor, which is observed for the time interval of about 20 minutes after the switch of the current in the PRT from 1mA to 5mA, is followed by the excessive cooling of the same elementary volumes during approximately the same time interval after the current switch from 5mA to 1mA. The effect changes the sign, but the magnitudes and the dependences on time of the corresponding parts of the process (presented in Fig.3c) are quite similar. The analysis of the numerical results of the measurements, presented in Fig.3c, indicates that for the cooling period of the cycle, after 25 minutes from the current switch in the PRT from 5mA to 1mA the possible deviations of the quantity **ΔV[1,2]** stays within ±2μK/minute. It means that after 25 minutes from the indicated current switch, the cooling processes in the parts of the artifact, located symmetrically relative to the heat source, are becoming, practically, identical, while at the beginning of the cooling period the difference between them exceeds 500μK/minute, in absolute value.

A somewhat different point of view on the results of Fig.3c, which will be used later in this paper, is based on the observation that the quantity **ΔV[1,2]** deals with the differential velocity measurements and also carries the information about the direction along the axis of symmetry of the GB. So, instead of the excessive cooling of the elementary volumes in the vicinity of R6 thermistor after the current switch in the PRT from 5mA to 1mA, we can interpret the same results as a relative excessive heating of the elementary volumes in the vicinity of the thermistor R3. And as the differences between the absolute values of the curves, presented by the dots and by rhombi in Fig.3c, are very small, we can say that during the heating period of the modulation cycle some excessive flux of energy is propagating from the heat source to the elementary volumes, located in the vicinity of the thermistor R6 close to the gauging surface. Meanwhile during the cooling period of the cycle, practically, the same amount of the flux of energy is propagating in the opposite direction from the heat source to the elementary volumes, which are located symmetrically relative to the heat source in the bulk material, in the vicinity of the thermistor R3. Thus, from the results of the studies, presented in Figs. 2 and 3, we can conclude that during the heating period, some excessive thermal energy is stored in the vicinity of the boundary (Fig.2, dots) as a result of a relatively short flux of energy (Fig.3c, dots), while by the end of the cooling period, the thermal energy is distributed almost homogeneously along the surface of the artifact (Fig.2, squares) as a result of a short energy flux (Fig.3c, rhombi), propagating in the opposite direction. Thus, *the positive quantities **ΔT[1,2]** and **ΔV[1,2]**, observed at the beginning of the heating period of the modulation cycle, directly indicate to the existence of the thermal surface energy (TSE), which can be reliably detected by the synchronous differential thermal measurements*.

The other important observation deals with statement that the propagating flux of energy in a material with absorption is always related to the force

density, acting on the material objects inside the elementary volume [15, 9h]. So, during a single modulation cycle, a variable in direction force is acting alternatively in two spatial regions of the artifact, located symmetrically relative to the source of EM field. In this our experimental situation is quite similar to the case of the hysteresis effect in Ferro-electric samples [9e], when the process of the build-up of the sample polarization is observed in the electric field of constant magnitude, but when the field direction is periodically changing in time to the opposite one. In the latter case, every time after the switch of the direction of the electric field, there appears a variable in time force, acting on the elementary volume inside the domain structure, as the domains are polarized predominantly in the direction of the previously existing electrical field. And then, the process of the change of the polarization of the medium starts (as a result of the re-orientation of the domain dipole moments in the new direction of the external electrical field [9e]) that inevitably changes the force, acting on the elementary volume. Thus, the observation method of the hysteresis loop in Ferro-electrics shows the way how to present the hysteresis loop in case the thermal hysteresis effect. Instead of presenting the experimental points as a continuous sweep in time (Fig.2), it is necessary to present the points in two separate time sequences (see Fig.7 below), which correspond to the two directions of the variable forces, acting on two spatially different parts of the system.

But first, we want to present another type of experiment, which unambiguously shows that the quantities **ΔT[1,2]** and **ΔV[1,2]** describe the thermal surface energy (TSE) by demonstration that the amplitudes of both quantities fall rapidly with the increase of the separation of the thermistor R6 from the gauging surface of the block. Thus, the effects, described in this paper, can be observed only when one of the thermistors is located close to the boundary of the artifact. The other result of paramount importance is the *experimental demonstration that the thermal evolution process, in the general case, is characterized by the spatial asymmetry*.

To prove this, we performed a special experiment, in which our measuring system, which included the PRT and both thermistors, was moved as a whole away from the gauging surface of the steel GB in two equal steps of 4.5mm, each. The separations between the surfaces of the PRT adapter and the corresponding surfaces of the adapters of thermistors were equal to 10 mm. They were installed with the help of a 10mm GB with very high precision. The magnitudes of the quantities **ΔT[1,2]** and $\mathbf{\Delta V[1,2]_{max}}$ for the heating period of the cycle are presented in Figs. 4a and 4b as a functions of the separation of the axis of the thermistor R6 from the nearest gauging surface of the block, which will be denoted here by Z. In Fig.4a, the vector quantity **ΔT[1,2]** corresponds to the magnitude of the surface energy, observed 13 minutes after the increase of the modulation current in the PRT. Here, the experimental points, corresponding to the Z-values of 4.5mm, 9mm, 13.5mm and 22mm, are shown as dots. The left data-point in Fig.4a (with the value Z=4.5mm) corresponds to the case when one of the side surfaces of the R6 adaptor lies in the plane of the gauging surface of the block. For this point, the experimental conditions correspond to the plots of Figs. 1-3, and the surface energy, characterized by the quantity **ΔT[1,2]**, has it maximum value. The right data-point (with the value Z=22mm) corresponds to the symmetric position of the PRT on the side surface of the block. For this point, the magnitude of the quantity **ΔT[1,2]** is becoming vanishingly small, as for the larger values of Z the quantity **ΔT[1,2]** is becoming negative: in this case the thermistor R3 is becoming closer to the opposite gauging surface of the block, and so, the quantity **ΔT[1,2]** changes the sign.

The part of the experimental curve in Fig.4a, corresponding to R6 axis distances less than 14mm, can be approximated by the Gaussian curve $\exp(-(z-z_o)^2/2\sigma^2)$, where z is the distance of the R6 axis from the gauging surface; z_o is an adjustable parameter (with the value of about 4.43mm), which corresponds to the maximum of the experimental dependence (shown as a solid line in Fig.4a) and takes into account the finite width of the R6 adapter; σ is the sigma value of the Gaussian curve, measured in mm. For the adopted type of the exponential fit, the value of the parameter σ, which describes the characteristic length of decrease of the **ΔT[1,2]** magnitude with the increase of the distance from the boundary, is estimated to be about 9.06mm. The corresponding plot of the Gaussian curve, with appropriate magnitude and with the sigma value of 9.06mm, is presented in Fig.4a with rhombi. It covers the Z-values from Z=4.5mm to the σ-value of the curve, representing the magnitude dependence of the Gaussian curve from its maximum to the relative value of 0.606. As it follows from Fig.4a, the thermal surface energy, characterized by the quantity **ΔT[1,2]**, falls very rapidly with the increase of the distance from the boundary, and so the term “surface” is quite appropriate in this case.

The corresponding dependence of the maximum value of the quantity **ΔV[1,2]** (which is clearly observed on the plot of Fig.3c) on the distance of the thermistor R6 from the gauging surface is shown in Fig.4b. Here, the left data-point corresponds to the experimental conditions of Fig.3c. The solid line in Fig4b is connecting all 4 experimental points, covering Z values in the range from 4.5mm to 22mm. The maximum values of the quantity **ΔV[1,2]** in Fig.4b (denoted here as $\mathbf{\Delta V[1,2]_{max}}$) were found from the plots analogous to the one of Fig.3c, but measured in the experiments with

larger values of the separation of the thermistor R6 from the gauging surface. The experimental dependence of Fig.4b can also be accurately approximated by the Gaussian curve from its maximum value to the relative amplitude of 0.606 (which corresponds to 1σ level of the abscissa variable of the Gaussian curve). The approximating part of the Gaussian curve is shown in Fig.4b by rhombi for the relative magnitudes from 1 to 0,606, and by open squares for the abscissa variable beyond 1σ level, i.e. for the R6 separation values in the range of 12-14 mm. The agreement between the fit and the experimental points, lying within 1σ range, is below 1μK/minute. Even for the point with Z-value equal to 13mm (where systematic differences are becoming already important), the difference is 3.3μK/minute. Here, it should be taken into account that the indicated value of the difference presents less than 1.3% of the measured quantity $\Delta V[1,2]_{max}$ at this point.

The other important observation concerns the widths of the curves in Figs. 4a and 4b. They are not equal. The width of the curve $\Delta V[1,2]_{max}$ in Fig.4b is smaller. This result can be immediately obtained from the comparison of the solid curves in these figures. In Fig.4b the experimental points describes a larger part of the corresponding Gaussian curve than the data-points in Fig.4a, corresponding to the same Z-values. The smaller width of the curve $\Delta V[1,2]_{max}$ means that the energy flux, described by this quantity, falls faster with the R6 separation value from the boundary than the quantity $\Delta T[1,2]_{max}$. A quantitative description of the widths of the experimental curves in Figs. 4a and 4b can be obtained from the Gaussian approximations of these curves. In Fig.4b the corresponding σ-value is equal to 7.7mm, which is substantially smaller than the σ-value in Fig.4a (9.06mm). The same conclusion will follow from the other experiment, which will be presented at the end of this section.

In Fig. 4a, the magnitude of *the surface energy is presented as a function of the separation Z* of the thermistor R6 from the gauging surface for the fixed value of the time interval after the increase of the modulation current in the PRT. Naturally, this plot has to be complemented by the experimental dependences of *the surface energy as a function of the elapsed time* after the current increase for several fixed values of the separation Z. The corresponding dependences are shown in Fig.4c. The dependence 1 (dots) corresponds to the Z value of 4.5mm, the curve 2 (rhombi) corresponds to Z=9.5mm and the curve 3 (squares) – to Z=13.5mm. If we compare the values of the surface energy obtained for the time intervals of 3 minute and 13 minutes, we shall see that the ratio of magnitudes for the curve 3 is 0.183, for the curve 2 it is equal to 0.299 and for the curve 3, corresponding to the smallest separation of the thermistor R6 from the gauging surface (boundary of the block), it has the maximum value of 0.342. It means that *not only the magnitude of the surface energy depends on the observation point*, but *the form of the time dependence varies with the change of the observation point*. The decrease of the ratio of the surface energy, observed at fixed time interval (3 minutes) relative to its maximum value, achieved in the experiment, gives a direct indication that the excessive energy flux, responsible for the creation of the thermal surface energy, arrives later to the distances with larger separations from the gauging surface. Consequently, this experiment supports the idea that the excessive energy flux arises as a result of the reflection of the momentum of the coupled field-particle system from the boundary of the artifact. The other fundamental result is that *the thermal evolution process*, arising due to interaction of the external EM field with the ensemble of atoms in a solid-state artifact, *is characterized by the amplitude, depending on the observation point on the artifact surface, and is also characterized by the specific time dependence (or time scale), which is characteristic only for a particular observation point.* As the philosophers claim nowadays, the time and the space concepts are relational ones (see further in Discussions).

The other very important property of the vector quantities $\Delta T[1,2]$ and $\Delta V[1,2]$ *is the lack of spatial symmetry*. As theses quantities carry the information about the relative positions of the thermistors, they are to have the asymmetric properties, relative to the center of the larger side surface of the block on which all the thermometers are located. This property follows from the third type of experiments whose results are presented in Figs. 5a-5c. In these experiments we used a 100-mm tungsten carbide (TC) GB, in order to demonstrate also the effect of material properties on the time dependence and on the magnitude of the thermal surface energy (TSE). So, in Fig.5a we present two curves, representing the dependences of the TSE on the time interval after the increase of the modulation current in the PRT and corresponding to two limiting cases. The first curve, marked by squares, corresponds to the external experimental conditions similar to the conditions of Fig.2, and when the axis of the R6 thermistor is located at Z=4.5mm from the nearest gauging surface. The comparison of the corresponding plots on Figs. 2 and 5a shows that the magnitude of the TSE, characterized by quantity $\Delta T[1,2]_{max}$, has dropped for the TC block (in comparison with the steel artifact) by, approximately, 3 times. It is also clearly seen from these figures that the process for the surface energy build-up is about 3 times faster in the TC block relative to the steel block, having exactly the same form and dimensions.

The second curve in Fig.5a, marked with dots, corresponds to the case when the system of thermometers was shifted as a whole to the opposite gauging surface of the block, so that the separation of

the thermistor R3 was at the distance Z=4.5mm from the other gauging surface. Both curves 1 and 2 in the figure are reaching the maximum values at the same time (7minutes) after the increase of the PRT current, and the magnitudes of the curves are quite symmetrically located relative to the abscissa axis of the plot. The difference between the curves is that the signs of the quantities **ΔT[1,2]** are opposite for both thermometers positions. Now we can plot the experimental points of the curves 1 and 2, corresponding to the time interval of 13 minutes (when the slopes of the dependences are quite small) and add the third point, corresponding to the symmetric positions of the thermistors *relative to the block center*. The obtained dependence is presented in Fig.5b. Here, the TSE is shown as a function of the position of the PRT relative to center of the side surface of the block. From the plot of Fig.5b it follows that the quantity **ΔT[1,2]**, which is used for the description of the TSE, presents an anti-symmetric function of the displacement relative to the block center, thus presenting another confirmation of the vector character of this quantity.

The total energy of the field-particle system, which affects the readings of the thermistors R6 and R3, consists of a symmetric part (which to about 1.1% uncertainty level is characterized by the R3 temperature record in Fig.1) and anti-symmetric component, represented by the TSE. Thus, directly from the thermistors records of Figs.1 and 5b, one can conclude that, *in the general case, the thermal evolution process of an open system is characterized by the lack of symmetry in space*.

To the same conclusion we can come after the studies of the excessive energy fluxes, described by the quantity **ΔV[1,2]** and presented as a function of the time interval elapsed after the increase of the PRT current (Fig.5c). The curve 1 (where data-points are presented by squares) shows the time dependence of the quantity **ΔV[1,2]**, which corresponds to the displacement of the thermistor R6 from the gauging surface Z=4.5mm. The curve 2 (shown by dots) corresponds to the displacement of the measurement system to the opposite gauging surface, so that the same value of the displacement Z=4.5mm is observed for the thermistor R3. All the data-points of the curves 1 and 2 lie, practically, symmetrically relative to the abscissa axis. And it shows that **ΔV[1,2]** is a vector quantity, anti-symmetric relative to the center of the corresponding side surface of the block. *The total energy flux*, which is presented in Fig.3b for the steel GB, *has clearly no spatial symmetry in the general case* (i.e. for arbitrary position of the heat source relative to the center of the block surface).

The comparison of the plots in Figs. 3c and 5c shows that the maximum value of the excessive energy flux, observed for the heating period of the modulation cycle, is about 401μK/minute in case TC block. It is definitely smaller than the maximum value of the energy flux in the steel GB, which exceeds 500μK/minute (Fig3c). More substantial is the difference in the time intervals, which are necessary for the realization of the maximum energy flux. In case of the TC block, the time interval is 1.5minutes after the current increase from 1mA to 5mA (Fig.5c), while for the steel block the corresponding interval is about 2.5minutes (Fig.3c). So, when in the observations of the effect the signal-to-noise ratio is of primary importance, we shall use the experiments with steel blocks. Meanwhile, for the detection of a larger portion of the evolution process, the use of TC blocks is more preferable.

The other important feature of the plots in Fig. 5c is the negligible amount of the contribution of random uncertainty in the measurement results. The main contributions are from systematic effects. This is illustrated by the following observations. For example, if the quantity **ΔV[1,2]** changes the sign for the time interval from 196 to 194 minutes, then it occurs simultaneously for both curves 1 and 2. If the absolute values of the effects are larger for the time values of 188 and 192 minutes relative to the time values of 190 and 194 minutes, then these observations are valid for both curves in the figure. The analysis of the numerical results of Fig.5c shows that the systematic effects of 5-7μK/minute can be reliably detected for the TC block under our experimental configuration. This observation will be later used in the analysis of the thermal evolution process in Fig.11.

One can also conclude from Fig.5c that the dependences of **ΔV[1,2]** on time are quite complicated and have small "damped periodic oscillations", which are not simply possible for the case of a random force (in accordance with the definition of a random physical quantity given in [10]). Though the data points (presented by squares and dots) belong to absolutely independent experiments, the positions of the data points in Fig.5c are correlated. When the magnitude of the curve 1 increases, then the magnitude of the curve 2, corresponding to the same time interval, also increases. Both curves reach the maximums of their absolute values at a time instant of 1.5 minutes. Only the signs of the two dependences on time are always opposite. The "synchronization" in **ΔV[1,2]** time of the two processes is realized in this case, as the abscissa variable in both plots of Fig.5c corresponds to the time interval, elapsed after the current increase from 1mA to 5mA during the heating periods of the modulation cycles in both experiments. The damped oscillations of the curves in Fig.5c, most probably, indicate to the specific features of the propagations of the energy and of the wave momentum [15] in rectangular metallic blocks, when reflections from all artifact boundaries are becoming significant.

From the dependences 1 and 2 of Fig.5c, we can conclude that the largest values of differential thermal powers, delivered to the elementary volumes of the artifact in the vicinity of the thermistors R6 and R3, are observed during the first 5 minutes of the heating period of the cycle. The comparison of the measured values of the induced temperature velocities **ΔV[R6]** and **ΔV[R3]**, realized in each channel during the heating period of the modulation cycle (Fig.3b), shows that for the steel block the maximum value of the ratio of the quantities **ΔV[R6] / ΔV[R3]** as a function of time is equal to 1.39±0.03. It is observed at the time instant of 2.5 minutes, when the dependence **ΔV[1,2]** in Fig.3c reaches its maximum value. For tungsten carbide GB this ratio, describing the maximum ratio of the energy fluxes in two channels, is equal to 1.9±0.07. But it is observed at a shorter time (1.5 minutes) after the increase of the current in the PRT, and, as it was already mentioned before, the magnitude of $\Delta V[1,2]_{max}$ in case of tungsten carbide blocks is somewhat smaller in comparison with steel blocks. Thus, the magnitude and dependence on time of the additional energy flux, described by the quantity **ΔV[1,2]**, are shown experimentally to depend crucially on the artifact material.

The fourth experiment of this study, which is used to clarify further the origin of TSE, establishes the linear relation between the vector quantities **ΔT[1,2]** and **ΔV[1,2]** and the Poynting vector (S), which characterizes the energy current density [15,13a] and the momentum density [13a,15] of the external EM field. This experiment can be regarded as an experimental check of the validity of the Poynting theorem of classical Electrodynamics, performed with huge signal-to-noise ratio for a wide-band thermal radiation. The main experimental results are shown in Figs. 6a and 6b. In Fig.6a it is demonstrated that the magnitude of the quantity **ΔT[1,2]** (and hence the magnitude of TSE) is linearly related to the increments in powers δP, delivered to the GB by the PRT. Actually, in Fig. 6a and 6b we present the results of four independent experiments. The curves marked with number 1 correspond to the displacement Z=4.5mm of the axis of the R6 thermistor from the gauging surface. The curves 2 correspond to the Z-value of 13.5mm. In Figs.6 the measurements were performed for two different current modulation cycles in the PRT. The first cycle presented a rectangular modulation with DC current values of 1mA and 5mA (as in Fig.1). The other cycle realized the smaller variations of the dissipated energy in the PRT and corresponded to the current values of 1mA and 3mA.

All the data points, shown in Fig.6a, correspond to values of the temperature differences **ΔT[1,2]**, arising in the channels 1 and 2 during the heating period, exactly 13 minutes after the increase of the modulation current. At this time interval the magnitude of the TSE is already close to its maximum value (see Fig.2), and the value of the reference function can be very accurately predicted. In Fig.6a we have two increments of the input power, corresponding to 3 power levels. The zero increment of power corresponds to the current in the PRT of 1mA. At this current value (at the end of the cooling period) we define our reference points, relative to which all the differences in the induced temperature variations **ΔT[1,2]** in the channels are then measured. From the equation of the reference function in Fig.2, we find that for the time instant of 13 minutes after the current increase, the reference function is about 0.009μK. This is a quite negligible quantity in comparison with other experimental points of Fig.6a. So, for the zero power increment we plot that vanishingly small quantity, as for the reference function the quantity **ΔT[1,2]** is equal, practically, to zero, in agreement with the basic idea of the MSD technique. Then two power increments are plotted as abscissa variables, with the values of 856μW and 2568μW, corresponding to the current variations from 1mA to 3mA and from 1mA to 5mA, respectively. The indicated values of δP take also into account small variations of the resistance of the platinum thermometer (defined as 100 Ohm resistance at 0°C) when it is used close to 20°C, where all our temperature measurements were performed. As in our automatic DC bridge, a digital current control system was used, the power increment δP at I=5mA, with very high precision, was three times larger than the corresponding power increment at I=3mA.

The data point in Fig.6a, belonging to dependence 1 and characterized by the largest value of **ΔT[1,2],** corresponds to the experimental conditions of Fig.2, when the PRT current during the heating period was 5mA and one of the surfaces of the R6 adapter was in the plane of the gauging surface of the artifact. The only differences from Fig.2 are that the presented data points in Fig.6a correspond to the mean values of the quantity **ΔT[1,2]**, obtained by the averaging procedure over all the modulation cycles of long experiments with total duration up to 16 hours, and also here, instead of the linear fit, we used the six order polynomial fit for the reference points of all modulation cycles. The second data point, belonging to dependence 1 and corresponding to the smaller power increment (δP =856μW), was obtained as a result of an independent experiment, in which the higher level of the modulation current was 3mA. The stability in time and uncertainty of the measurement procedure in Fig.6a can be estimated from the spread of the data relative to the linear regression line, obtained for the 3 presented experimental points. The equation of the fit is shown in the inset. The maximum deviation of the experimental points for dependence 1 relative to the fit is 0.3μK. The standard deviation of the data-points is 0.24μK. These values should be compared with the TSE value of more

than 2500μK, observed for the power increment of 2568μW. Consequently, with very high precision it has been demonstrated experimentally, that the TSE magnitude depends linearly on the power, delivered to the artifact by the external heat source. And it has been shown above that the induced temperature variation **ΔT[1,2]** is a vector quantity. Among the external influence factors, we have the Poynting vector of the broad-band EM field, radiated by the heat source (PRT), that is also a vector quantity and whose magnitude is linearly related to the power dissipated in the heat source. As the PRT is separated from the block by a layer of isolating, thermo-conducting paste, the tunneling of particles from the PRT is not possible. So, the energy to the charged particles inside the artifact can be delivered only by means of the external EM field [14a], and, in accordance with the integral form of the Poynting theorem of electrodynamics, the power delivered to the field-particle system inside the artifact is defined by the flux of the Poynting vector through the boundary surface of the artifact [13a, 14b, 15]. Thus, *the linear relation between the vector quantity* **ΔT[1,2]**, *which describes the thermal surface energy, and the Poynting vector, representing the energy current density of the external EM radiation, has been established experimentally with the signal-to-noise ratio of several thousands*.

Taking into consideration that the fit equation in Fig.6a is linear to a very high accuracy level, we can infer that the TSE value, under the experimental conditions of the dependence 1 and 13 minutes after the increase of the modulation current from zero to 1mA, should be at the level of ~107μK (representing 1/8 of the TSE effect for the second point of this series). So, the contribution of TSE due to power dissipation in 100 Ohm PRT at I=1mA under our experimental conditions is usually substantially smaller than the contributions of the poorly controlled external heat sources, defining the temperature difference **T[1,2]** at the locations of the thermistors. For example, the total temperature difference between the channels even for the specially selected experimental conditions of Fig.1 is about 470μK, i.e. more than 4 times higher than the surface energy, produced by the PRT at 1mA. Still, much smaller values of TSE can be very precisely measured as a result of the used combination of the modulation technique with the synchronous differential temperature measurements.

The dependence 2 in Fig.6a, marked with squares, shows the results of the corresponding measurements, when the measuring system, consisting of the PRT and of the pair of thermistors, was moved as a whole away from the gauging surface by 9mm, so that the distance Z of the axis of the thermistor R6 from the nearest gauging surface increased from 4.5 mm to 13.5mm. As the separations between the surfaces of the PRT adapter and the surfaces of the adapters of the thermistors R6 and R3 were established with the help of a 10mm gauge block, the separations between the adapters were exactly the same in all these experiments. From Fig.6a it follows that the data points of the dependence 2 are also quite close to the corresponding linear fit, passing through the origin and establishing the linear relation between the TSE and the power increment δP. The corresponding fit equation is presented in Fig.6a below the dependence 2. The comparison of the fit equations for the dependences 1 and 2 shows that the increase of the distance of the R6 thermistor from the gauging surface by 9mm resulted in the decrease of the TSE (**ΔT[1,2**]) magnitude by 1.664 times, when this decrease is characterized by the ratio of the slopes of the dependences 1 and 2.

Similar experimental studies were performed for the maximum value of the additional energy flux, which was characterized by the quantity $\Delta V[1,2]_{max}$ and which was observed during the initial stages of the heating period of the modulation cycle, similar to the one of Fig.3c. The experimental linear relations between the quantity $\Delta V[1,2]_{max}$ and the power increments δP, equal to 2568μW and 856μW, are presented in Fig.6b. Here we show two plots, corresponding to the separations of the R6 axis relative to the gauging surface Z equal to 4.5mm and 13,5mm (as in Fig.6a). The equations of the linear regression lines for the experimental dependences 1 and 2 are presented in text boxes of Fig.6b. The decrease of the maximum energy flux with the increase of the separation Z from the gauging surface can be found from the ratio of the slopes of the experimental dependences 1 and 2 of Fig.6b. The obtained ratio is 1.981. This means that the experiment with power modulation of the external energy source has also shown that the maximum value of the energy flux $\Delta V[1,2]_{max}$ falls with the increase of separation Z from the gauging surface substantially faster than the value of the surface energy **ΔT[1,2]**, for which the corresponding ratio was 1.664. If we divide the first ratio by the second ratio, we shall obtain the number 1.1905. Here, it can be noted that the conclusion about faster decrease of the energy flux $\Delta V[1,2]_{max}$ with Z separation from the gauging surface relative to the corresponding decrease of the surface energy **ΔT[1,2]** follows from both experiments with modulation cycles of 1mA-5mA and 1mA-3mA. So, the results and conclusions, following from the plots of Figs.4a and 4b, are confirmed by the experiment with the smaller power increment in Figs. 6a and 6b, but the signal-to-noise ratio is smaller in this case.

The result of fundamental importance follows from the linear dependences of Fig.6b, passing through the origin of the X/Y system. It means that the maximum value of the induced energy flux, described by $\Delta V[1,2]_{max}$, is linearly related to the power increment δP,

produced by the variations of the Poynting vector of the external EM field. For example, for the dependence 1 in Fig.6b, the standard deviation for all three experimental points is about 0.3μK/minute. Meanwhile, the quantity $\Delta V[1,2]_{max}$ exceeds 500μK/minute for the power increment of 2568μW. So, from the plots of Fig.6b follows *the linear relation between the maximum value of the additional energy flux in the artifact* $\Delta V[1,2]_{max}$ *and the Poynting vector of the external EM field, supplying the energy and momentum to the artifact.* This relation has been demonstrated experimentally with the signal-to-noise ratio of ~1000.

III. Thermal Hysteresis Effect and Evolution in Time of Thermal System

As it follows from the plots of Figs.1 and 2, the build-up of TSE does not occur instantaneously with the irradiation of the surface of artifact with a broad-band EM field, produced by the step-type increase of the current in the PRT, but there is an easily detected experimentally time delay, whose magnitude increases with the increase of the separation of the thermistor R6 from the gauging surface. Besides the time delay, the experiment shows that the amplitude of TSE is dropping with the increase of the R6 distance from the artifact's boundary (see Fig.4a), and the form of the $\Delta T[1,2]$ dependence on time is also changing with this distance (Figs. 4c and 5a). So, we have a complicated process that evolves in time and varies from point to point inside the artifact, depending also crucially on the material of the artifact. It looks that we have a typical hysteresis effect, as in cases of ferromagnetic [9d] or ferroelectric materials [9e], when the induction inside the artifact does not track instantaneously the changes of the external field, but its build-up depends on the pre-history of the process, when the whole path to the particular state of the system should be indicated.

Additionally, the plots of Figs.5a-5c give a clear proof that the build-up process of the TSE on time is not symmetric in space. And this is again the typical feature of the hysteresis effects in the well studied ferromagnetic and ferroelectric materials. As pointed out in [9e], when an external electric field is applied to a ferroelectric sample ($BaTiO_3$, for example), there starts a gradual process of the growth of the domains with the favorable direction of the polarization (when the polarization vector coincides with the direction of the applied field) at the expense of the domains with the unfavorable polarization. This effect as a function of time can be detected experimentally by the observation of the domains in a polarized light. And this type of experiments, which are known for ferromagnetic [9c] and ferroelectric materials [9d], presents a clear experimental proof of the asymmetry in space in case of these hysteresis effects. The other key feature, typical for the system with hysteresis effect, is the appearance of the *differences in the properties* of the material under the application of the external field that can be considered as the manifestation of the evolution of the material (or the demonstration of the "self-ordering" effect in the material). For example, it has been observed experimentally that in $BaTiO_3$ crystal, the positive edge of the domain is etched faster by an acid than its negative edge [9e]. These considerations give an indication that the dependencies of Figs.2-6 can be presented as a closed loop of a thermal hysteresis effect, especially, when we notice that the area of the curve above the reference line in Fig.2 defines the amount of energy, radiated by the particular parts of the block into the environment during one modulation cycle, and the area below the reference line defines the energy absorbed by these parts from the environment, so that *the thermal evolution process of Fig.2 has no symmetry in time* in accordance with the Clausius-Thomson-Plank formulations of the second law of Thermodynamics [9b]. The proof can be performed exactly in the same way as it is done for the well-studied hysteresis effects in ferroelectric [9e] and ferromagnetic materials [9d]. Indeed, the key feature of the process in Fig.2 is that it is periodic in time, and the system under the study (the gauge block with the PRT and thermistors) during each cycle realizes the transfer of the energy and of the momentum of the oriented motion of the electrons in the PRT (and of the energy and momentum of the propagating EM field irradiating the block) to the non-oriented thermal energy of the surrounding material objects on the Earth, with the corresponding transmission of the excessive momentum to the environment through the areas of mechanical support of the gauge block. This process is irreversible in time, as the process in the opposite time direction is strictly forbidden by the Clausius-Thomson formulations of the Second Law of Thermodynamics [9b].

After this, it is becoming probably clear that, in accordance with the discussion of the previous section, the indication to the way of the presentation of a closed loop of the thermal hysteresis effect gives the experimental procedure in ferroelectric materials. Instead of presenting the experimental points as a continuous sweep in time, it is necessary to present the points in two separate time sequences, each corresponding to one of the two possible directions of the variable forces, acting on the particles of the system. For materials with absorption, the direction of the EM force, acting on the charged particles, is defined by the direction of the energy propagation in the medium [15, 9g]. As it follows from Fig.3c, and the direction of the energy flux is changed during our modulation cycle. So, to obtain the form of the thermal hysteresis loop it is sufficient to present the data of Fig.2 as a function of the direction of the external force (acting on the field-particle system inside the artifact) by inverting the time for the

cooling period of the cycle. The corresponding plot is shown in Fig.7. Here, the induced temperature variations **ΔT[1,2]** for the heating period are presented in the same time scale as in Fig.2. The corresponding data points are shown as dots between the two arrows 1 and 2, indicating to the beginning and to the end of the heating period. The data points for the cooling period of the cycle in Fig.7 are shown by rhombi, corresponding to the path indicated by arrows 2-3-1. Along this path the time variable is (111 – *t*), which means time inversion relative to the point t=111 minute, marked with arrow 2. Between the time interval, indicated by the arrows 2 and 3, the time scale is the same as in Fig.2. For the time interval between the arrows 3-1, where the variations of **ΔT[1,2]** are negligible, the data points are presented for much larger time intervals, so that the end of the cooling period coincides with the beginning of the heating period. As the quantity **ΔT[1,2]** is measured relative to the mean value of the several reference points at the very end of the cooling period of the cycle, we have a perfectly closed loop, only with some random jitter at a few μK level, which is negligible in comparison with the amplitude of the TSE effect.

The energy, which is radiated by the system during the modulation cycle and which is responsible for heating the environment, is defined by the form of the thermal hysteresis curve. As for the other, well studied hysteresis effects, the TSE process is an irreversible one. To prove this, we shall use the Plank formulation [9b] of the Second Law of the Thermodynamics (the most simple for interpretation), which says that no weight can be lifted in the field of gravity by periodic process when cooling thermal reservoir. We assume that the modulation of the current in the PRT is produced by an electronic switch with negligible losses and rechargeable battery, and the state of the battery charge is continuously monitored by the device, which is used in all portable computers. All the results of the measurements are assumed to be recorded. Then for the normal time direction (or the normal play of the record) we shall observe that the battery is gradually discharged, and the environment is heated by the energy radiated by the gauge block. For the backward play of the record, we shall observe that for the purely periodic process, the energy of the battery is increased only as result of cooling of the environment (thermal reservoir). The energy of the battery can be used to lift some weight. Thus, for the opposite play record (or time direction) we encounter the violation of the Thomson-Plank formulation of the Second Law of Thermodynamics (which presents the result of the analysis of a huge number of experimental facts and is known to have no exemptions). Consequently, such a process is strictly forbidden. So, the thermal evolution process, described by the vector quantity **ΔT[1,2]**, is irreversible. In other words, it has no symmetry in time, strictly in accordance with the Weyl idea how to check the symmetry in time of an arbitrary physical process [16].

Thus, experimentally we have demonstrated that *the thermal evolution process*, presented by the experimental plots of Figs. 1-7, *is characterized by the lack of symmetries in space and in time and shows clearly hysteresis effect, when the polarization of the medium in the external EM field depends on the pre-history of the system.*

Now we shall describe the fifth type of experiments of this study that discovers the other fundamental property of the surface energy, which, together the above mentioned properties of TSE, creates a new concept of the evolution process in physics, which is equivalent to the evolution concept in biology, for example. Experimental dependencies in the following figures show the effect of non-linearity of the material on the thermal evolution process, or, in other words, the invalidity of the superposition principle for the external EM fields in the process of energy and momentum propagations inside the material artifact.

In Fig.8, we show the evolution in time of the magnitude of the TSE, characterized by the quantity **ΔT[1,2]**. As we were interested in obtaining maximum resolution in the amplitude of the effect, the measurements were performed with the steel block. The TSE magnitudes are presented for the first 13 minutes after the increase of the modulation current to 5mA. The averaging time for each experimental point was 2 minutes. The main differences relative to the experiment of Fig.2 are the following.

First, two additional, auxiliary heat sources (resistors) were located inside the Dewar, symmetrically and at the same distances from the gauging surfaces of the artifact. When one of them was energized, the adjusted value of the stabilized dc current through this resistor could produce a desired temperature difference between the locations of the thermistors R6 and R3. Thus in this experiment, the difference in the induced temperature variations, recorded by the channels 1 and 2, was measured when there was a systematic temperature difference on the artifact surface at the locations of the thermistors belonging to the channels 1 and 2. The temperature difference between the channels, **T[1,2]**, shown as an additional parameter in Fig. 8, was measured as a mean value of the temperature difference between the two thermistors, observed for the last 30 minutes of the cooling period of the modulation cycle. In Fig.8 the range of the variation of the parameter **T[1,2]** was between -2.46mK and 61.06mK. Second, the separations between the adapters of the PRT and thermistors were increased from 10mm to 13.5mm, in order to study for the steel block the effect of the heat source separations from the thermistors adapters on the TSE amplitude.

As it is clearly seen in Fig.8, the temperature variation **ΔT[1,2]**, induced by the increase of the current in the PRT, is also affected by the temperature difference **T[1,2]**, which is produced by an independent heat source with a constant dissipated power. It means that the steel gauge block acts as a non-linear device when its surface is irradiated by the EM fields of two independent sources. It also follows from the plots of Fig.8 that for all of the presented time intervals the magnitude of the TSE, represented by the quantity **ΔT[1,2]**, is increasing with the increase of the temperature difference **T[1,2]**. It means that the larger surface energy is observed when the auxiliary energy source produces excessive heating of the gauging surface in the vicinity of the location of the thermistor R6. It is also clear from Fig.8 that for any data-points, corresponding to the same value of the time interval, the separation between the plots, corresponding to different values of the temperature difference **T[1,2]**, is steadily increasing with the increase of the observation moment. So, we have records of several complicated evolution processes, as each plot in Fig.8 represents a considerable part of the hysteresis loop (similar to the one of Fig.7), and *the parameters of this hysteresis loop can be easily changed by an auxiliary energy source*.

The resolution of the modulation technique is very high and gives the opportunity to observe clearly the difference between the TSE values, resulting from the increase of the temperature difference between **T[1,2]** by only 4mK. For example, for dependences in Fig.8, corresponding to the temperature differences of 57.1mK and 61.1mK, the systematic differences in **ΔT[1,2]** are well above the noise level for all the presented time intervals in the range between 3 and 13 minutes. As the quantity **ΔT[1,2]** corresponds to the difference in the temperature variations in the channels 1 and 2, which are induced by the increase of the current in the PRT and *this induced temperature difference is affected by the presence of the other heat source*, this means that *the superposition principle is not valid for the sources of external EM radiation as a result of the existence of the thermal surface energy*. It should be specially emphasized here that *the violation of the superposition principle for EM fields is observed also in a free space, which is not occupied by the material artifacts*. This is a consequence of the fact that the energy, recorded by the thermistor, corresponds to the energy of the oriented motion of the field-particle system, which is radiated by the block into the auto space. When the accuracy of the experiment is sufficient to detect the energy, reemitted by the material objects, the principle of superposition of the EM fields is becoming invalid even for the free space.

From the experiments (presented above) it follows that the thermal evolution process (Figs.2, 7), observed in metallic blocks for periodic power modulation, is irreversible, or in other words, it has no symmetry in time. This process changes from point to point inside the artifact (Figs.4a, 4b, 6a, 6b) and has no symmetry in space (Figs.3b, 5a, 5b). So, the parameters, characterizing the properties and state of the artifact, should be specified for a particular time instants and for the particular observation points. If in Fig.8, we choose the data points corresponding to measurements, obtained 13 minutes after the increase of the current in the PRT, and plot them as a function of the temperature difference **T[1,2]** for the locations of the thermistors indicated above, we obtain the plot of Fig.9a. By this plot, we present experimental demonstration of the non-linear properties of the thermal process in steel blocks: the magnitude of the TSE depends not only on the amplitude of the PRT current, but is also affected by the presence of an auxiliary heat source. The non-linearity of the system, which in this case is characterized by the linear dependence of the TSE magnitude on the temperature difference **T[1,2]**, is demonstrated with a huge signal to noise ratio. For this it is sufficient to compare the maximum deviation of the 4 data-points relative to the linear fit (which is 1.75μK in Fig.9a) with the total variation of the quantity **ΔT[1,2]**, exceeding 700μK. Thus, Fig.9a shows that the non-linearity of the artifact can be measured with the signal-to-noise ratio of several hundreds with the use of modulation technique, in spite of the fact that we are dealing with the next order effect in comparison with the detection of the surface energy as a function power, which is dissipated in the PRT.

In Fig.9a, the equation of the linear fit is presented in a separate text box. When X and Y variables of the plot are both measured in the same units (mK), the quantity R_1, which is defined as the ratio of absolute values of the vector quantities **ΔT[1,2]** and **T[1,2]**, is becoming equal to 1.2%. So, the non-linearity of the system is not that small. But this value characterizes the non-linearity only for the indicated time interval of 13 minutes. As, the plots of Fig.8 describe some portions of the hysteresis loops and the hysteresis effect means some memory in time of the preceding states of the system, the response of the system to the variation of the external EM field, characterized by the non-linearity of the system, inevitably should be some function of time. *Important variations of the non-linearity in time, as a main property of the steel block in the thermal evolution process, follow from the comparison of Figs. 9a and 9b*. In Fig.9b, the induced temperature variations **ΔT[1,2]** are presented as a function of temperature difference **T[1,2]** for the time interval of 3 minutes after the increase of the PRT modulation current. From the equation of the fit in Fig.9b, we find that the value of the ratio R_1 is only 0.25%. So, the non-linearity in this case is 4.8 times less than the one in Fig.9a. If we choose the third time interval as 9 minutes,

we shall find that the ratio R_1 will be 0.95%. When plotting these values as a function of elapsed time, we find that at the beginning of the thermal hysteresis loop, the rate of the increase of the non-linearity value increases rapidly with time, reaches its maximum value and then the rate decreases.

And now we are to explain why in Figs.9 we have such a high signal-to-noise ratio. The answer is simple. In this case we performed special *modeling of the evolution process*. First, we applied a synchronous modulation technique, using the most accurate (square-wave) type of modulation. If, for example, during the total measurement time of ~7 hours we have a record of six modulation cycles, then the averaging procedure over all of them keeps, practically, only induced variations for each specified time interval of the quantity **ΔT[1,2]**. The spurious perturbations of the signal are significantly reduced as a result of effective isolation of the investigated system by the Dewar enclosure, resulting in a very large thermal time constant of the system. The other important factor is the use of the temperature control system, so that when the averaging procedure over several cooling and heating cycles of the temperature control system is realized, the effect of the external temperature perturbations is diminished to the acceptable level. Second, the temperature difference between the locations of the thermistors was produced by the stabilized heat source, which was located inside the Dewar. The effect of the spurious perturbations was about two orders of magnitude smaller. So, even for relatively small signals of Fig.9b, where the total variation of the quantity **T[1,2]** is about 150μK, the signal-to-noise ratio is still considerable, as the standard deviation of the points relative to the fit is only 0.22μK. But the price for this is also clear. In this case we observe the influence on the TSE magnitude only of the static temperature difference **T[1,2]**, represented by the mean value of this quantity over the whole measurement time. The effect of the temperature transients on the TSE can not be observed in this case.

The violation of the superposition principle in combination with hysteresis effect results in important consequences: the presence of an additional heat source can change drastically the evolution process, which can be observed as a result of the energy modulation cycle inside the PRT at any point of the artifact. In more detail this is illustrated by Fig.10, where we present the dependences **ΔT[1,2]** versus time for a 100mm tungsten carbide GB, in which the creation of the TSE occurs much faster than in steel blocks. In this case, even during the first 13 minutes after the increase of the modulation current in the PRT, a considerable part of the evolution process can be observed. The separations between the adapters of the thermometers were 14 mm in this case. The other distinguishing feature of the experiments (presented in Fig.10) is that in all cases the auxiliary heat source irradiates more efficiently the gauging surface, which is far away from the thermistor R6 (belonging to channel 1). So, the external heat source produces the heat flux in the same direction in the vicinity of the thermistor R6 as the PRT does, when the current inside it (during the heating period of the modulation cycle) is increased to the value of 5mA. The dependences 1-3, marked with dots, squares and rhombi, correspond to the mean values of the temperature differences between the channels **T[1,2]** equal to -1,17mK, -8.2mK and -17.2mK, respectively. These values were measured at the ends of the cooling periods of several modulation cycles. So, we show here three independent experiments with three different power levels, dissipated by the auxiliary heat source. For each sequence of the data-points, the mean value of the temperature difference between the channels was the additional parameter.

As it is clearly demonstrated by the dependences 1-3, the additional heat source changes significantly the thermal evolution process. The maximum of the curve **ΔT[1,2]** versus time is clearly detected for the negative values of the quantity **T[1,2]**. The key features of the evolution process are the variations of the maximum values of the TSE magnitude with the increase of the absolute value of the temperature difference **T[1,2]**, and the shift of the maximum value of the quantity **ΔT[1,2]** on the time scale. For example, for the dependences 1-3 the maximum values are, approximately, equal to 915μK, 863μK and 846μK, respectively. The uncertainty of these measurements is ~2-5μK. With the increase of the value of the negative temperature difference **T[1,2]**, the position of the maximum value shifts to the smaller time intervals, elapsed after the increase of the modulation current in the PRT. For the dependences 1-3, the corresponding time intervals are, approximately, equal to 7.5, 5.45 and 4.15 minutes, respectively. Thus, we have a record of the evolution process when *the external heat source changes the shape of the dependence of the surface thermal energy on the time elapsed*.

One can see in Fig.10 that the difference between the dependences 1- 3 is steadily increasing with the time increase for the time intervals in the range of 3-13 minutes. For example, for the time intervals 3, 7 and 13 minutes after the increase of the modulation current, the differences between the dependencies 1 and 3 are equal to 13μK, 123μK and 255μK, respectively. When choosing the data-points of Fig.10, corresponding to the time interval of 13 minutes and plotting them as a function of the temperature difference **T[1,2]**, we obtain (as in Fig.9a) the linear dependence, where the slope for the TC block is somewhat larger than the slope in Fig.9a. The corresponding non-linearity coefficient R_1 is equal to 1.4% in this case. And it is also clear from Fig.10 that the value of the coefficient R_1 will

continue to grow with the further increase of the time interval (at least, in some range).

The other important result follows from Fig.10 when we analyze the presented dependences in the time interval between 0.5-1.5 minutes. The non-linearity ratio R_1 is negative in this range, showing that we have a hysteresis effect of the opposite sign! In this time interval, the auxiliary heat source, producing in advance a stationary energy flux in the direction of the thermistor R6, is increasing the quantity **ΔT[1,2]**. Or in other words, the additional energy flux, stimulated by the increase of the PRT modulation current, is increased if the steady-state energy flux in the same direction has been created in advance by an auxiliary energy source. Here, it is important to note that for this time interval we have, practically, a pure running wave of the propagating energy, as the reflection from the gauging surface is quite small: the product of the indicated time interval and the mean velocity of the energy propagation in the medium is smaller than the distance from the PRT to the gauging surface. Thus, it is demonstrated experimentally that when the energy reflection from the boundaries is negligible, *the energy flux, which is propagating in a homogeneous medium and which is induced by a step increase of the magnitude of the Poynting vector of the external EM field, is significantly increased, if the energy flux in the same direction has been created in advance by an auxiliary source of EM radiation*. Some preliminary studies of this effect have been reported also in [3f, 3i]. In some cases, this effect can be of primary importance. For example, for the time interval of 0.5 minute after the increase of the modulation current, the quantity **ΔT[1,2]**, corresponding to the temperature bias **T[1,2]** of -17.2mK, exceeds by more than 2 times the quantity **ΔT[1,2]**, observed for the bias of -1.2mK.

Some additional information dealing with this experiment is presented by the plots of Fig.11. Here, we show the differences in the induced temperature velocities **ΔV[1,2]** as a function time for the tungsten carbide (dependences 1 and 2) and for the steel block (dependence 3). As it follows from Fig.11, the main parameter, defining the properties of the evolution process, is the type of the material. For the dependence 3, representing the corresponding part of the plot in Fig.3c, the area between the curve and the abscissa axes is much larger than that for the dependence 1, so that the TSE magnitude in steel is about 3 times larger than in tungsten carbide (in agreement with the plots of Figs. 2 and 10). But the process in the TC block evolves much faster, as the maximum value of the additional energy flux in the TC block is observed substantially earlier (Fig.11).

For TC block we show two plots. Dependence 1, represented by dots, corresponds to the temperature difference between the channels **T[1,2]** of -0.2mK, PRT current modulation amplitudes 1-5mA and the separations of 14mm between the adapters of all thermometers. Dependence 2, shown by squares, corresponds to the value of the temperature difference **T[1,2]** of -17.2mK. As there are differences between the dependences 1 and 2, it means that the auxiliary heat source changes the induced variations of the temperature velocity **ΔV[1,2]**, and consequently the principle of superposition is not valid for EM fields. Here, we are to note that the positive value of the quantity **ΔV[1,2]** means that the power, emitted into the outer space by the elementary area of the block surface in the vicinity of the thermistor R6 (close to the gauging surface), is larger than the power, emitted by the elementary area of the block surface in the vicinity of the thermistor R3. The negative value of the quantity **ΔV[1,2]** means that the power emission capability of the block surface is larger in vicinity of the thermistor R3. So, the plots of Fig.11 show that *the power emission capability of the block surface is changed by auxiliary heat source both in space and in time*. And the interesting thing is that these variations are observed during a relatively small part of the heating period of the modulation cycle. Probably, the evolution process depends on the enormous quantity of influence parameters. As it follows from Fig.3c, the uncertainty of the measurements are smaller than the dimensions of the symbols used for the presentation of the data-points, and, consequently, the error bars cannot be shown on the plot. The consideration is valid for the experimental curves in Fig.11. So, the comparison of the dependences 1 and 2 in Fig.11 shows that the effect of the auxiliary heat source on the induced thermal velocity difference **ΔV[1,2]** is well beyond the uncertainty of the experiment. For example, for the time interval of 0.5 minute the negative value of the quantity **T[1,2]** increases the velocity difference. Meanwhile in the range of intervals from 1.5 to 13 minutes, the negative value of **T[1,2]** diminishes the value of the quantity **ΔV[1,2]**, thus reducing the excessive energy flux density associated with the TSE. A complicated form of the difference between the dependences 1 and 2 gives an indication that even for our experiment, when the mean value of the temperature difference **T[1,2]** and the PRT modulation current value characterize sufficiently accurately the external experimental conditions, the number of internal influence parameters is enormous. As it will be shown in the next section of the paper, the cycle-averaged rate of the conversion into heat of the energy of the oriented motion of the field-particle system [15] is linearly related to the total force density [15], acting on the field-particle system inside the material with arbitrary level of absorption. So, if in Fig.3 the quantity **ΔV[1,2]** is changing the sign at the beginning of the heating and cooling periods of the modulation cycle, then there are the corresponding variations in the

energy flux densities in time and in space that immediately result in the differences in the total force densities in time and in space. But the variation of the force, acting on the elementary volume of the medium, means that force results in deformations and stresses in the medium, which change the properties of the medium and which lead to the creation of a non-uniform medium in the presence of the EM field. So, it is not astonishing that the non-linearity parameter, which is one of the fundamental in Electrodynamics and which is characterizing the response of the medium to the EM field, is also changing in time and in space (see Figs. 8-10).

For the steel block, it is natural to expect that the process of the propagation of the field-particle system is crucially affected by the presence of the domain structure. So, in the list of influence factors we are to include the size of each domain, its orientation relative to axis of the block and its position relative to the gauging surfaces. The dislocations inside the domain structure are also inevitably affecting the propagation of the free electrons and displacement of the ions of the lattice. So, among the internal influence factors we are to include the position, orientation and the size of each dislocation. Thus the number of influence parameters, affecting the thermal evolution process in a steel block, is always enormous. But, similar situation with enormous number of influence factors is observed in case of ferromagnetic materials, which have been studied experimentally for many decades. And it is known from the book of Ch. Kittel that the description of the hysteresis effect in ferromagnetic materials presents too complicated problem for theoretical physics [16a]. Even larger number of internal influence factors is typical for tungsten carbide gauge block. The domain structure is not present in that material and the positions of all atoms are to be specified (the nearest order does not exist in this case).

The enormous number of internal influence factors in case of the thermal evolution process should be added to the huge number of external factors, which define the magnitude and direction of the resulting Poynting vector of the EM field at each point of the surface of the gauge block under investigation. When we use an auxiliary heat source, its radiated energy is partially transmitted through the side walls of the Dewar and part of it propagates along the walls in the direction of the Dewar axis, so that the mean temperature of the gauge block over the time interval of the modulation cycle is, practically, constant. To solve the problem, it would be necessary to write the equations for the continuity of energy, momentum and angular momentum, but the solution is not possible as, for the realized accuracy of the experiment, it is necessary to take into account the radiated energy of the Sun that propagates through turbulent atmosphere and the walls of the building. And the description only of turbulent atmosphere requires an infinite number of macroscopic parameters [9a]. Besides that, when the energy, radiated by the Sun reaches any material object it produces the surface energy and some part of the energy is reemitted as a result of the oriented motion of the field-particle system. So, *the resultant Poynting vector of the EM field, irradiating the Dewar surface, is the vector sum of the contributions of the enormous number of material objects, which cannot be considered as independent, as all of these objects are interacting with the common EM field* [17-19]. The same considerations are valid for the investigated gauge blocks, as the Dewar (or any other experimental set-up) cannot produce adiabatic isolation of the system. Thus, for the investigated material objects, for which evolution process, as shown experimentally, is characterized by the hysteresis effects, produced by the infinite number of correlated influence factors, it is very doubtful that the description of the corresponding process can be realized in terms of mathematical tools, specially developed and only quite adequate for the description of relatively simple cases of Newtonian mechanics. Indeed, as it follows from the fundamental principle of thermodynamics even for a specific theoretical model of an ideal gas, the presentation of the evolution process by a continuous line on the pressure versus volume diagram is only possible for the (so-called) quasi-static processes of the isolated systems [9b], that is only for the sequence of thermally equilibrium states, following each other without any transient intermediate processes. The experimental observation of the evolution processes in thermal systems gives sufficient proofs for the validity of the Niels Bohr statement that the description of arbitrary system in terms of time and space is not possible in the general case. This is a direct consequence of the famous incompleteness theorem of Kurt Gödel in mathematics. In the described experiments it is shown that the interaction of the EM field with the ensemble of atoms of a solid-state artifact results in a clearly observed hysteresis effect, while the theoretical physics, equipped with the standard mathematics (specially developed for the description of Newtonian systems with the finite number of independent *variables*), *has not been able, so far, to describe adequately the "simplest case" of the hysteresis effect in ferromagnetic materials in a constant magnetic field. Thus, the description in the general case of the evolution process*, characterized by the infinite number of interacting material objects, which produce the common Poynting vector over the whole space and consequently cannot be regarded as independent, *is far beyond the possibilities of all Modern Physics, as even its basic concepts of isotropic time and of isotropic space (borrowed from mathematics) are in dramatic contradiction with all Natural sciences* (see Discussions).

Besides that, our experiments have demonstrated that the time dependence of the thermal

evolution process and the magnitude of the surface energy are specific for a particular point inside the artifact, and that both quantities can be significantly changed by the auxiliary external heat source (see Figs. 3-11). *As philosophers say nowadays, the time and space concepts are relational ones* (see Discussions). On the other hand, the very fact of the existence of the thermal hysteresis effect means that there is a time scale, which is characteristic to each material object and which is defined by its own evolution process. The two time scales, corresponding to any two material objects, are inevitably somewhat different: among the huge number of internal parameters, characterizing each object, there will be some difference. Besides that, the driving source of each thermal evolution process is the Poynting vector of the resultant common EM field, is also somewhat different as a result of spatial difference in the locations of the two objects. On the same reasons, the record of the evolution process of a particular material object in time scales of two clocks (including quantum atomic clocks) will be always somewhat different. This is the consequence of a well-established experimental fact that the Allan variance as a function of the averaging time for any quantum clock starts to increase (after reaching the "flicker floor") [20], or in other words *the time scales of the two clocks start to deviate in unpredictable manner when the observation time exceeds the flicker floor averaging time*. Thus, *the processes in material objects cannot be synchronized in time, and this is the manifestation of the fact that isolated systems do not exist in Nature.* All these are experimental proofs to the Niels Bohr's famous observation that *"Isolated material particles are abstractions*, *their properties being definable and observable only through their interaction with other systems"*.

IV. Conclusions and Discussions

Before starting discussions, it is worth noting that the main parameter, affecting the indications of a resistance thermometer (thermistor) is the energy of the external EM field, irradiating the surface of the thermometer. This field is mainly produced by the irregular motion of the charged particles and the EM field inside the artifact, which is in contact with the thermistor. As the adapter of the thermistor is isolated from the artifact by nonconductive paste and charged particles cannot tunnel through the gap of ~0.1mm between the adapter and the artifact, the only way for the energy transfer is the radiation of the EM field, with the following absorption of it in the thermistor adapter. The part of the EM energy, absorbed in the thermistor, changes the number of carriers in the valence and in conductance bands, thus effectively changing the recorded resistance value of the sensor. This is the consequence of the Poynting's theorem of Electrodynamics [13a, 14a], which says that the rate of change of the electromagnetic energy plus the total rate of doing work by the fields over the charged particles within the volume of a material artifact is equal to the flux of the Poynting vector (see eq.(6.109) in [13]), S, entering the volume of the artifact through its boundary surface (see eq.(6.111) in [13]). So, the vector S describes the energy-flux density of EM field [13], or the energy current density (as it is called in [15]). For the dielectric material with arbitrary level of losses, the continuity equation for the total energy density for the coupled EM field and dielectric lattice, under the approximations made in [15], can be presented in the form (see eq.(2.17) in [15]):

$$\frac{\partial}{\partial t}W + m\Gamma\left(\frac{\partial}{\partial t}s\right)^2 = -\boldsymbol{\nabla S} \qquad \ldots(1)$$

Here, W presents the total energy density, which contains in addition to the EM field energy density, the kinetic and potential energy densities of the optic vibrational mode; *s* is the relative spatial displacement field of two ions in the primitive unit cell; *m* is the reduced mass of two ions in the primitive unit cell, and Γ is the damping rate of the optical mode.

The rate of the energy variations, described by the first two terms in Eq. (1), can be detected by thermistors and corresponds to the experimentally measured thermal velocities at the specified points of the material artifact (**ΔV[1]** and **ΔV[2]**). Indeed, the reading of the thermometer depends on the power absorbed from the EM field, as in accordance with the Poynting's theorem, the power, radiated by the material artifact, is defined by the total rate of the energy loss of the EM field and of the energy loss of the optical mode, which is directly coupled to the EM field [15]. The second term in Eq. (1) describes the rate of loss of the energy of the optical mode, which is converted into heat as a result of intrinsic non-linearity of the system [15]. And this contribution is also detected by thermistors, as all the thermometers are traditionally used to characterize the random part of the thermal energy of the material artifacts. So, if in Fig.3 we see that the quantity **ΔV[1,2]** is not equal to zero during a short interval of time after the change of the PRT current, it means that there is an additional energy flux (positive or negative) to the elementary volumes (dx)(dy)(dz) in the vicinity of the thermometer R6 relative to the elementary volumes in the vicinity of the thermometer R3. And in accordance with the continuity equation in the differential form [13a, 15], these energy fluxes arrive inside these volumes through their boundary surfaces as a result of the total-energy current density $\boldsymbol{\mathcal{S}}$ **[15]**, which is present at a particular point of the artifact and describes the interacting field-particle system. As the difference in the induced temperature velocities **ΔV[1,2]** is not equal to zero, it means that the total-energy current densities [15] at two different locations inside the

artifact, located symmetrically relative to the energy source, are also different at that time moments. And this difference in the energy current densities *S*, representing the oriented motion of the coupled field-particle system inside the artifact, is shown experimentally to be linearly related to the energy current density of the EM field, irradiating the surface of the artifact (section 2.1). Thus, *the oriented motion of the energy and momentum of the field-particle system, which is stimulated and supported by the Poynting vector of the external EM field, is the physical reason for the existence of the thermal surface energy* **ΔT[1,2]**.

Simultaneously, the above presented experimental studies have clearly demonstrated that *the basic assumption of the Fourier thermal conductivity theory* (TCT), which is borrowed from the steady-state experiments and which states that the thermal energy flux is defined by the temperature gradient [9c], *is not valid for any period of the heat transfer process*. Especially, it is not true for the "transients" of the propagation process of the thermal energy. As it follows from Figs.1-3, for the heating period of the cycle, the maximum energy fluxes to the unit volumes inside the steel artifact, which are located symmetrically, but in the opposite directions relative to the energy source, differ by ~40% and the energy flux to the vicinity of the R6 sensor is larger. But the temperature in the system was adjusted in such a way that the temperature of the artifact surface, close to R6 sensor, was already somewhat higher than the temperature, close to R3 sensor, just before the increase of the modulation current. During the whole heating period of the modulation cycle, the induced temperature difference **ΔT[1,2]** continues to increase and at the end of the heating period, characterized by the equal thermal fluxes (see Fig.3), the largest induced temperature difference **ΔT[1,2]** of about ~2.5mK is observed. Meanwhile, at the end of the cooling period of the modulation cycle, the energy fluxes to the unit volumes in the vicinities of both sensors are again, practically, equal, but the temperature difference between the PRT and the thermistor R6 is somewhat smaller (by approximately 0.47mK) than the temperature difference between the PRT and the thermistor R3. From this it follows that the *TCT can be expected to give reasonable agreement with the temperature measurements of moderate precision only for the steady-state periods of the heat transfer process,* but the TCT predictions about the initial periods of the heat transfer are very doubtful.

The other very important observation, which is necessary for the interpretation of the presented experimental studies, follows from the solid-state physics [16b]. It is known that for a charged particle inside the solid-state, the conserved quantity is the total momentum, which consists of the kinetic momentum of the translational motion of the charged particle and the potential momentum of the EM field [16b]. As pointed out by Ch. Kittel, this requirement on the total momentum of the field-particle system is correct, because it results in the proper equation for the Lorentz force acting on the charged particle [16b].

This is in agreement with the conservation laws of electrodynamics [13a, 14c, 15]. The electromagnetic momentum density $\mathbf{G}_{EM}$ (in accordance with eq. (6.118) [13a]) is given by:

$$\mathbf{G}_{EM} = \mathbf{S} / c^2 \qquad \ldots (2)$$

where *c* is the velocity of light in vacuum. The continuity equation of Electrodynamics in the integral form (see eq. (6.122) in [13a]) states that the first derivative in time of the total momentum of the field-particle system in the artifact volume, consisting of the EM momentum and the momentum of the charged particles, is defined by the flow through the boundary surface inside the artifact volume of the EM momentum current density, given by the Maxwell stress tensor (see eq.(6.120) in [13a]). Thus, from the fundamentals of Electrodynamics and the Solid-state Physics it follows that the "conserved" quantities of the field-particle system inside material artifact can be only the total momentum and the total energy densities (Poynting's theorem, section 3 above) of the field-particle system. So, in agreement with the presented experimental studies, the temperature, as a physical parameter, which characterizes the variations of the internal energy of a macroscopic elementary volume inside the artifact that can be detected by EM radiation, should inevitably correspond to the variations of the total energy of the field-particle system. Thus, the total energy has to include the energy of EM field in addition to the energy of the charged particles. And the experimental result of the primary importance of these studies is that *the internal energy includes both: the energy of the random type of the motion of the field-particle system (with the mean values of the linear momentum and angular momentum equal to zero) and the energy of the systematic part* (**ΔT[1,2]**), *which describes the oriented propagation inside the medium of the thermal energy with the corresponding wave-momentum* [15]. In this respect our experiments present the necessary confirmation of the theoretical studies of R. Loudon, L. Allen and D. F. Nelson [15], dealing with the propagation of the energy and momentum through an absorbing dielectric with an arbitrary level of losses. The essential features of the theory [15] are the inclusion of the contributions from EM field and from dielectric medium to the total energy density *W* and to the wave momentum density, and taking into account the Rőntgen term in the current density in the Maxwell equations. The Rőntgen term changes drastically the relation between the magnetic field **H** and magnetic induction **B** (by introducing the term, depending on the

polarization of the medium **P**, which is induced by electrical field). In accordance with [15], the wave-momentum density consists of the EM field momentum $\mathbf{G_{EM}}$ and the pseudomomentum density $\mathbf{G_{psm}}$, found to be equal to [P x B] plus a dispersive term, which accounts for the thermal losses in the system. The main results in [15] are illustrated by the one-dimensional case of a plain transverse EM wave, propagating in z-direction of dielectric material with arbitrary losses. The intensity of the EM field in z-direction is assumed to fall exponentially with the characteristic length *L*, as a result of the gradual conversion of the energy of the optical mode into heat (see eq.(3.11) in [15]).

As pointed out in section 2.1, our measurement procedure is sensitive to the variations of temperature only in one *z*-direction, along the longer side of the GB. Also, from the experimental plots of Fig.12 in [3c] we can infer that a thermal wave, induced by power dissipation in the PRT located on the surface of a long (900mm) steel block, can be quite well approximated by inhomogeneous plane wave, if its amplitude and attenuation coefficient in the direction of the propagation are obtained from experiment. But for the plane transverse EM wave, propagating along the dielectric medium with arbitrary large losses [15], all the basic solutions (including the energy of the system which is converted into heat) can be obtained in a closed form as a function of the total-energy current density (see eq. (2.18) in [15]). So, from the temperature measurements, described in this paper, we can define quite accurately the variable part of the total-energy density of the field-particle system, W:

a) the induced temperature variations along the artifact can be precisely measured;
b) the thermal capacity of steel at room temperature is well known;
c) the distribution of temperature in the vertical direction inside the GB (at some distance from the heat source) is quite homogeneous;
d) the thickness of the block (9mm) is much smaller than its length;
e) the adapters of thermometers cover the whole width of the GB.

Additionally, from the experiments presented here, the *velocity of the energy propagation* inside the steel GB *can be found*, so that we can have a reliable estimation of the basic processes inside the artifact. For example, for the plane TEM wave (in accordance with [15]), the cycled-averaged value of the total-energy current density $\langle S \rangle$ (which has the only nonzero component in the direction of the energy propagation *z*) is related to the cycle-averaged energy density $\langle W \rangle$ (see eq.(2.19) in [15]) by a simple relation (4.16):

$$\langle \mathbf{S}_z \rangle = \mathbf{v_e} \langle W \rangle \qquad \dots (3)$$

where, v_e is the velocity vector of the energy propagation in the material. This is a standard relation between the energy current density and the energy density that describes quite precisely an arbitrary medium with absorption [9f]. And all the parameters on the right side of eq.(3) can be accurately enough measured experimentally for any particular point of the artifact. Meanwhile, the total energy density W can not be properly calculated by theory by using the parameters of the external EM field irradiating the object, as the *as the constitutive relations for the medium are not known* [13b].

For the wave vector *k* in the medium, given by the usual expression [15]:

$$k = [\eta + i\kappa]\, \omega / c \qquad \dots (4)$$

where ω is the EM field frequency; c is speed of light; η is the refraction index of the medium; and κ is the extinction coefficient, the expression for the energy velocity v_e, in accordance with eq.(4.16) in [15], is

$$v_e = c /(\eta + c/(L\Gamma)) \qquad \dots (5)$$

Here, Γ is the parameter showing how fast the energy of the optical mode is converted into heat through Rayleigh dissipation function, and $L = c / (2 \omega \kappa)$ is the characteristic length of the decay of the intensity of the EM field with the distance along the propagation direction. The parameters η and κ in different materials can be precisely determined from the studies of optical reflections from the surfaces [3g]. For example, for steel gauge blocks in red light the refractive index η is 2.2 and κ=3.4; for tungsten carbide GB, η=3.4 and κ=2.4 [3b]. These values are in agreement with very accurate measurements of the phase change at optical reflection by optical interferometry [3a]. The velocity value v_e of the energy propagation in steel can be estimated from the present studies, when using the dependencies of **ΔT[1,2]**, obtained for different distances from the gauging surface. (These studies are similar to the ones resulting in the plots of Fig.5). From these studies the velocity v_e is found to be of the order of 10mm per minute for the steel block.

We can have also a reliable estimation of the wave momentum density **G** in the medium, which consists of the momentum density of the EM field and of the pseudomomentum density of the medium (see Eq. (3.21) in [15]). Pseudomomentum contains the contribution of the polarization, which is induced in the medium by the propagating EM field. In accordance with equation (4.32) in [15], the cycle-averaged value of the wave momentum density **G** in the propagation direction z of the plane wave is also related to the Poynting vector of EM field inside the medium and is given by the expression:

$$\langle \mathbf{G}_z \rangle = \mathbf{v_e} \langle W \rangle / (v_p\, v_{wm}) \qquad \dots (6)$$

where $v_p = c/\eta$ is the phase velocity of EM field and the velocity v_{wm} of the wave momentum current density is

$$v_{wm} = c/(\eta + c/(L\Gamma) + \kappa^2/\eta) \quad \ldots (7)$$

It follows from equations (3) and (5) that in case when $v_e << c$, the velocities v_e and v_{wm} are, practically, equal. So, in accordance with Eq. (6), the value of the z-component of the wave momentum density G_z is, approximately, equal to the ratio of the energy density $<W>$ and the value of the phase velocity v_p. Both parameters can be quite precisely determined from the experiments.

For the plane, transverse EM wave, the cycle-averaged values of the wave momentum current density T_{ji}, defined by equations (3.18) and (3.24) in [15], presents the sum, taken with the sign minus, of the Maxwell stress tensor [13a] and the product of the corresponding components of the EM field and of the arising polarization of the medium. The quantity T_{ji} describes the values of stresses and sheers, acting on the unit areas inside the artifact material [14b]. For example, the component T_{zz} is given by the relation [15]:

$$-<T_{zz}> = <W>(v_e/v_p \quad \ldots (8)$$

Under the same approximations, the total force density $<F_t>$, consisting of the Lorentz force density (which is acting on the particles) and of the time derivative of the EM field momentum density [15], can be presented by the expression:

$$<F_t> = [(1 + \eta^2 + \kappa^2)/(2\eta^2 L)] <W> (v_e/v_p) \quad \ldots (9)$$

Meanwhile, the cycle-averaged rate of the energy conversion into heat $<R_H>$ in accordance with continuity equation (2.17) in [15], written for the energy density of the coupled field-particle system, can be presented in a form:

$$<R_H> = <S_z>/L = v_e <W>/L \quad \ldots (10)$$

So, from equations (9) and (10) it follows that the cycle-averaged rate of the energy conversion into heat $<R_H>$ is linearly related to the total force density $<F_t>$ for dielectric material with arbitrary level of losses [15]. So, *the propagation of thermal energy and momentum are always accompanied by stresses and deformations in the material that can be estimated from the experimental data.*

But the theoretical model in [15] uses an approximation of a simple Lorentz oscillator, which is characterized by an instantaneous, linear response to the external EM field. So, the hysteresis effect, which forms the basis of the thermal evolution process, is beyond the scope of this theory. In this respect it can be noted here that the thermal hysteresis effect in the bulk material was first observed for the external heat source in a 900mm steel GB (see Fig.9 in [3f]). Also, from the experimental dependence of Fig.8 in [3h]) it follows that the heat energy (described by the energy density W) in a homogeneous, well thermally isolated material artifact can propagate large distances with very small damping. It means that when in the experiments presented here, the gauge block surface is irradiated by an EM field of the PRT, then, in accordance with [15], the wave momentum density **G** of a coupled field-particle system should be detectable at any point of a 100mm block. But if the total momentum, consisting of the momentum of the charged particles and the momentum of the EM field, is not equal to zero, then some part of the total momentum will be inevitably reflected from the boundary, and the reflected total-energy and momentum densities will produce an additional energy flux to the unit volumes of the artifact in the vicinity of the boundary. From this we can conclude that the general theoretical observation of A. Einstein about the importance of taking into account the surface energy has been confirmed experimentally for a particular case of the thermal surface energy **ΔT[1,2]** (see Figs.2-5).

Here, we are to note also that the *velocity error studies* in thermal systems, described in [3a, 3b] and performed under thermally non-equilibrium conditions, do present a particular kind of the of the thermal hysteresis effect, when we studied the propagation of the oriented part of the thermal energy in the bulk material under the influence of an external heat source. There, the energy transfer was studied in a specially designed system, in which the energy propagation vector lied along the same line both for heating and cooling periods of the evolution process (as a result of the spatial symmetry of the system), and the time constant of the system exceeded 20 hours. When the input of the thermal energy to such system is constant and when the quasi steady-state phase of the thermal process is realized ($V_1 = V_2 = V$), then the temperature difference between the locations of two thermometers inside the material artifact can be described by the velocity error correction $V\tau$, where τ is the propagation time of the thermal signal between the locations of the thermometers [3a-3c].

It is also worthy of note here that under the approximation of a plane TEM field, adopted in section IV of [15], the z-component of the wave momentum can be described by equation (6), and the rate of the energy conversion into heat by equation (10). The parameters $<W>$ and L, which enter these equations and correspond to the wave, reflected from the gauging surface and propagating in the z-direction away from the boundary, can be determined quite accurately from the experimental plots of Figs. 2a, 2b, 6 and 7. Indeed, these plots are obtained from the differential energy measurements, performed synchronously at the specified time intervals for several distances from the gauging surface, and the averaging procedure of the

results of the measurements in x,y-directions has been used. From these plots it follows, for example, that the energy density <W> is changing continuously in time and in space and represent one of the parameters of the evolution process, which is irreversible in time, has no symmetry in space and exhibits a clearly detectable hysteresis effect. Some other parameters of this process are: rate of energy conversion into heat R_H, the wave momentum density $\mathbf{G}$, the total force density $\mathbf{F_t}$ and tensor quantity $\mathbf{T_{zz}}$, which corresponds to the force acting in z-direction on the unit area inside the material that is oriented in the same direction. All *these parameters*, which can be approximately described by the relations (6),(8-10), *correspond to the new properties of the artifact medium that are acquired as a result of interaction with the external energy and momentum sources of the environment*. All of these parameters of the evolution do not simply exist under the thermal equilibrium conditions. So, we have an evolution process, when the properties of a material artifact, representing the part of the interacting system are changed in response to the variations of the external conditions. Such process in literature is sometimes called as a "self-ordering" process, but it is much more appropriate to call this process as *synthesis*, as in this meaning it was first introduced into philosophy by the XVIII century German philosophers H. M. Chalybäus and J. G. Fichte and is commonly used nowadays in Chemistry. Indeed, *the thermal evolution process is the simplest one, when the material artifact changes its properties and characteristics (see Figs.9a and 9b) as a result of the exchange with the environment of only three material quantities: linear momentum, angular momentum and the energy, which are delivered to the object by the external EM field*.

In general, the irreversible in time changes of the properties of the material objects, subjected to hysteresis evolution process, are well known in many fields of Natural Science. Some example results in case of ferroelectric and ferromagnetic materials were presented above in section 2.2. But, probably, the most spectacular and well studied example is our planet [21]. As a result of interaction with material objects of the Universe and evolution processes in the Earth, the pole of the planet is in continuous motion with respect to the Earths crust, with well-detected daily, unpredictable wobble of the pole, with the presence of the quasi-periodic components (characterized by the durations 1.0 and 1.2 years) and with the relatively slow secular drift of the pole along the meridian 80° [21]. When these pole variations are combined with the variations of the magnitude of the angular velocity of the Earth's rotation that have "random", quasi-periodic and secular components, the total effect, obtained during 50 years of continuous observations, is equal to -34 seconds relative to the time scale of atomic standards [21]. So, as a result of unpredictable, systematic changes in the Earth's rotation, the amount of the energy, received from the Sun by the objects on the Earth's surface is continuously changing, and *as a consequence of the violation of the superposition principle for the thermal surface energy, all the thermal processes on the Earth are definitely irreversible in time*. For example, the measurement of Fig.1, performed for the duration of several days, presents a *spiral type curve*, for which the form and amplitude of each cycle is slightly different as a result of some input of momentum and energy from the time irreversible environment, and *also as a result of constant changes of the properties of the particular* artifact. Even without the realization of the square-wave modulation of the energy by the PRT, we shall have the same spiral type of the thermal evolution process of the system as a result of the daily, seasonal and secular variations of the level of EM radiation of the Sun on the Earth's surface. Naturally in this case, the span of the spiral will be much smaller, as a sophisticated air temperature control system was used in our experiments and the effective thermal isolation of the artifact from the environment was realized inside the Dewar. Summarizing this part, we can conclude that *the demonstration of the thermal evolution process in the form of a spiral under the influence of the infinite number of the continuously changing parameters presents an experimental confirmation of the basic concepts of the dialectics of the Ancient Greek philosopher Heraclitus of Ephesus (6-5 centures BCE)*.

It should be also noted here that the time irreversible evolution processes of material objects are well known in Astronomy for many years. So, that the concept of the arrow of time was introduced in 1927 by the British astronomer Arthur Eddington. According to A. Eddington, the distinguished direction of the time can be determined by the study of organizations of material objects in the Universe. Thus, the lack of symmetry in time, demonstrated here for the thermal evolution process, is an agreement with the experimental studies of ferromagnetic [9d] and ferroelectric materials [9e], is an agreement with the huge number of astronomical observations (including the studies of the Earth's rotation process [21]) and with all biological studies, naturally including the fundamental discovery of Ch. Darwin and A. R. Wallace [22].

From the presented studies we can conclude that the discovery of the thermal surface energy has a fundamental impact on the Electrodynamics in general. Indeed, as described by N. Ramsey theoretically and first shown experimentally by P. Kusch, the process of interaction of the EM field with the quantum system is always nonlinear [23]. So, from our experimental results and the equation (V, 55) in [23] it follows that *if in the "thermal" range of energies of EM field for the process of interaction of the field with matter is irreversible in time and exhibits hysteresis effect, then the hysteresis effects should be observed in the whole range of energies of the*

EM radiation, *if the proper accuracy of measurements can be realized in the corresponding range*. Here, it is also worth noting that our experimental demonstration of the invalidity of the superposition principle for thermal systems is in agreement with the experiment of P. Kusch [23], showing the fundamental property of nonlinearity of atomic systems that are exposed to EM radiation. P. Kusch used atomic beams, monochromatic EM radiation, and performed the analysis of the spectral response of the system. While for the thermal broad-band radiation and metallic artifacts (used in our studies), the amplitude analysis of the interaction of the two energy sources with material artifact is preferable, and it is definitely simpler from the point of view of the interpretation of the results of the measurements. But both approaches can be considered as complementary for the studies of the nonlinearity of the field-particle system.

It should be also specially emphasized that the violations of symmetries in space, which are clearly demonstrated by the plots of Figs. 1-3 and 6 in case of thermal evolution processes, are also known from other fields of Natural science. Similar effects were reported earlier in the experimental studies of the hysteresis effects in ferromagnetic [9d] and ferroelectric [9e] materials, as discussed above in section 2.2. The lack of spatial symmetry is well known in biology, and many examples can be found in the University text-book [24]. Here, we find: "Proteins consist of chains of amino acids. The one that comes from the living thing is called *L-alanine. All proteins use L-alanine exclusively* [24]". So, in biology the violations of symmetries in time and space are well established facts, and the importance of the prehistory of the system on its future evolution is clearly realized. In theoretical physics it is acknowledged nowadays that the law of conservation of parity, following from quantum-mechanical equations of the weak decays under reflection [24], is in obvious contradiction with numerous experimental observations. And one of the first experimental observations of the violation of the reflection symmetry was performed using β–disintegration of radioactive isotope of cobalt in strong magnetic fields at low temperatures [24]. As pointed out by R. Feynman himself: "*Fundamentally, the law of reflection symmetry, at this level in physics, is incorrect*"[24]. But in accordance with the approach of K. Popper and A. Einstein (that are generally accepted by the physical community nowadays), if a theory is in contradiction with a single experiment it should be considered as the falsified one (or the wrong one).

The violations of symmetries in time and in space are known in Astronomy for a long time. Relatively recent astronomical studies of the radiation levels in the Universe, performed with radio-telescopes, clearly demonstrated the anisotropy of the Universe [25]. Here, it is worth noting that our experimental observations of violations of symmetries in time and in space in case of thermal evolution processes are in agreement with more general asymmetries [26, 27], which have been predicted and explained theoretically by the prominent Russian physicist A. D. Sakharov in case of the physics of elementary particles [27].

It should be specially emphasized that the results of our studies and conclusions are in deep agreement with the fundamental discovery of Charles Darwin and Alfred Russel Wallace, first formulated in their article "On the Tendencies of Species to form Varieties, and by Perpetuation of Varieties and Species by Natural Means of Selection" [22]. In this paper, the effect of the long-term influence of the surrounding Nature on the evolution process of living species (organisms) has been unambiguously established for the first time. In this paper, we have demonstrated that basically similar *thermal evolution process, with the continuous creation of the new properties of the material object, does occur continuously in non-living material objects under the influence of infinite number of material objects, which are (at least) partially correlated and which produce a common Poynting vector, interacting with the investigated material artifact*. Naturally, in case of living objects the evolution process due to interaction with the outside Nature is much more spectacular, as besides the energy and momenta, the living objects absorb from environment different material objects, starting with atoms and molecules and finishing with different gasses, liquids and dissolved minerals. The evolution process in living organisms has more manifestations, can be observed even with "naked eye", but its detection requires usually very long observation time intervals. Meanwhile, in the presented experiments on the thermal evolution process, as a result of the use of the sophisticated measurement procedure, the change of the properties of the material artifact can be clearly detected within a couple of minutes (see Figs. 10 and 11).

It can be also emphasized that *in case of our very precise experiments with water triple point (WTP) cells* [3a], when the ensemble of different isotopes is located in the field of gravity, each isotope has different temperatures of phase transitions, and the whole system is exposed to super-cooling in the process of creation of the ice mantle, *the thermal evolution process is much more complicated than in metallic blocks, and has, at least, three different time scales.* For example, the record, presented by the plot of Fig.8a in [3a], demonstrates the part of the evolution process with the smallest time scale. It is associated with the gradual changes of the isotopic composition and chemical impurities in a thin water layer between the ice mantle and the thermometric well in a short period of time after the thermal shock, which makes possible the ice mantel to rotate freely relative to the thermometric well. As in case of the WTP cells, the temperature measured by thermometer differs by less than 0.2mK from the

temperature of the triple point in water (due to hydrostatic pressure effect), the sensitivity of temperature on different influence factors is much higher than in metallic blocks. So, the thermal differential measurements are not necessary, and the study of the evolution process can be performed with the use of only one thermometer. It is also worth noting here that the evolution process in WTP cells has two additional hysteresis effects, which are detected at longer observation times. The first effect is associated with origin of the water (arctic or equatorial) [7a], and the second (with much smaller characteristic time) depends on time interval, elapsed after the creation of ice-mantle, and the pre-history of keeping the cell and its use in temperature calibrations.

As pointed out above, the thermal hysteresis effect has many common features with hysteresis effects in ferromagnetic and ferroelectric materials, associated with the change of the direction of the constant magnetic or electric fields. But as in our experiments we study the interaction of EM radiation with the ensemble of atoms, which are forming material artifacts, we can establish correspondence between our experimental results and the standard technique of laser cooling of the ensemble of the free moving neutral atoms [28] that is currently used in all modern time and frequency fountain standards [20]. It is known from laser cooling experiments that if the frequency of the laser light is red-shifted (i.e. lower than the mean frequency emitted by a stationary atom), then the free atoms are cooled, and when the frequency is blue-shifted, the atoms are heated. If we have an atomic beam propagating in vacuum device, then the blue-shifted resonant radiation of sufficient intensity can easily remove the atoms from the measurement zone. Similar effects are demonstrated here by the plots of Figs.3a-3b. If the average energy of the external thermal radiation is higher than the average energy, radiated thermally by the artifact, then the temperature of the artifact is rising and there is the excessive energy flux and the excessive force, acting on the charged particles absorbing radiation, in the direction of the nearest gauging surface. If the average energy of the external radiation is lower (frequency is red-shifted) relative to the average energy value of the emitted radiation, then the artifact is cooled, and the energy flux and the force are directed from the gauging surface. These properties are properly described by expressions (8) and (9), which show that the direction of the stresses in the artifact and the direction of the force, acting on the unit volume inside it, are both defined by the direction of the energy propagation vector. And as the energy density inside the artifact, in accordance with presented experimental studies, is changing significantly in space for a particular specified moment of time (Fig.4a), and is changing in time for the specified positions in space (Fig. 5a), then the forces and the stresses in the artifact, described by the equations (9) and (8), are continuously changing in the evolution process both in space and in time. But the forces, acting on the unit volumes, are responsible for the mass transfer of the particles inside the artifact, and the stresses and shears are responsible for the deformations inside it. Thus, the one dimensional theory of [15] cannot describe in detail 3-dimensional experiment, but it clearly predicts that propagation of energy and momentum inside the artifact is inevitably accompanied by the complicated processes of material deformations and free carriers mass transfer, both evolving in time and in space. So, any adequate thermal conduction theory has to describe in detail the mass transfer and deformation processes, which are always the necessary components of the thermal evolution process.

As it follows from the previous discussion, the *rigid body approximation* is not sufficient for the precise description of the propagation of energy and momentum in thermal processes. On the other hand, the force of the EM pressure, which also changes with distance L and in time, does produce the systematic motion of free electrons in the artifact as a result of the momentum acquisition of the EM field in the process of the EM energy absorption. And the systematic motion of free electrons in the presence of the external force results in the *mass transfer* in the thermal evolution process that must be taken into account in an adequate heat conduction theory. The systematic motion of electrons also results in the additional lattice deformations, which can be can be understood and described theoretically on the basis of the electron-lattice interaction [29]. Most probably, the lattice deformations are responsible for the fast, negative part of the dependence $\Delta V[1,2]$ on time, shown in Fig.3c. It follows from Fig.3c that the forms, magnitudes and time scales are, practically, equal for the heating and cooling periods of the modulation cycle. The total time of the observation of the effect in the induced differential thermal velocities $\Delta V[1,2]$ is about 25 minutes. It is much shorter than the time interval of several hours, which is necessary for the acquisition of the steady-state condition between the block and the environment (see the R3 temperature dependence in Fig.1). At the beginning of the heating period of the cycle, the electrons are moving in a systematic way, as a result of the uncompensated force, associated with the absorption of energy and momentum of the field-particle system. At the beginning of the cooling period, when the external force is switched off (or diminished), the electrons have to return to their steady-state, equilibrium positions as a result of the uncompensated force, produced by the deformed lattice whose magnitude has been tuned to compensate the higher level of the forces, acting on the unit volumes inside the artifact and described approximately by eq. (9).

In general, the process of the gradual changes of the properties of the material standards in the presence of stresses and deformations is known in many fields of physics, where accurate measurements are available. For example, in interferometric length measurements, the measured length of the material standard (gauge block) is found to depend on the level of deformations [3b, 3c], arising in the wringing procedure of the reference plate to the gauging surface of the block. So traditionally for optical interferometry, the length of the gauge block is defined in the wrung condition. Also, to minimize the effect of deformations, arising in the field of gravity, on the optical length measurements, the support of a long gauge block inside the optical comparator is performed at the special (Airy) points. Using modern fringe-pattern analyzing interferometers it is possible to study the process of the build-up of the wringing deformations of the surface of the reference plate in time and in space [3c]. As a common practice, the length measurements by optical interferometry in international comparisons are realized after a certain time interval, when the variations of the measured length in time due to the wringing procedure are becoming less, or comparable with the total uncertainty of the length measurement. The method, resulting in the crucial decrease of the wringing deformations on the result of the interferometric length measurement, has been also developed [3a].

The effect of the presence of stresses in the solid state parts of temperature standards on their performance is also well known. In WTP cells, the temperature standards that are used for the definition of the unit of temperature – Kelvin, the stresses in the ice mantel, which are produced in the process of the ice crystallization from the super-cooled very clean water, can produce the systematic shifts to lower temperatures. These shifts are usually much larger than the resolution of modern temperature-measuring equipment. So, the WTP cells are suitable for the accurate comparisons only after the relaxation of stresses, by keeping the standard for several days at the temperatures, which are slightly below the triple point value. In temperature standards, using the phase transition in pure metals, the effect of deformations and stresses on the reproduced temperature can be an order of magnitude larger than in the WTP cell. But probably, the most spectacular demonstration of the effect of stresses on the properties of the matter is known from material science. It is found that in mechanical tests, performed under the multiple mechanical deformations variable in time, metallic and plastic artifacts demonstrate specific hysteresis effect: they are getting "tired" and dismantle to smaller pieces when subjected to stresses, an order of magnitude smaller than stresses, which they can withstand at the beginning of the test. As the mechanical perturbations have EM origin, then combining the observation of the material science with the result of this study that the propagating EM field inevitably produces stresses and deformations inside the irradiated material artifact, we can infer that all the material processes under the typical Earth's conditions should be considered as transient: there is a period of creation and growth of material object, there is a period of time when its properties and parameters are changing very slowly, and there is a period of relatively fast decline and demolishing of the object. In this we can see common features with the evolution of the living species known in Biology. And it is worth special note that all these experimental observations are in agreement with the principles of dialectics of Heraclitus, which were concisely formulated by his disciples in the form: "everything is continuously flowing and changing; no person steps in the same currents (river) twice; no one can experience the state of death twice".

We can also consider that our experimental results present some clarification to the famous philosophical triad (thesis – antithesis - synthesis), which was introduced by the German philosopher H. M. Chalybäus and then was greatly elaborated by J. G. Fichte. In the presented thermal measurements, thesis and antithesis, which are to describe the opposite properties of the entity that coexist simultaneously in a material object, correspond to the two types of internal energy. The first type of the internal energy, which is characterized by the mean value of the momentum of the field-particle system equal to zero, represent the result of a long-term evolution process of the hysteresis type under the influence of a huge number of external sources of EM radiation. This type of internal energy can be quite precisely described by a random quantity. The other type of the internal energy, complementary to the first one, corresponds to the thermal surface energy and represents the oriented motion of the field-particle system under the influence of a few, closely located heat sources. This type of energy is characterized by the total momentum, which is not equal to zero. As it follows from equations (2)-(10), the properties and parameters of the material object for these two types of motion of the field-particle system are also opposite, complementary to each other. There are two observations of primary importance, which are to be mentioned in this respect. First, in each elementary process of absorption or emission of the EM energy by free electrons inside the metallic blocks, the laws of conservation of energy and momentum are realized with tremendous accuracy, so that these two types of thermal energy should be considered as independent for short time observations. Second, as the skin depth for the external EM field, irradiating the surface of material artifact, is by orders of magnitude smaller than the characteristic length of the observation of the reflected wave from the boundary surface of the artifact (see Fig.5), these elementary processes are repeated a huge number of times [3d],

so that at time intervals of about 15 minutes after the increase of the PRT current, the physical laws of conservations of energy and momentum are no more valid for the blocks, as a consequence of the fact that the system is an open one. During this time interval, the absorbed momentum and energy of the external EM field are sufficient to realize a complicated pattern of lattice deformations and stresses inside the artifact, and to produce systematic displacements of free electrons. In accordance with the equations (2)-(10), the external field will produce a continuously changing in time and in space the distributions of wave-momentum and energy densities inside the artifact, which correspond to the oriented motion of the field-particle system and which can be observed simultaneously with the distribution of the thermal energy of the random type. Thus, the thermal evolution process, or the thermal synthesis (when following the terminology of J. Fichte), can be observed when the physical laws of the conservations of energy and momentum are no more valid, as the blocks (as any material objects in the Universe) present typical examples of the open systems. In this respect, our experiments present a spectacular illustration to the basic ideas of Heraclitus, who is famous for his insistence on ever-present changes in the Universe ("All entities move and nothing remain still.") and his cryptic utterances that "Ever-newer waters flow on those who step into the same stream", and "All entities come to be in accordance with this Logos". (Here, the term Logos corresponds to the present day concept of the Law of Nature).

It is also worth noting here, that there is an experimental observation of primary importance from the point of view of basic concepts, which has no analogue in Fichtean dialectics. But the corresponding philosophical concept can be found in the Ancient Indian (Jain) philosophy. It is known that the fundamental Jain doctrine (Anekantavada) states that all entities have infinite number of modes of existence and qualities, and, consequently, these entities cannot be completely perceived in all their aspects and manifestations by human beings as a result of the inherent, intrinsic limitations of a human person. Only the Kevalis – the omniscient beings – can comprehend the object in all its aspects and manifestations, while human beings are capable of knowing only some part of it. Consequently, no one view can claim to represent the absolute truth. This fundamental doctrine is clearly in agreement with the presented experimental studies. Indeed, it has been shown experimentally that for the TSE the principle of superposition is not valid, and this result is in agreement with P. Kusch experiments [23], demonstrating that quantum systems, interacting with EM field, are basically nonlinear systems. As a result of the TSE existence and the non-validity of the superposition principle, all the energy sources of the Universe are in continuous interaction with each other through hysteresis type evolution processes. And for the description of the TSE, as a part of this process, the Poynting vector, representing the vector sum of the corresponding vectors of all the external EM fields, has to be specified for each point of the artifact surface and for all the preceeding time moments, as the properties and parameters of the wave-momentum, propagating inside the artifact, are defined by the Poynting vector of the external field and the material (constitutive) relations for the artifact medium [6b, 8] (which have to be treated as evolution processes and which cannot be described by standard mathermatical functions due to the presence of the hysteresis effect). Correspondingly, the energy and momentum of the EM field, radiated by the artifact, depend, in particular, on the wave-momentum and energy distributions, existing inside the artifact for the specified time moment, and thus depend on the prehistory of the interaction between the external field and the artifact. As the radiated field amplitude is dropping with distance [6, 7], among the influence parameters for the resultant Poynting vector of the external field (even in the simplest case of a free space) we are to include all the distances from the energy sources to the artifact, the mutual orientations between each energy source and the artifact, mutual angles of observation and energy excitation levels of all the sources. So, for the achieved level of temperature measurements (of about 1μK), the number of energy sources, which are to be taken into account, is becoming enormous. Consequently, the number of the influence parameters, which increases much faster than the number of sources, is approaching infinity, even in a free space. In the standard case of the propagation of the part of thermal energy in a turbulent atmosphere, when the propagating energy represents the coupled field-particle system and the particles are also participating in the macroscopic turbulent motion in the field of gravity with the dissipation of energy and with the important mass transfer on the macroscopic level, the number of influence parameters should be considered as infinite one [4a]. The infinite number of influence factors inevitably results in the infinite number of modes of existence of a thermal system and in the infinite number of the manifestations of the thermal evolution process. Thus, in accordance with the Jain philosophy (which is kept in the memory of the mankind for several thousands of years) and in accordance with the results of the present experimental studies, the thermal evolution process has infinite number of influence factors, cannot be perceived in all aspects and in all of its manifestations by any human being, and, consequently, cannot be adequately described by any experiment. The experiment, under these conditions, is fundamentally incomplete, covering only a few of the influence factors. And *the most important result of this experimental study is that the original evolution process of the artifact is in irreversible way damaged by the*

presence of the measuring instrument, *with which the artifact forms a new coupled, interacting system*. And this is one of the experimental confirmations of the famous observation of N. Bohr that isolated system is a mere abstraction of theoretical physics.

Finally, we shall perform in a concise way the comparison of our experimental results with the main conclusions of the series of theoretical papers [17-19], dealing with the interaction of the EM field with an ensemble of atoms or molecules. It was R. H. Dicke, who first pointed out that that the standard theoretical treatment of spontaneous radiation by a dilute gas of molecules, in which it is considered that separate molecules radiate independently of each other, "is wrong in principle and many of the results obtained from it are incorrect"[17]. In accordance with [17-19], the parameters of the radiation process critically depend on the pre-history of the system and the type of its excitation. In [17] we find an important observation: "consider a gas of two-level molecules, all excited", when "an intermolecular spacing is large compared with the radiation wavelength. Assume that a photon is emitted in the k direction". Then it follows from [17] that "the radiation probability in the direction k has twice the probability, averaged over all other directions" that "corresponds to the ordinary, incoherent spontaneous radiation of a single molecule". Thus, such system of molecules has an angular correlation between the successively emitted photons [17].

In [17] it is specially emphasized that if the dimensions of the molecular system are large in comparison with the wavelength of the resonant radiation, *the coherent spontaneous decay of the system is still possible, but only in the single direction*, as "the polarization of the emitted or absorbed radiation is uniquely given by the direction of propagation". It is pointed out in [17] that if "in the present case the incident radiation is assumed to be plane with the propagation vector k, then after the excitation, the gas radiates coherently in the k direction". Because of the difference in the selection rules for coherent and incoherent spontaneous radiation (see equations (51) and (52) in [17]), "radiation in directions other than k tends to destroy the coherence with respect to the direction k "[9]. So, the *theoretical description of an ensemble of molecules, interacting with EM field [17], shows that the coupled field-particle system is the anisotropic one, and the considerations of space symmetry are not valid for it*. This is in strict agreement with our experimental results (see Figs.1-6).

The other basic property of the Dicke's ensemble of molecules, following from the theoretical analysis in [17,18], is the irreversible in time evolution process, described by the coherent spontaneous emission. In accordance with [18], the evolution of the ensemble of two-level atoms in equivalent positions can be described by the motion of the super Bloch vector R on the Bloch sphere, when in the process of this motion the length value R of this vector is kept constant. The X- and Y- components of R are related to the dipole moment of the transition and its time derivative, and describe (in combination with the field amplitudes) the interaction process in time between the field and the ensemble of atoms. The projection of the vector R on the Z-axis describes the dependence of the total energy of the atomic system in time, which is measured in terms of the energy difference $h\omega$ between the two levels of the unperturbed molecular transition. As the quantity R^2 is conserved in the process of the coherent spontaneous radiation [17, 18], its length value R is defined solely by the initial excitation of the system [18, 19]. It is demonstrated in [18] that "the rate of change of the super Bloch vector R is R times as rapid as the rate of change of the vector describing an isolated single atom". Under the approximations of [18], the expression for the total energy of the atomic system can be obtained in a closed form. The energy of the atomic ensemble decays in time as a negative of the hyperbolic tangent (see Eq. (35) in [18]), where the corresponding time scale is equal to $\tau_o/(2R)$ and τ_o represents the time of incoherent spontaneous decay of an isolated atom. The theoretical models in [17, 18] correspond to open systems, and the coherent spontaneous radiation process is inevitably terminated, when the vector R acquires the $-Z$ direction on the Bloch sphere, which corresponds to the zero value of the total dipole moment of the system [18]. In that state, in the general case, some part of the excitation energy is still trapped in the atomic system (as a consequence of the conservation of R^2). Thus, "the system of atoms can no longer radiate coherently, and the remaining energy will be dissipated by whatever incoherent processes are available to the atoms" [18]. So, when comparing this property of the solution in [18] with our studies of the interaction of the EM field with ensembles of atoms, forming rectangular metallic blocks, we can see that in both cases the processes are irreversible in time. And the lack of symmetry in time for all natural processes is nowadays explicitly formulated in the University text-books [2c]. It is interesting that this property of Nature immediately follows from the fundamentals of Ancient Greek and Indian philosophies that are kept in the memory of the mankind for thousands of years.

The other very important property of the theoretical solution of [18, 19], which has a complete experimental confirmation of our studies, deals with the huge number of influence factors, which determine the process of coherent spontaneous radiation. The EM field, which is acting on a arbitrary atom in the ensemble, is produced by all other atoms, and the expression for the near field of an ensemble of dipoles (see Eqs. (10)-(11) in [18]) depends explicitly on all the distances and on all the mutual orientations between the

specified atom and its partners. So, in accordance with [18], among the parameters, characterizing the system, we have all the separations between the atoms and their mutual orientations, that is, approximately, 2N influence parameters (where *N* is the total number of atoms in the ensemble). But as it is also necessary to specify initial conditions, and the super Bloch vector is defined as a vector sum of the Bloch vectors of individual atoms (in accordance with Eq. (19)-(20) in [18]), this procedure requires additionally 3*N* influence factors. If the number of atoms *N* is much larger than 1 (as it is in the majority of practical cases), then the number of influence parameters, in accordance with [18], in fast way approaches infinity. In the real experiments on the thermal evolution process the number of influence parameters is even greater, as for the experiments with material objects, performed in a free space, the additional information about the forms of material objects, properties of material properties and the solid angles, at which each object is seen from the positions of its partners, are expected to be added to the enumerated influence factors of the theoretical paper. At the resolution level of about 1μK (typical for the presented experiments), when the propagation in a turbulent atmosphere of the Earth of the wave-momentum, generated by the EM radiation of the Sun, had to be taken into account, the number of influence parameters in the thermal evolution process can be considered as infinite [9a]. So, the theories of [17, 18] and our experimental studies are presenting a clear support from the physical point of view to one of fundamentals of the Jain philosophy that the number of modes of existence of the processes in Nature is infinite, and so, no human being is capable to perceive such process in all of its manifestations.

In conclusion, we would like to discuss the N. Bohr observation that *in the general case* the theoretical description of the material objects, interacting with the surrounding material objects through different fields, is not possible. Here, it is necessary to remind again the letter of E. Schrödinger to W. Wien: "*Bohr's standpoint, that a space-time description is impossible*, I reject a *limine*... *The aim* of atomic research *is to fit our empirical knowledge* concerning it *into our other thinking*. *All of this other thinking, so far as it concerns the outer world, is active in space and time.* If it cannot be fitted into space and time, then it fails in its whole aim and one does not know what purpose it really serves". From the following short analysis it can be concluded that none of the E. Schrödinger's contributions to the Natural sciences can present a slightest trace of refutation to the fundamental N. Bohr's "standpoint". Indeed, the theoretical model for the Schrödinger's equation is an isolated stationary atom, and it is natural that the solution presents a set of stationary energy levels, specific for each type of atom. As in accordance with the solution, the atom can stay indefinitely long in each state, M. Born gave the statistical interpretation of the wave function, so that in case of a hydrogen atom, the square of the modulus of the wave function in the arbitrary point of space corresponds to the probability of finding the electron, bound to the proton, in the elementary volume, corresponding to that point of space. But in accordance with N. Bohr observation "Isolated material particles are abstractions, their properties being definable and observable only through their interaction with other systems". So, the solutions of the Schrödinger's equation should be compared with spectroscopic studies. And from numerous experiments in the field of optical spectroscopy it definitely follows that in hydrogen atom, for example, only the ground state is stable, and all others decay through spontaneous radiation to the ground state. For the first excited state in hydrogen, which is connected to the ground state by the electrical dipole transition, the life-time is about 1.5ns, and for the similar higher excited states the life-time is further dramatically reduced. Such short time intervals, representing the whole life-time, cannot be measured for a single isolated atom, as the modern electronic counters can have the necessary time resolution of about 1ns for the electrical pulses, which have not only a shorter rise time but which possess the electrical power, producing ~20mA current on 50 Ohms input of the counter that makes the signal observable against the background noise level. Also it should be taken into account that in mathematics, the concept of probability was introduced by C. F. Gauss for the description of *stationary processes*, as the measurement of the probability distribution with the infinite resolution, which is assumed for the presentation of the distribution function as a continuous one, requires an infinite time of the measurement process. Besides that, for the existence of the probability function it is necessary that any new procedure of the measurement of the probability function for any real process should give the identical results with the previous determinations. This is also only possible for stationary processes.

The discrepancies between the solutions of the Schrödinger's equation (supported by the statistical interpretation of M. Born) and the numerous experiments in the field of optical spectroscopy were so important, that in the year 1949 N. Bohr considered it necessary to publish in his article "Discussions with Einstein on Epistemological Problems in Atomic Physics" the following statement: "…evidently the interpretation of the spectral laws implies that an atom in an excited state in general will have the possibility of transitions with photon emission to one or another of its lower energy states. In fact, *the very idea of stationary states is incompatible with any directive for the choice between such transitions and leaves room only for the notion of the relative probabilities of the individual transition processes*".

There is also another fundamental discrepancy between the solutions of the Schrödinger's equation and the historic Stern – Gerlach experiment, performed before the publication of the Schrödinger's theory. In this experiment it was demonstrated that the beams of silver or hydrogen atoms in their ground state were splitted into two lines by inhomogeneous magnetic field, while the Schrödinger's theory predicted no splitting. In 1925 Uhlenbeck and Gouldsmit showed that the splitting in the Stern – Gerlach experiment and the fine structure of atoms in spectroscopic studies could be explained by the intrinsic angular momentum of the electron, which they called spin. And this new quantum number is not present in the Schrödinger's equation. But in accordance with Carl Popper – Albert Einstein principle, if a theory is in contradiction even with a single experiment, the theory should be considered as the falsified one.

Still, there is the general contradiction of the Schrödinger's equation with the properties of Nature. As the equation is of the first order in respect to time, the knowledge of the wave function at some arbitrary time moment is sufficient for the prediction of the state of the system at any past or even future time moment. This is in dramatic contradiction with numerous experimental observations in various natural sciences, such as biology (including the discovery of the evolution process by Ch. Darwin and A. R. Wallace in 1858), geology or astronomy, for example, including the arrow of time by Arthur Eddington of 1927 or fundamental Edwin Hubble experiment of 1929. Lee Smolin, in his book "Time reborn" writes: "The central principle is that time must be real and physical laws must evolve in that real time" [30a]. It is pointed out there that the idea of evolving laws is not new, and the American philosopher Ch. S. Pierce wrote in 1891:"Now the only possible way of accounting for the laws of nature and for uniformity in general is to suppose them the results of evolution". The same idea was expressed later by the famous British physicist Paul Dirac in a more general way [30a]:" At the beginning of time the laws of Nature were probably very different from what they are now. *Thus, we should consider the laws of Nature as continually changing with epoch, instead of as holding uniformly throughout space-time*." It is specially noted in [30b] that for "complex systems, involving large numbers of atoms, we must deal *with the laws of thermodynamics, which are not reversible in time*". And there is a special emphasis in [30b] that "*many laws in physics are time-reversible. One is Newtonian mechanics, another is general relativity, still another is quantum mechanics*". In this respect, of primary importance is the record of the conversation with A. Einstein by the Viennese philosopher R. Carnap [30c]: "Once Einstein said that the problem of the Now worried him seriously. *He explained that the experience of the Now means something special for man, something essentially different from the past and future, but* ***this important difference does not and cannot occur within physics. That this experience cannot be grasped by science seemed to him a matter of painful but inevitable resignation***". After this citation there can be no ambiguity about the meaning of Albert Einstein's historical observation:" *No amount of experimentation can ever prove me right; a single experiment can prove me wrong*". This is a rigorous refutation of all "Modern Physics", which is based on the fundamentally wrong, illusionary concepts of "symmetrical" space and "symmetrical" time, typical both for Relativity theories and Quantum mechanics. It was evidently clear to A. Einstein that the concept of space-time, introduced into his theories, was not only in contradiction with the principles of thermodynamics or E. Hubble experiment, but it was in the obvious disagreement with the natural processes, studied in many Natural sciences, such as Biology, Geology, Paleontology, Astronomy or even in some parts of Classical Physics (ferromagnetism, for example). And from the very formulation of A. Einstein statement it follows that every natural process depends on the infinite number of influence parameters, and so, in agreement with K. Popper observation, only the infinite number of experiments, performed under all possible conditions, can only prove the validity of a theory. To realize clearly what advancement in physics presented A. Einstein's statement, it is sufficient to compare it with some observations of R. Feynman made more than 10 years later. In the course of University physics he writes that "all electrons are the same, all protons are the same, all positive pions are the same; and so on" [24b]. And on the next page we read: "*Apparently it is true that the fundamental physical laws, on a microscopic and fundamental level, are completely reversible in time"*. Only much later, R. Feynman has changed crucially his point of view, musing in an interview [30a]: "*The only field which has not admitted any evolutionary question is physics. Here are the laws, we say*,…but how did they get that way, in time? So, *it might turn out that they are not same all the time and that there is a historical, evolutionary question*".

In the recent book [31], published by B. Greene, we can find: "*The concept of symmetry's breaking*, and its realization through the electroweak Higgs field, *clearly plays a central role in particle physics and cosmology*. Like the aether, a condensed Higgs field permeates space, sweeps through everything material, and as a nonremovable feature of empty space, it redefines our conception of nothigness" [31]. In [30a] we find a more general observation: "There can be no absolute time that ticks on blindly whatever happens in the world. Time must be consequence of change; without alteration in the world there is no time. Philosophers say that time is relational – it is an aspect of relations, such as causality, that govern change. Similarly, space must be relational; indeed, every property of an object must be a reflection of dynamical relations between it and other things in the

world". Further, in [30c] we find: "Leibniz's principle of *the identity of the indiscernibles* follows from the basic idea that physical properties of bodies are relational. What about two electrons, one of which is in the atom in the bedspread, the other on top of the mountain on the dark side of the moon? These are not identical particles, because their location is one of their properties. From a relational point of view, they are distinguishable by having distinguishable surroundings". It is clear that this statement is supported by the experiments of P. Kusch of the year 1954, when the non-linear character of interaction between EM field and atomic beam was established, using spectral type of measurements. It is in agreement with our studies, in which the non-linear properties were demonstrated with high precision in interaction of the ensemble of atoms in the solid state with EM field, resulting in a clearly observed hysteresis effect.

Also, in [30d] we read: "Darwinian evolutionary biology is the prototype of thinking in time, because at its heart is the realization that natural properties developing in time can lead to creation of genuinely novel structures". This observation is in complete agreement with our studies. As in natural selection in biology, in our experiments there is always infinite number of external parameters (as discussed in detail above). The *Poynting vector of the external field is the result of the interaction between the numerous material objects during the whole preceding time epoch, including the instant of the last measurement point in the series.* The EM field, re-emitted by the each object, depends on its own pre-history, simply as a consequence of the existence of the surface energy and the accompanying hysteresis effect. The evolution process in the studied artifact presents the synthesis process, occurring under the influence of infinite number of internal and external influence factors. And *the basic result of this study is the experimental demonstration that thermal evolution process, or thermal synthesis, means the appearance of the new properties in the object, which were not present in the parts of it before the open system absorbed the momentum and energy of the external EM field*. This is an experimental proof for the particular case of electromagnetic fields of more general principle of *driven self-organization* [30c]: "Flows of energy through open systems tend to drive them to states of higher organization". We can say that our experimental result presents an additional confirmation of the fundamental observation, known to the mankind thousands of years since the time of Ancient Buddhism, that the properties and the structure of material objects are defined by the processes, occurring inside and outside this object. We can also emphasize that the specific character of the time dependence, observed at any point of the artifact in its evolution process, gives a clear experimental indication that processes cannot be synchronized. This is in agreement with the well-known observation in medicine that the person dies when some vital organ (heart, for example) stops to function normally, and there are no "normal" cases when all the body of the person starts to disintegrate simultaneously to small parts just as a result of the general ageing of the organism of the person. From these observations it is becoming evident that the unambiguous, accurate description of material processes by mathematics in term of imaginary reference system, consisting of homogeneously spaced three "coordinate" axis's and one homogeneous "time" axis, with the assumed possibility to make infinitely accurate projection even of a point object (electron in a hydrogen atom, for example) on each axis, which is commonly used in theoretical physics, is only a primitive illusion. This expectation contradicts the fundamental Kurt Gödel incompleteness theorem, which says that "Any effectively generated theory, capable of expressing elementary arithmetic, cannot be both consistent and complete", and the observation of C. F. Gauss that the queen of mathematics is arithmetic. From the physics point of view this should be absolutely clear. Indeed, mathematics is incapable of description of the synthesis process under the influence of infinite number of external parameters, which are, at least, partially correlated and the properties of the object under consideration are continuously changing in time and in space. So, the mathematical description can be only applicable for relatively short periods of time, only when the properties of the object can be considered as invariable. And this time period can be only established from the comparisons with the corresponding experiment. In many cases the mathematical description is simply not possible. For example, in the studies of ferromagnetic properties of materials, the theoretical physics is unable to present any description of the process, resulting in the observation of the well-established experimentally hysteresis loops in different materials. The other important example follows from astronomical observations. Since 1887 it is known that the pole is moving with respect to the Earth [21]. These motions cannot be predicted theoretically; their measurement requires a continuous monitoring which started in 1900 [21]. Nowadays, besides regular optical measurements, the information about the daily rotation of the Earth relative to stars is obtained from laser ranging to the satellites and to the Moon, from very long baseline radio-interferometry of quasars and from the Doppler shift measurements between the clocks on the satellites and on the ground stations. And in spite of a huge number of experimental data, the theoretical predictions of the Earth's rotation with the precision, comparable with the uncertainty of the indicated experimental observations is found to be impossible [21]. The result is clear: the change in the properties of the Earth can be observed on the daily time interval. Something similar is observed in the presented studies.

The time of propagation of a thermal signal, measured at its half-amplitude value (due to significant dispersion in velocities), exceeds 30 minutes in a 1m steel gauge block. Meanwhile, the variation of the properties of the block under the application of the external EM field, is recorded in 1-2 minutes. Taking these observations into account, it is not very surprising the comparison in [30] that in theoretical physics, mathematics appears nowadays not as a queen, but as an ordinary room maiden.

The long term irregularities of the Earth's rotation were demonstrated in the first half of the 20-th century, by comparison with the orbital motion of planets in the Solar system (called Ephemeris Time) [21]. Since the middle of the last century the rotation of the Earth was in detail studied relative to the International Atomic Time (TAI) scale, and since January 1958 up to January 2011, 34 leap seconds have been added to the Universal Coordinated Time, which has the dimension of TAI second, to keep in agreement with the Earth's rotation to within 1 second. And it was found that sometimes, the leap seconds had to be added every consecutive year, and sometimes this interval (by unknown reasons) was increased to 7 years [21]. Combining these results with the presented experimental studies of the thermal evolution process, we are coming to the experimental confirmation of N. Bohr – A. Einstein statement that the material objects and the processes in Nature cannot be adequately described in terms of the time-space concepts of Modern Physics. The historic statement of A. Einstein that "No amount of experimentation can ever prove me right…" should be, probably, complemented by an important observation that in all natural process the enormous number of influence factors cannot be regarded as independent ones, as all material objects are participating in the generation of the resultant field, which reflects the process of interaction between them in all the preceding time epochs up to the moment of the last measurement or observation. Thus, the hysteresis effect presents one of the main, characteristic features of the evolution processes in Nature. The famous observation of Paul Dirac that "we should consider the laws of Nature as continually changing with epoch, instead of as holding uniformly throughout space-time" presents another, relatively late admission of the importance of N. Bohr – A. Einstein idea that the description of processes of Nature in terms of the existing space-time concepts of Modern Physics is not possible. Only, instead of K. Popper terminology (which was used by A. Einstein), P. Dirac preferred to use the notions of the 19th century American philosopher Ch. S. Pierce.

V. Acknowledgements

The author gratefully acknowledge financial support of the studies at INMETRO by the CNPq of Brazil and a fruitful cooperation with Igor Malinovsky during that period. The technical and moral support of our studies by the staff of INMETRO is highly appreciated and will never be forgotten. The author is grateful to members of Physical department of the Yeditepe University (Turkey) for useful discussions and for the afforded possibility to present some results of this study at the International Conferences.

References Références Referencias

1. L. Rosenfeld, "Niels Bohr's contribution to epistemology", Physics Today, **v.16**, No.10, pp. 47-53, (1963).
2. D. G. Giancoly "Physics for Scientists and Engineers", Prentice Hall, 3-ed., pp.958-959 (2000) [2a]; 3-ed., p.981 (2000) [2b]; 4-ed., p.543 (2009) [2c], p. (2009) [2d].
3. A. Titov, I. Malinovsky, H. Belaïdi, R.S. França, C.A. Massone, "Advances in interferometric length measurements of short gauge blocks", *Metrologia*, **37**, (2), pp. 155-164 (2000) [3a];.
   a) Malinovsky, A. Titov, J.A. Dutra, H. Belaïdi, R.S. França, C.A. Massone, "Towards sub-nanometer uncertainty in interferometric length measurements of short gauge blocks." *Applied Optics,* **38**, No.1, pp.101-112 (2000) [3b];.
   b) A. Titov, I. Malinovsky,"Advances and new techniques in length measurements by optical interferometry", pp. 1-6, XVIII IMEKO WORLD CONGRESS, September, 17 – 22, 2006, Rio de Janeiro, Brazil [3c];.
   c) A. Titov, I. Malinovsky and C. A. Massone, "Wringing deformation effects in basic length measurements by optical interferometry", *Proc. SPIE*, **5190,** *Recent Developments in Traceable Dimensional Metrology*, ed. by J.E.Decker, N.Brown, pp. 43-53, San Diego, CA, USA, 4-6 August, (2003) [3d];.
   d) A. Titov, I. Malinovsky and C. A. Massone, "Scientific basis for traceable dimensional measurements in a nanometer range: methods and concepts", *Proc. SPIE*, vol. **4401** Recent Developments in Traceable Dimensional Measurements:, eds. J. E. Decker & N. Brown, pp. 33-43, (2001) [3e];.
   e) A. Titov, I. Malinovsky, "Nanometrology and high-precision temperature measurements under varying in time temperature conditions", *Proc. SPIE*, **5879,** *Recent Developments in Traceable Dimensional Metrology*, ed. by J. E. Decker, Gwo-Sheng Peng, pp. 587902-1 – 587902-10,

San Diego, CA, USA, 31 July-1 August, (2005) [3f];.

f) A. Titov, I. Malinovsky, H. Belaïdi, R. S. França, M. Erin, "Primary level gauge block interferometers for realization of the SI length unit", Proc. SPIE, **5190,** *Recent Developments in Traceable Dimensional Metrology*, ed. by J.E.Decker, N.Brown, pp. 24-33, San Diego, CA, USA, 4-6 August, (2003) [3g];.

g) A. Titov, I. Malinovsky, "New techniques and advances in high-precision temperature measurements of material artefacts", *Can. J. of Scientific and Industrial Research*, vol.2, no.2, pp. 59-81(2011) [3h];.

h) A. Titov, I. Malinovsky, M. Erin, H. Belaïdi, R. S. França, "Precise certification of the temperature measuring system of the original Kösters interferometer and ways of its improvement", *Proc. SPIE*, **5879,** *Recent Developments in Traceable Dimensional Metrology*, ed. by J. E. Decker, Gwo-Sheng Peng, pp. 587904-1 – 587904-10, San Diego, CA, USA, 31 July-1 August, (2005) [3i].

4. E. Engelhard "Precise Interferometric Measurement of Gage Blocks", Proc. "Metrology of Gage Blocks", Symposium on Gage Blocks, August 1955, NBS, Circ.581, pp.1-20, 1957.
5. H. Darnedde, "High-precision Calibration of Long Gauge Blocks Using the Vacuum Wavelength comparator", Metrologia, **V. 29**, pp. 349-359, (1992).
6. "Documents Concerning the New Definition of the Metre", Metrologia, V.19, pp. 163-177, (1984).
7. J. V. Nicholas and D. R. White, "Traceable Temperatures", J. Wiley and Sons, 2-nd ed., pp. 96-111 (2000) [7a]; pp. 203-220 [7b]; pp. 13-18 [7c].
8. R. L. Rusby, *et al,* "A review of progress in the measurement of thermodynamic temperature", TEMPERATURE. Its Measurement and Control in Science and Industry, J. F. Schooley, Ed., Vol. 6, pp.9-14, American Institute of Physics, New York, (1993).
9. D. V. Sivukhin, "General Course of Physics", Physmatlit, Moscow, (2008):

   "Thermodynamics", **V2**, pp.44-71 ([9a]);
   "Thermodynamics", **V2**, pp. 85-110 [9b];
   "Thermodynamics", **V2**, pp.162-182 [9c];
   "Electricity", **V3**, pp.293-317 [9d];
   "Electricity", **V3**, pp. 159-172, [9e];
   "Electricity", **V3**, pp. 613-621 [9f];
   "Optics", **V.4**, pp. 466-480 [9g];
   "Optics", **V.4**, pp. 466-480 [9h].

10. Einstein, "Investigations on the Theory of the Brownian Motion", *Annalen der Physik*, **v.17**, No.3, pp.549-566, (1905).
11. A. Einstein, Theory of the Foundations of Thermodynamics", *Annalen der Physik*, **v.11**, pp.170-187, (1903).
12. E. R. G. Eckert and R. M. Drake, Jr., "Analysis of heat and mass transfer", International Student Edition, McGraw-Hill, Kogakusha Ltd, Tokyo, pp. 38-56, 1972.
13. J. D. Jackson, "Classical Electrodynamics", J. Willey and Sons, 1999, 3-ed, p.239-262 [13a]; p. 14 [13b].
14. D. J. Griffiths, "Introduction to Electrodynamics", Prentice Hall, 3-ed, 1999, pp.435-460 [14a]; p.346-348 [14b].
15. R. Loudon, L. Allen and D. F. Nelson, "Propagation of electromagnetic energy and momentum in absorbing dielectric", Phys. Rev. E, **55**, 1071 (1997).
16. C. Kittel, "Introduction to Solid State Physics", Wiley and Sons, 8-ed., pp.323-355 [16a]; p. 661 [16b] (2005).
17. R. H. Dicke, "Coherence in Spontaneous Radiation Processes", Phys. Rev., **93**, 99 (1954).
18. C. R. Stroud, Jr. and J. H. Eberly, W. L. Lama and L. Mandel, "Superradiant Effects in Systems of Two-Level Atoms", Phys. Rev. A, **5**, 1094 (1972).
19. F. W. Cummings and Ali Dorri, "Exact solution for spontaneous emission in the presence of N atoms", Phys. Rev. A, **28**, 2282 (1983).
20. V. Gerginov *et al*, "Uncertainty evaluation of the caesium fountain clock PTB-CSF2", *Metrologia*, **47**, p.65 (2010).
21. B. Guinot, "Solar time, legal time, time in use", *Metrologia*, **48**, pp. S181-S185 (2011).
22. Ch. Darwin and A. R. Wallace, "On the Tendencies of Species to form Varieties, and by Perpetuation of Varieties and Species by Natural Means of Selection", Journal of the Proceedings of Linnean Society of London, Zoology 3, **3** (9), pp.46-50 (1858).
23. N. F. Ramsey, "Molecular beams", Oxford, Clarendon Press, pp. 115-144 (1963).
24. R. P. Feynman, R. B. Leighton and M. Sands, "The Feynman Lectures on Physics", Addison-Wesley, 1-ed, **V.1**, Ch.52, pp.1-12 (1964).
25. G. Smoot, M. Gorenstein, and R. A. Muller, "Detection of anisotropy in the cosmic background radiation", Phys. Rev. Let. **39**, 898-903 (1977).
26. A. D. Sakharov, "Violation of CP Symmetry, C-Asymmetry and Baryon Asymmetry of the Universe", JETP Lett. **5**, 24 (1967).
27. A. D. Sakharov, "Topological structure of elementary particles and CPT asymmetry", in "Problems in theoretical physics", dedicated to the memory of I.E. Tamm: Nauka, Moscow, pp.243-247, (1972).
28. D. J. Wineland, R. E. Drullinger and F. L. Walls, Phys. Rev. Lett., **40**, 1639 (1978).
29. J. Bardeen, L. N. Cooper, and J. R. Schrieffer, Phys. Rev. **108**, 1175 (1957).

30. Lee Smolin, "Time reborn", Houghton Mufflin Harcourt, Boston – New York (2013), pp. XXV-XXVI [30a]; pp. 52-53 [30b]; pp. 214-219 [30c]; pp. 27-29.
31. B. Greene, "The fabric of the cosmos: space, time and the texture of reality", p. 268, Alfred A. Knopf, New York (2006).

Figure Captions

Fig.1. Simultaneous records of the resistance variations of the platinum resistance thermometer (PRT) and of the two thermistors R6 and R3, which are located symmetrically relative to the PRT on the surface of the gauge block (see insert). During the modulation cycle, the current in the PRT is kept at the level of 5mA for ¼ of the modulation period, and it is kept at 1mA for the rest part of the period. As the sensitivities of the thermistors are equal, these records demonstrate that the induced temperature variations in the channels are different for the asymmetric PRT position relative to the gauging surfaces. The location of one of the gauging surfaces of the block is shown by an arrow. (See text for other details).

Fig.2. The dependence on time of the thermal surface energy (TSE), represented by the difference in the induced temperature variations **ΔT[1,2]**, recorded in the two thermistor channels 1 and 2 during one modulation cycle. Dots and rhombi show the experimental points, obtained during the heating and cooling periods of the modulation cycle, respectively. Squares correspond to the reference points for the two adjacent cycles, and the linear fit to these points is shown as a solid line, with the corresponding expression presented in the inset.

Fig.3a. The thermal velocity dependence **V[R6]** as a function of time is presented for two modulation cycles under the experimental conditions of Fig.1. The experimental points corresponding to the heating period are shown as dots, while the cooling period is presented by rhombi and the reference points, corresponding to the last 30 minutes at I=1mA, are shown as rectangles. The solid line presents a 6-th order polynomial fit to all reference points for all modulation cycles in that experiment.

Fig.3b. The variations in time of the quantities **ΔV[R6]** and **ΔV[R3]**, which are measured relative to their 6-th order fits and which are averaged over a couple of modulation cycles of Fig.3a. The values of **ΔV[R6]** and **ΔV[R3]** are shown as dots and triangles, respectively, for the heating period of the modulation cycle, and as rhombi and circles, respectively, for the cooling period of the cycle. The reference points are shown as squares.

Fig.3c. Variations in time of the difference between the induced temperature velocities in the channels 1 and 2, **ΔV[1,2]**, observed during the heating period of the modulation cycle (dots) and during the cooling period of the cycle (rhombi). The reference points are shown as squares. The linear fit equation is presented in the inset.

Fig.4a. The dependence of the maximum value of the quantity **ΔT[1,2]** on the separation value of the axis of the thermistor R6 from the nearest gauging surface. The zero value of the quantity **ΔV[1,2]** corresponds to the symmetric position of the PRT on the block surface. Rhombi show the values of the Gaussian fit to the experimental points.

Fig.4b. The dependence of the maximum value of the quantity **ΔV[1,2]** on the separation of the axis of the thermistor R6 from the nearest gauging surface. The zero value of the quantity **ΔV[1,2]** corresponds to the symmetric position of the PRT on the block surface. (See text for other details).

Fig.4c. The dependences of the vector quantity **ΔT[1,2]** on time for the separations of the R6 thermistor from the gauging surface of 4.5mm (dots), 9mm (rhombi) and 13.5mm (squares). The reference points are shown as triangles.

Fig.5a. The dependences of the surface energy **ΔT[1,2]** on time, obtained for a tungsten carbide block when the R6 thermistor is close to the gauging surface of the block (curve 1), and when the R3 thermistor is close to the opposite gauging surface (curve 2).

Fig.5b. The dependence of the maximum value of the quantity **ΔT[1,2]** on the displacement of the PRT relative to the center of the gauge block surface.

Fig.5c. The dependences of the quantity **ΔV[1,2]** on the time interval, elapsed after the increase of the PRT modulation current, for two opposite cases of the thermistors positions: dependence 1 (shown by squares) corresponds to the separation of the R6 thermistor of 4.5mm from one of the gauging surfaces of the block, while the dependence 2 (shown by dots) corresponds to the case when the measuring system as a whole was shifted along the surface of the block, so that the separation of 4.5mm of the thermistor R3 from the other gauging surface was realized.

Fig.6a. The effect of the PRT power increment on the quantity **ΔT[1,2]**. Dependences 1 and 2 correspond to the separations of the R6 axis from the nearest gauging surface of L=4.5mm (dots) and L=13.5mm (squares), respectively. These plots establish the linear relation for the heating period of the modulation cycle between the two vector quantities: the Poynting vector of the external EM field and the quantity **ΔT[1,2]**, characterizing the TSE. The decrease of the magnitude of the TSE with the increase of the R6 separation from the nearest gauging surface is clearly demonstrated by the dependences (1) and (2). (See text for other details).

Fig.6b. The effect of the PRT power increment on the maximum value of the quantity **ΔV[1,2]**. Dependences 1 and 2 correspond to the separations of the R6 axis from

the nearest gauging surface of L=4.5mm (dots) and L=13.5mm (squares), respectively. These plots establish the linear relation for the heating period of the modulation cycle between the Poynting vector of the external EM field and the maximum value of the additional energy flux in the gauge block, described by the quantity **ΔV[1,2]**.

Fig.7. The thermal hysteresis loop for the quantity **ΔT[1,2]** that corresponds to the temperature records of Figs. 1 and 2. The heating period of the cycle (between the arrows 1 and 2) is shown by dots, while the cooling period of the modulation cycle (between the arrows 2, 3 and 1) is presented by rhombi. (See text for other details).

Fig.8. The records of the build-up in time of the thermal surface energy in a steel GB during the first 13 minutes of the heating period of the modulation cycle when the temperature differences between the channels **T[1,2]**, equal to 2.46mK (dots), 9.12mK (rhombi), 57.1mK (triangles) and 61.06mK (squares), were realized with the help of an auxiliary energy source in the Dewar. These dependences show that the principle of superposition is not valid for the external EM fields, and that the external energy source changes the dependence on time of the thermal evolution process, which is irreversible in time and specific for a particular point of the artifact.

Fig.9a. The dependence of the quantity **ΔT[1,2]**, measured 13 minutes after the increase of the PRT modulation current in steel gauge block, on the temperature difference **T[1,2]** between the positions of the thermistors R6 and R3. The maximum deviation of the measured values relative to the fit is 1.75μK and the standard deviation for a single measurement is 1.34 μK. (See text for other details).

Fig.9b. The dependence of the quantity **ΔT[1,2]**, measured 3 minutes after the increase of the PRT modulation current in steel gauge block, on the temperature difference **T[1,2]** between the positions of the thermistors R6 and R3.

Fig.10. The dependencies of the quantity **ΔT[1,2]** on time for the first 13 minutes of the heating period that were obtained for the tungsten carbide gauge block for the temperature differences **T[1,2]** of -1.72mK (dependence 1; dots), -7.2mK (dependence 2; squares) and -12mK (dependence 3; rhombi).

Fig.11. The dependencies of the quantity **ΔV[1,2]** on time for the first 13 minutes of the heating period that were obtained for the tungsten carbide gauge block (dependences 1 and 2) and for the steel block (3) for the temperature differences between the locations of the thermistors **T[1,2]** of -0,2mK (dependence 1; dots) and -17.2mK (dependence 2; squares). Note that the thermal evolution process is described by a complicated function of time, which is specific for the selected points inside the artifact, and whose form and magnitude depend on the direction and magnitude of the constant heat flux, created in advance by an auxiliary heat source. (See text for other details).

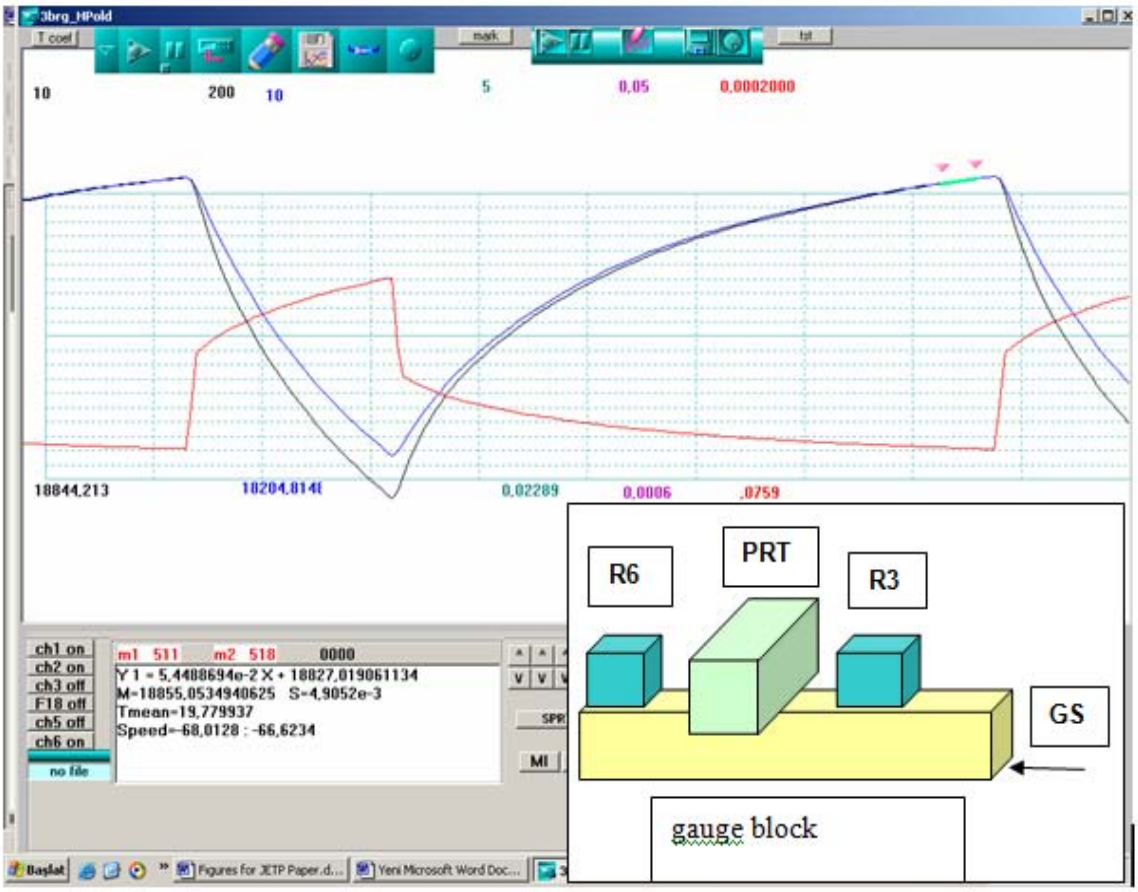

Fig.1 : Simultaneous records of the resistance variations of the platinum resistance thermometer (PRT) and of the two thermistors R6 and R3, which are located symmetrically relative to the PRT on the surface of the gauge block (see insert). During the modulation cycle, the current in the PRT is kept at the level of 5mA for ¼ of the modulation period, and it is kept at 1mA for the rest part of the period. As the sensitivities of the thermistors are equal, these records demonstrate that the induced temperature variations in the channels are different for the asymmetric PRT position relative to the gauging surfaces. The location of one of the gauging surfaces of the block is shown by an arrow. (See text for other details)

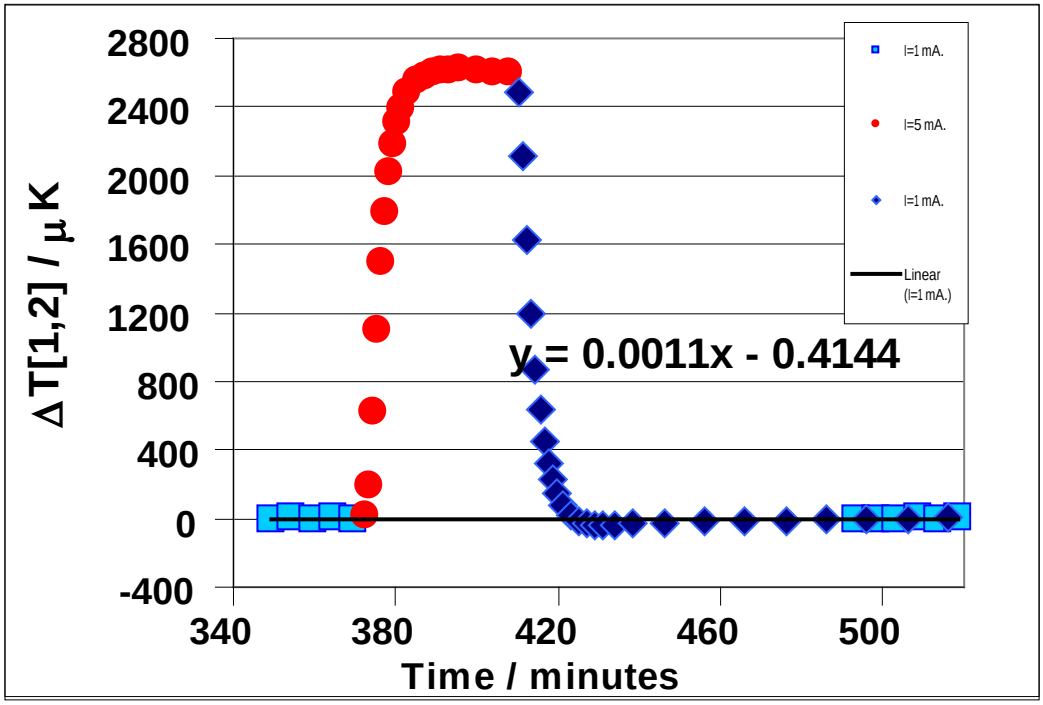

Fig. 2 : The dependence on time of the thermal surface energy (TSE), represented by the difference in the induced temperature variations **ΔT[1,2]**, recorded in the two thermistor channels 1 and 2 during one modulation cycle. Dots and rhombi show the experimental points, obtained during the heating and cooling periods of the modulation cycle, respectively. Squares correspond to the reference points for the two adjacent cycles, and the linear fit to these points is shown as a solid line, with the corresponding expression presented in the inset

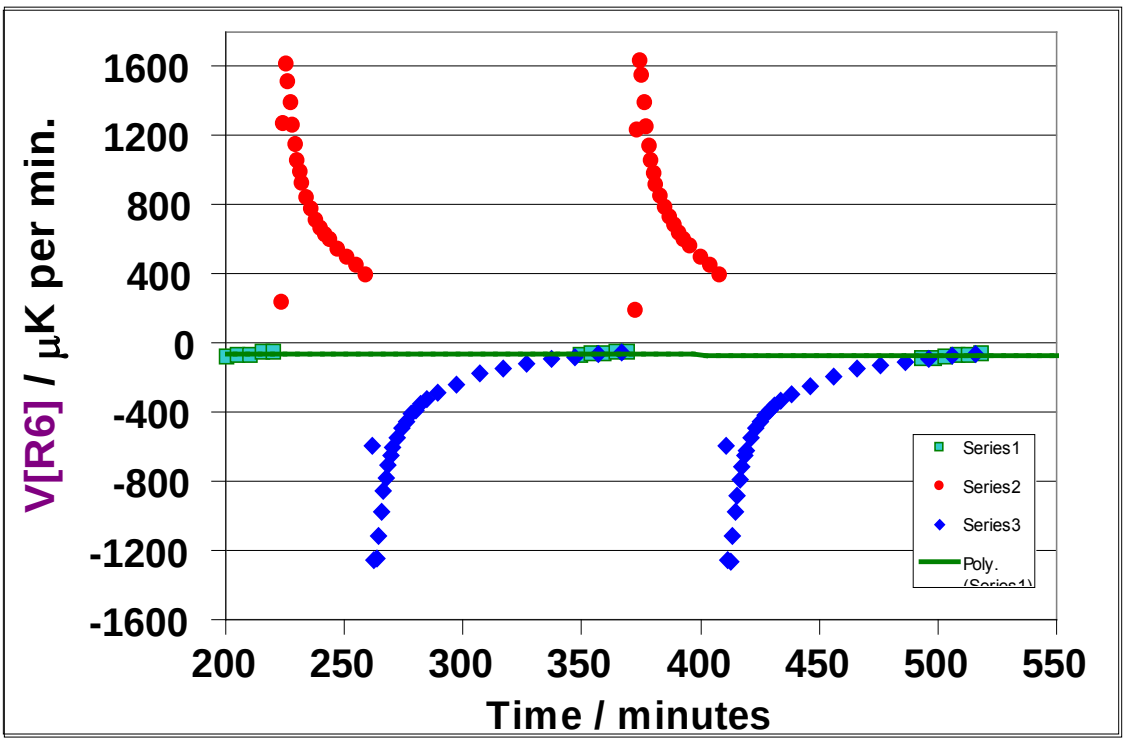

Fig. 3a : The thermal velocity dependence **V[R6]** as a function of time is presented for two modulation cycles under the experimental conditions of Fig.1. The experimental points corresponding to the heating period are shown as dots, while the cooling period is presented by rhombi and the reference points, corresponding to the last 30 minutes at I=1mA, are shown as rectangles. The solid line presents a 6-th order polynomial fit to all reference points for all modulation cycles in that experiment

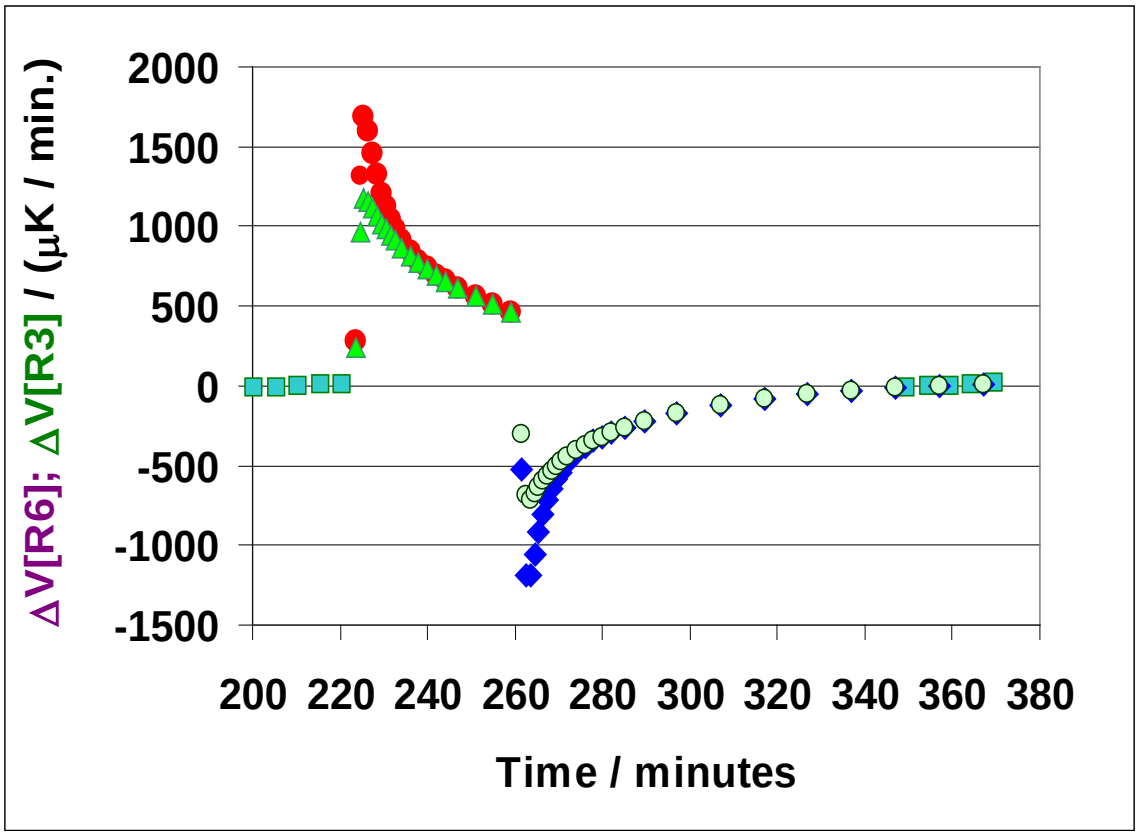

Fig. 3b : The variations in time of the quantities **ΔV[R6]** and **ΔV[R3]**, which are measured relative to their 6-th order fits and which are averaged over a couple of modulation cycles of Fig.3a. The values of **ΔV[R6]** and **ΔV[R3]** are shown as dots and triangles, respectively, for the heating period of the modulation cycle, and as rhombi and circles, respectively, for the cooling period of the cycle. The reference points are shown as squares

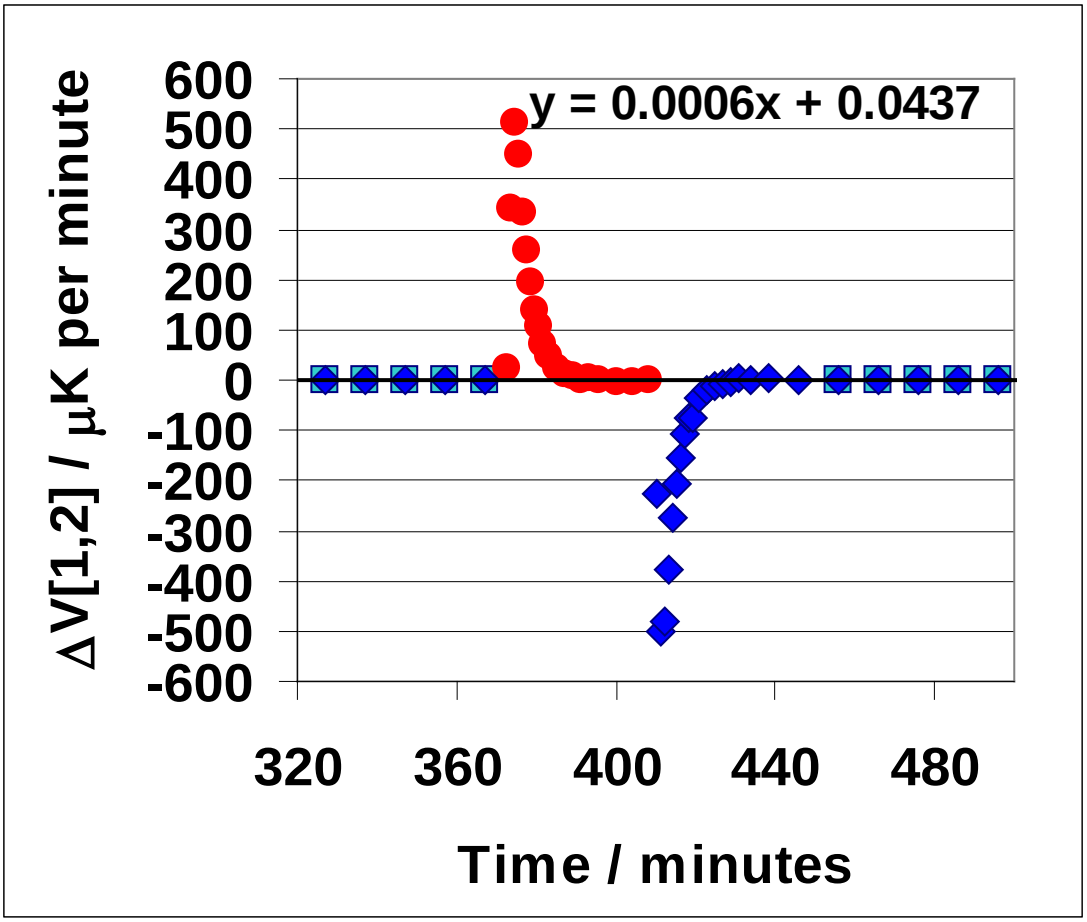

Fig. 3c : Variations in time of the difference between the induced temperature velocities in the channels 1 and 2, **ΔV[1,2]**, observed during the heating period of the modulation cycle (dots) and during the cooling period of the cycle (rhombi). The reference points are shown as squares. The linear fit equation is presented in the inset

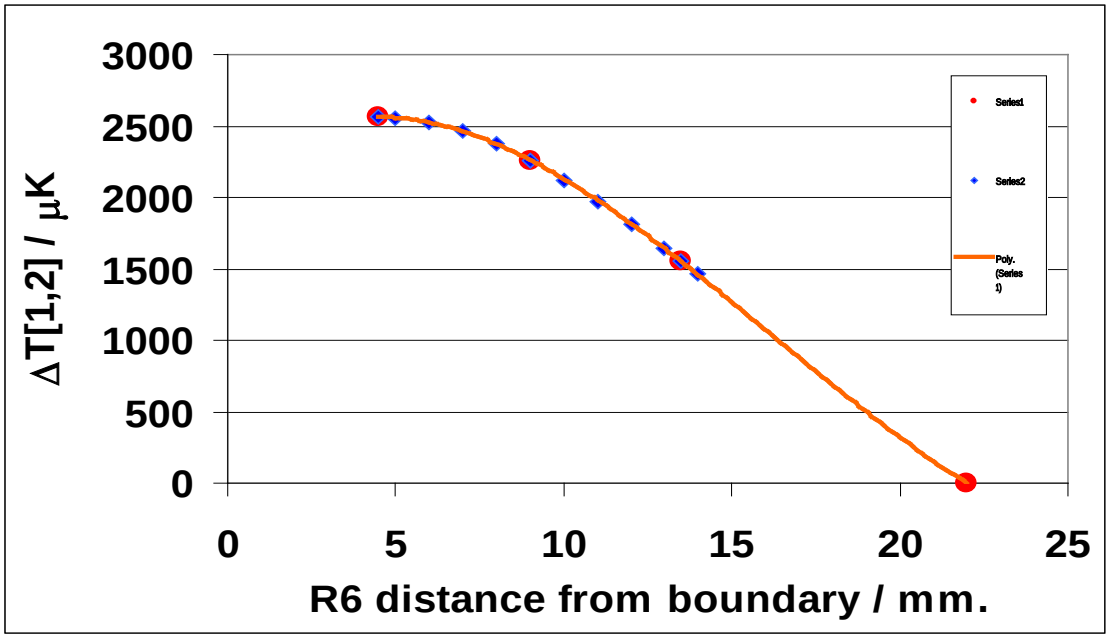

Fig. 4a : The dependence of the maximum value of the quantity **ΔT[1,2]** on the separation value of the axis of the thermistor R6 from the nearest gauging surface. The zero value of the quantity **ΔV[1,2]** corresponds to the symmetric position of the PRT on the block surface. Rhombi show the values of the Gaussian fit to the experimental points

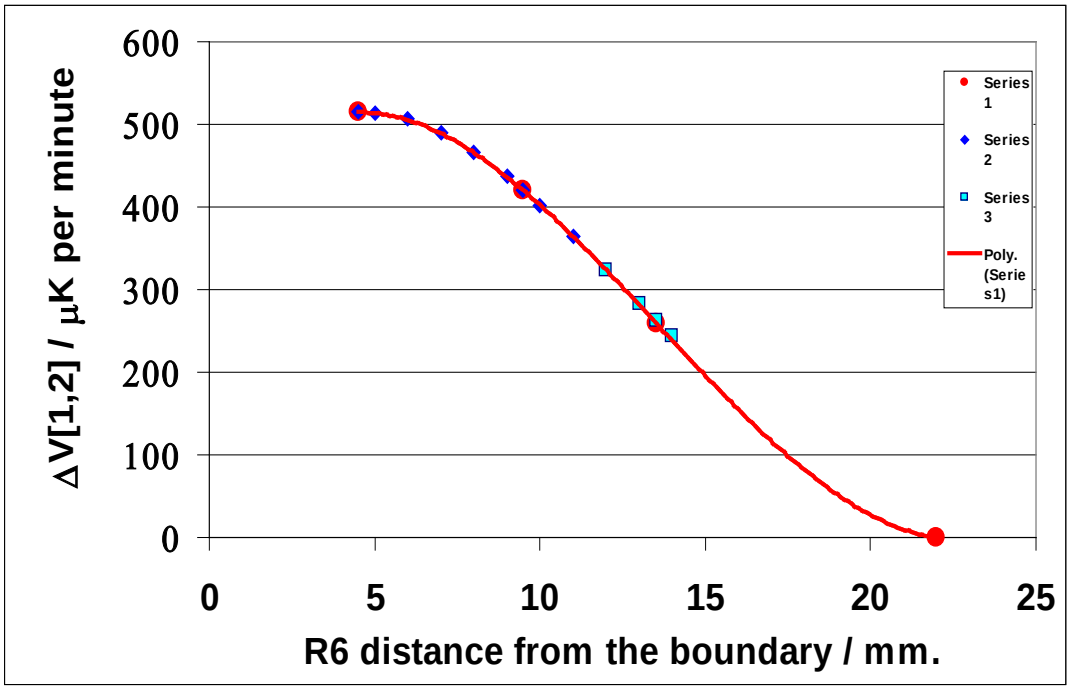

Fig. 4b : The dependence of the maximum value of the quantity **ΔV[1,2]** on the separation of the axis of the thermistor R6 from the nearest gauging surface. The zero value of the quantity **ΔV[1,2]** corresponds to the symmetric position of the PRT on the block surface. (See text for other details)

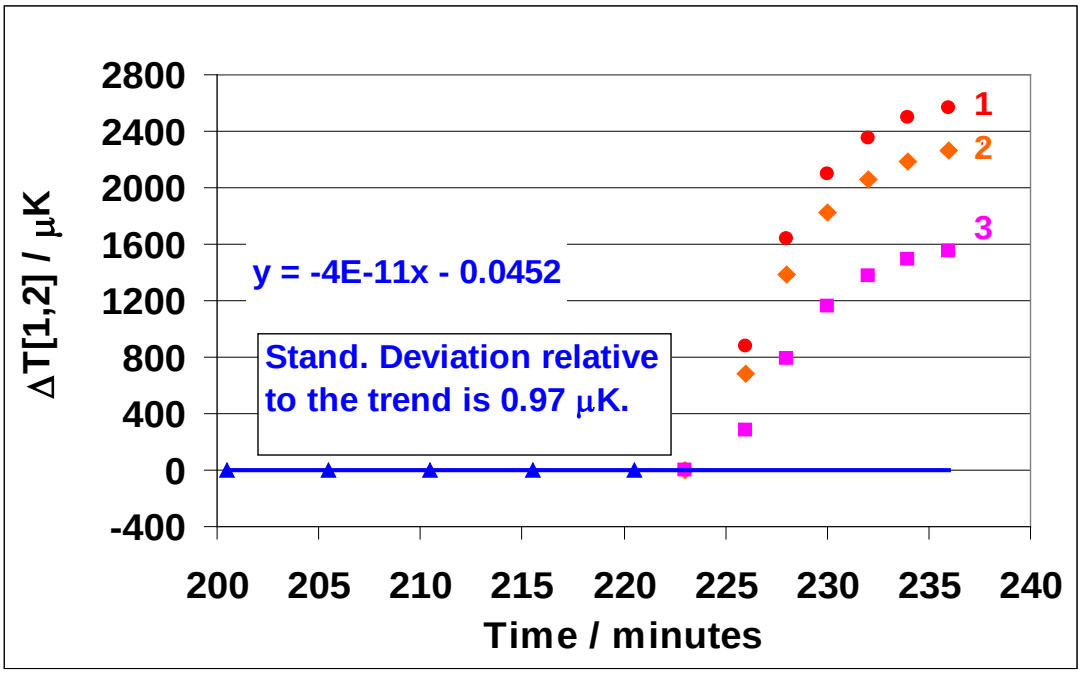

Fig. 4c : The dependences of the vector quantity **ΔT[1,2]** on time for the separations of the R6 thermistor from the gauging surface of 4.5mm (dots), 9mm (rhombi) and 13.5mm (squares). The reference points are shown as triangles

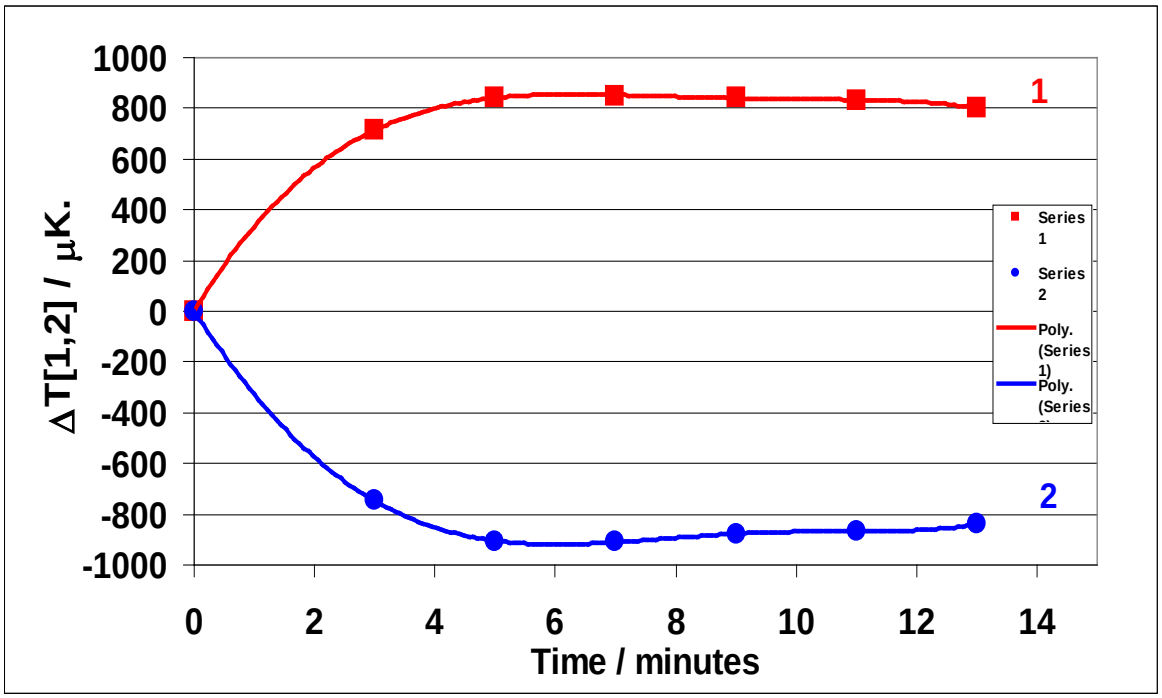

Fig. 5a : The dependences of the surface energy **ΔT[1,2]** on time, obtained for a tungsten carbide block when the R6 thermistor is close to the gauging surface of the block (curve 1), and when the R3 thermistor is close to the opposite gauging surface (curve 2)

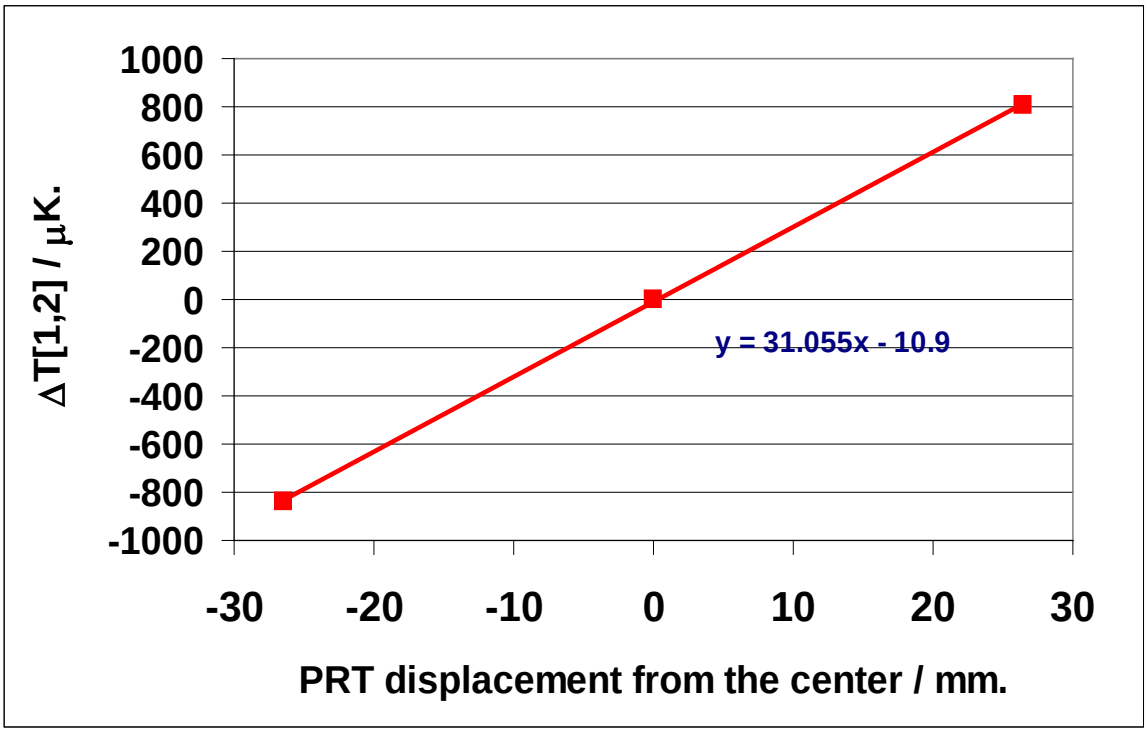

Fig. 5b : The dependence of the maximum value of the quantity **ΔT[1,2]** on the displacement of the PRT relative to the center of the gauge block surface

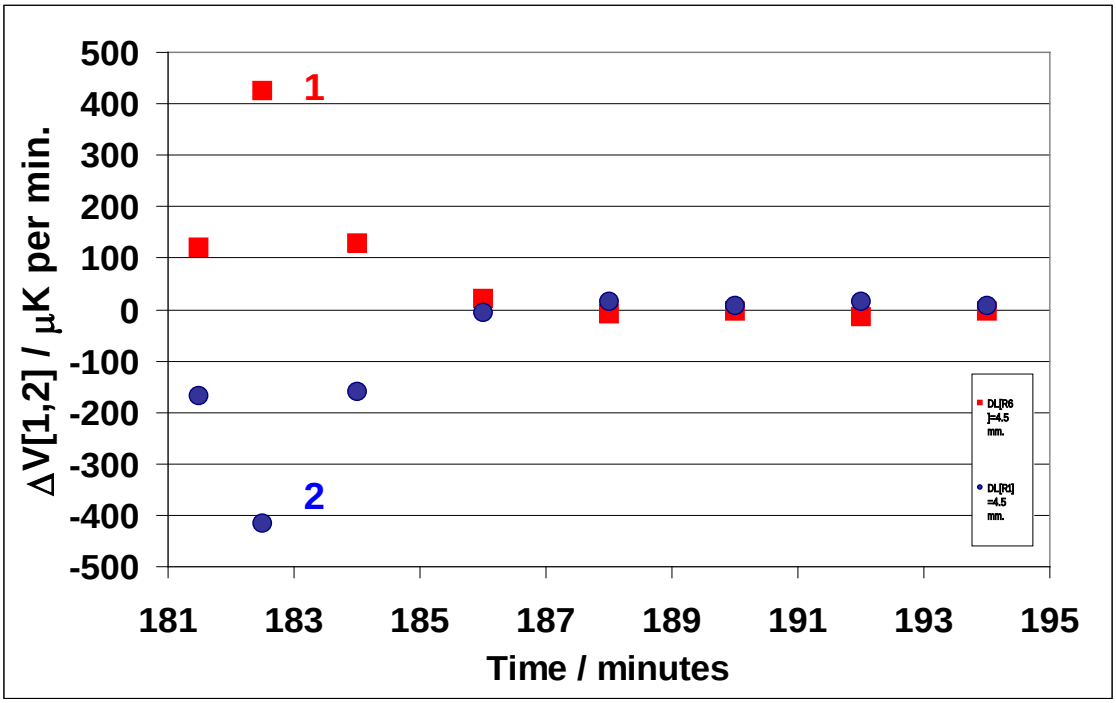

Fig. 5c : The dependences of the quantity **ΔV[1,2]** on the time interval, elapsed after the increase of the PRT modulation current, for two opposite cases of the thermistors positions: dependence 1 (shown by squares) corresponds to the separation of the R6 thermistor of 4.5mm from one of the gauging surfaces of the block, while the dependence 2 (shown by dots) corresponds to the case when the measuring system as a whole was shifted along the surface of the block, so that the separation of 4.5mm of the thermistor R3 from the other gauging surface was realized

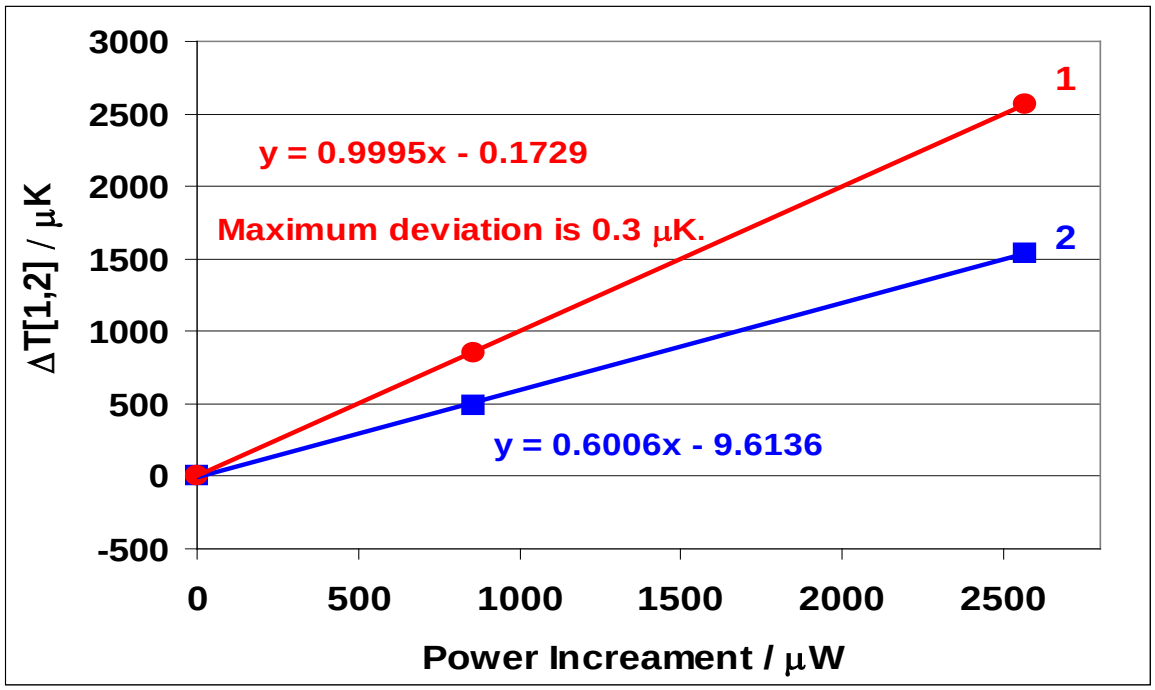

Fig. 6a : The effect of the PRT power increment on the quantity **ΔT[1,2]**. Dependences 1 and 2 correspond to the separations of the R6 axis from the nearest gauging surface of L=4.5mm (dots) and L=13.5mm (squares), respectively. These plots establish the linear relation for the heating period of the modulation cycle between the two vector quantities: the Poynting vector of the external EM field and the quantity **ΔT[1,2]**, characterizing the TSE. The decrease of the magnitude of the TSE with the increase of the R6 separation from the nearest gauging surface is clearly demonstrated by the dependences (1) and (2). (See text for other details)

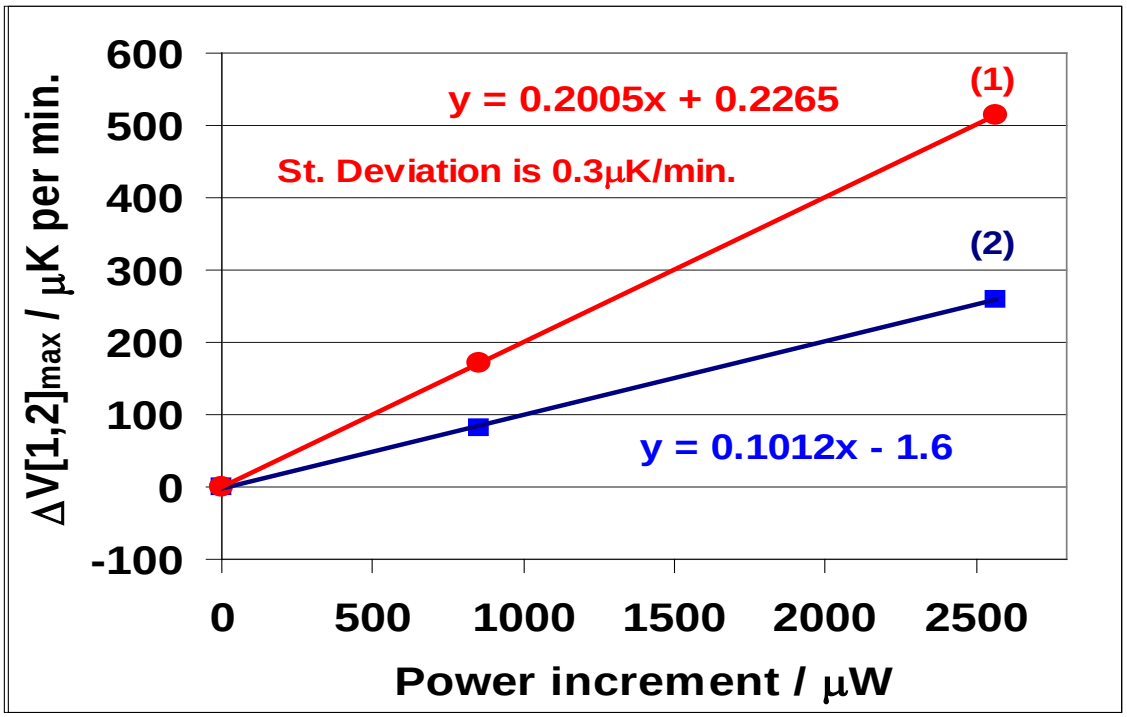

Fig. 6b : The effect of the PRT power increment on the maximum value of the quantity **ΔV[1,2]**. Dependences 1 and 2 correspond to the separations of the R6 axis from the nearest gauging surface of L=4.5mm (dots) and L=13.5mm (squares), respectively. These plots establish the linear relation for the heating period of the modulation cycle between the Poynting vector of the external EM field and the maximum value of the additional energy flux in the gauge block, described by the quantity **ΔV[1,2]**

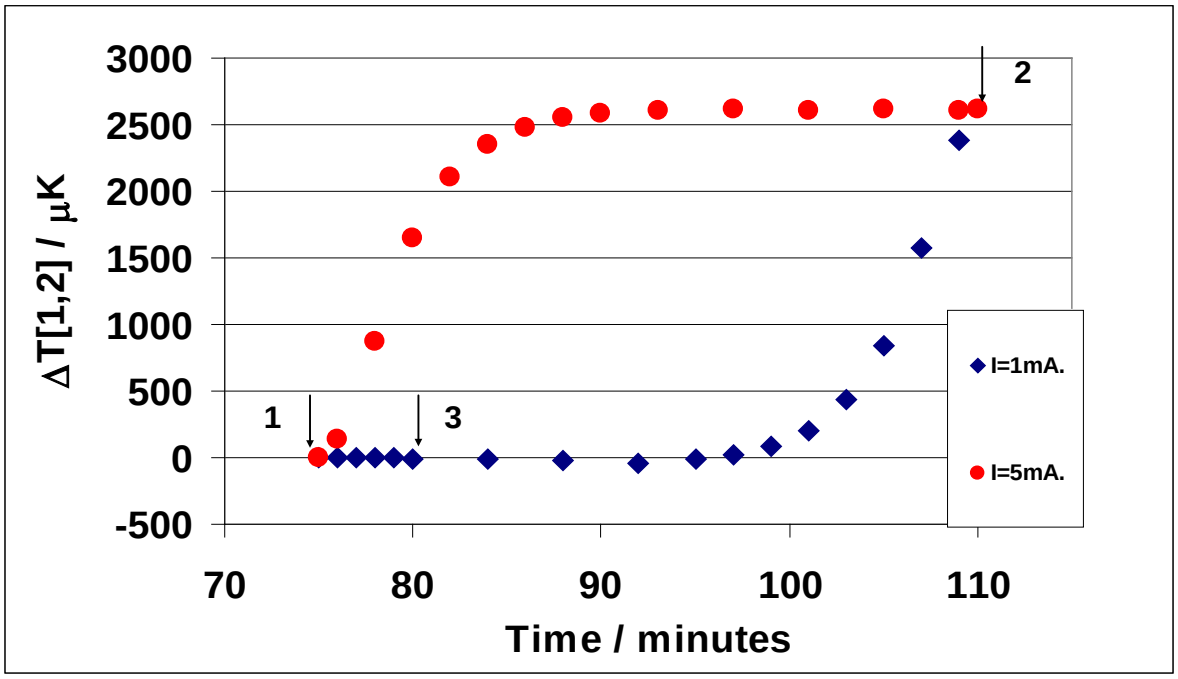

Fig. 7 : The thermal hysteresis loop for the quantity **ΔT[1,2]** that corresponds to the temperature records of Figs. 1 and 2. The heating period of the cycle (between the arrows 1 and 2) is shown by dots, while the cooling period of the modulation cycle (between the arrows 2, 3 and 1) is presented by rhombi. (See text for other details)

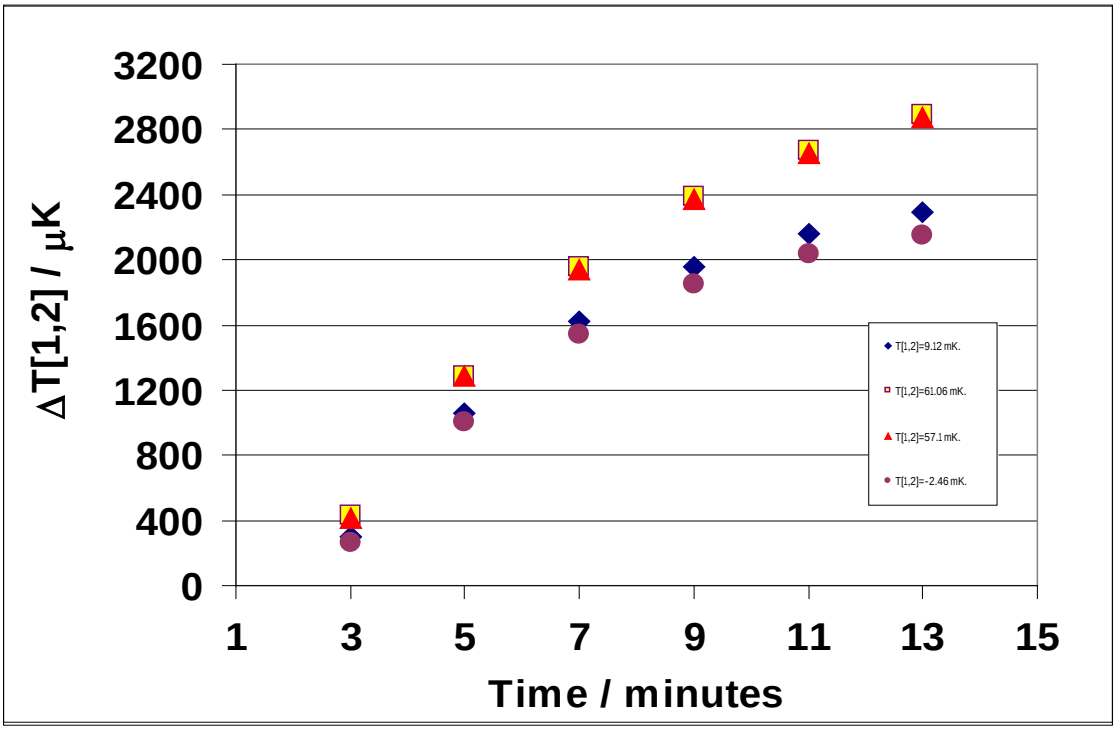

Fig. 8 : The records of the build-up in time of the thermal surface energy in a steel GB during the first 13 minutes of the heating period of the modulation cycle when the temperature differences between the channels **T[1,2]**, equal to 2.46mK (dots), 9.12mK (rhombi), 57.1mK (triangles) and 61.06mK (squares), were realized with the help of an auxiliary energy source in the Dewar. These dependences show that the principle of superposition is not valid for the external EM fields

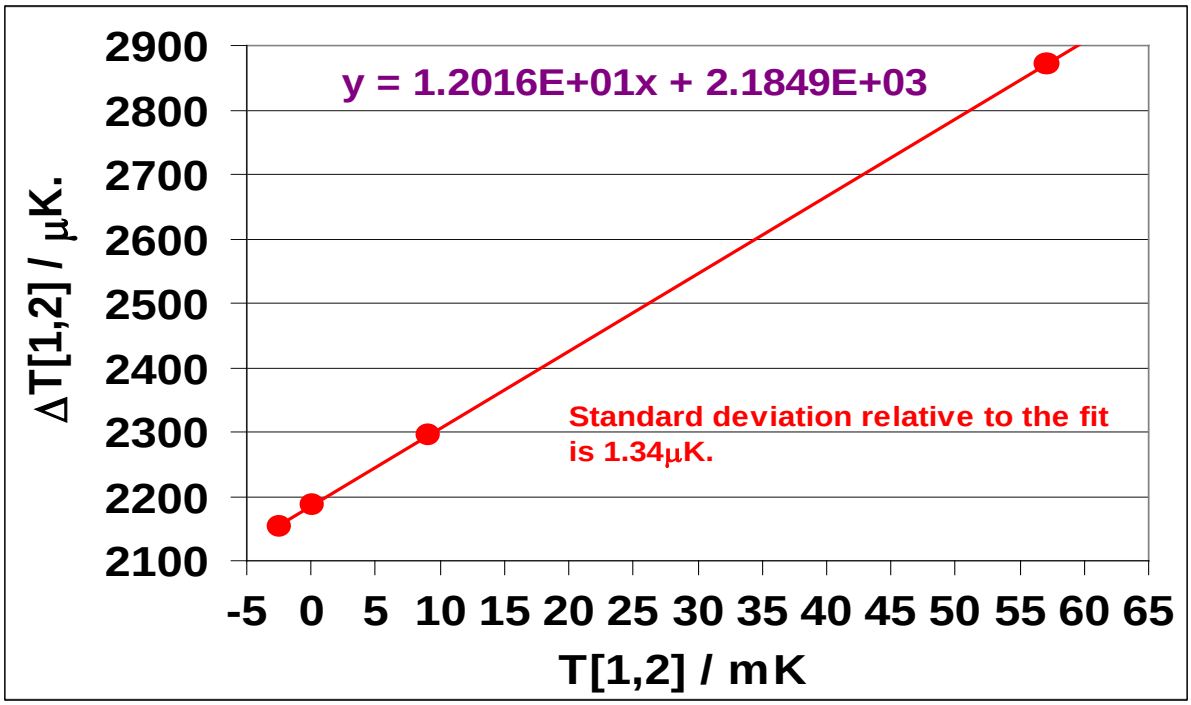

Fig. 9a : The dependence of the quantity **ΔT[1,2]**, measured 13 minutes after the increase of the PRT modulation current in steel gauge block, on the temperature difference **T[1,2]** between the positions of the thermistors R6 and R3. The maximum deviation of the measured values relative to the fit is 1.75μK and the standard deviation for a single measurement is 1.34 μK. (See text for other details)

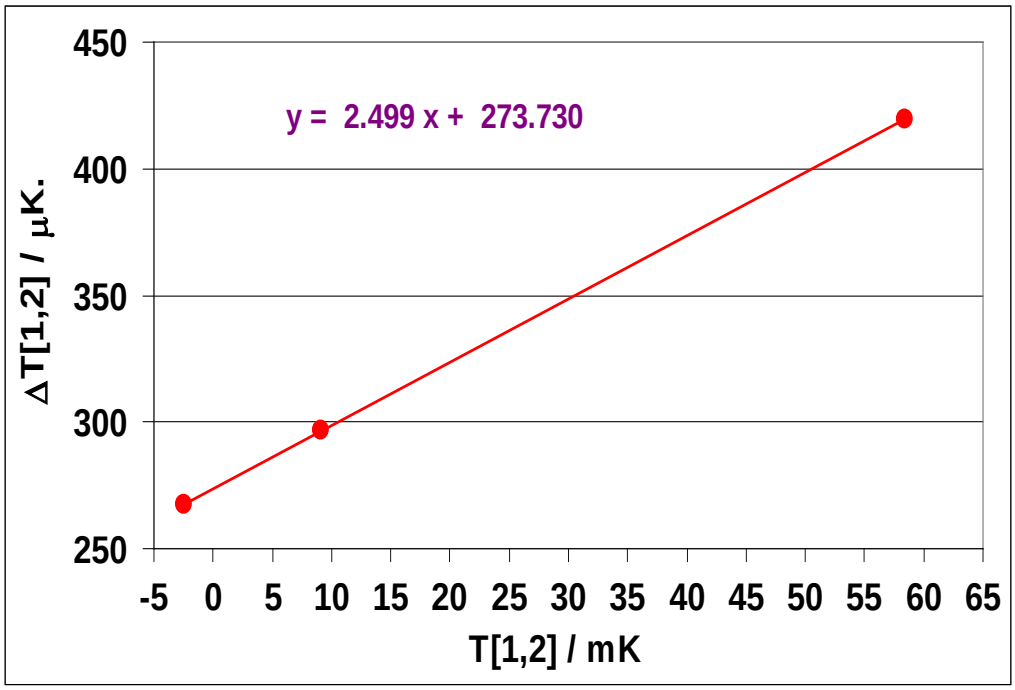

Fig. 9a : The dependence of the quantity **ΔT[1,2]**, measured 3 minutes after the increase of the PRT modulation current in steel gauge block, on the temperature difference **T[1,2]** between the positions of the thermistors R6 and R3

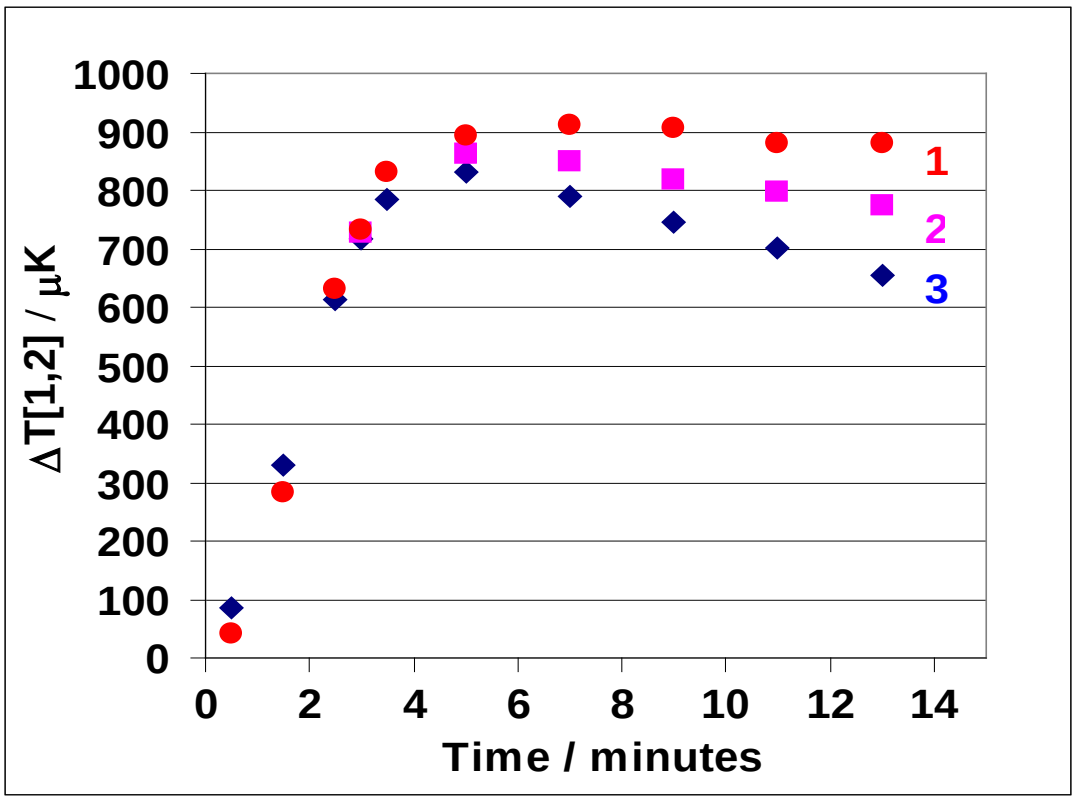

Fig.10 : The dependencies of the quantity **ΔT[1,2]** on time for the first 13 minutes of the heating period that were obtained for the tungsten carbide gauge block for the temperature differences **T[1,2]** of -1.72mK (dependence 1; dots), -7.2mK (dependence 2; squares) and -12mK (dependence 3; rhombi)

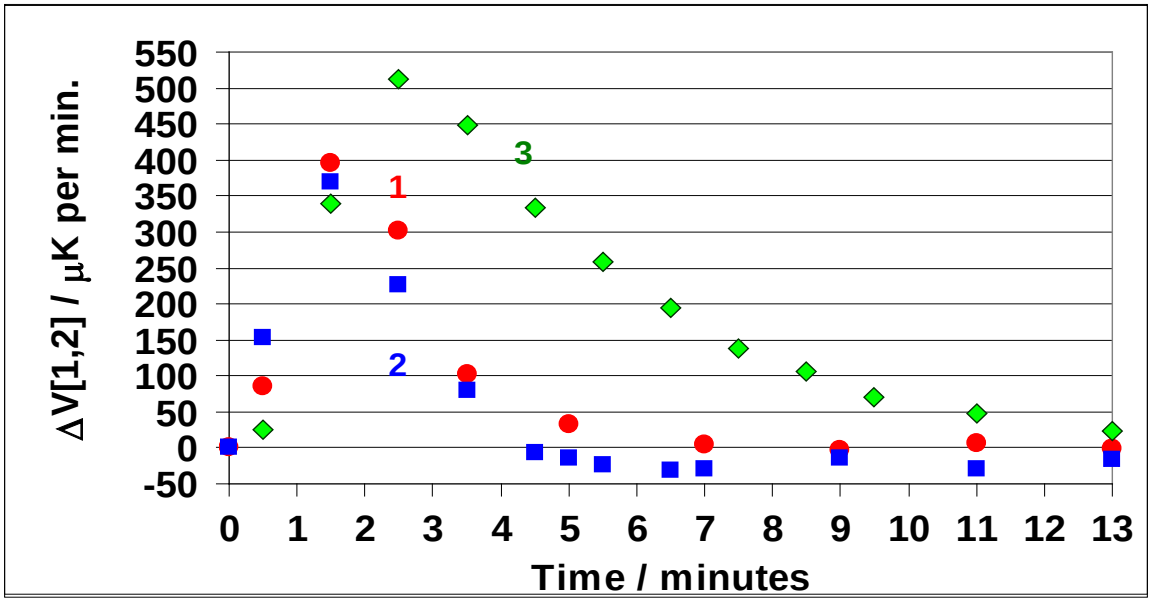

Fig. 11 : The dependencies of the quantity **ΔV[1,2]** on time for the first 13 minutes of the heating period that were obtained for the tungsten carbide gauge block (curves 1 and 2) and for the steel block (3) for the temperature differences between the locations of the thermistors **T[1,2]** of -0,2mK (dependence 1; dots) and -17.2mK (dependence 2; squares). Note that the thermal evolution process is described by a complicated function of time, which is specific for the selected points inside the artifact and whose form and magnitude depend on the direction and magnitude of the constant heat flux, created in advance by an auxiliary heat source. (See text for other details)

This page is intentionally left blank